AD_____

Award Number: W81XWH-11-1-0334

TITLE:
Evaluation of Acid Ceramidase Overexpression-Induced Activation of the Oncogenic Akt Pathway in Prostate Cancer

PRINCIPAL INVESTIGATOR:
Thomas H. Beckham

CONTRACTING ORGANIZATION:

Medical University of South Carolina
Charleston, SC 29425-0001

REPORT DATE: January 2014

TYPE OF REPORT: Annual Summary

PREPARED FOR: U.S. Army Medical Research and Materiel Command
Fort Detrick, Maryland 21702-5012

# REPORT DOCUMENTATION PAGE

*Form Approved*
*OMB No. 0704-0188*



| 1. REPORT DATE | 2. REPORT TYPE | 3. DATES COVERED |
|---|---|---|
| January 2014 | Annual Summary | 11 April 2011 - 10 October 2013 |

**4. TITLE AND SUBTITLE**
Evaluation of Acid Ceramidase- induced Activation of the Oncogenic Akt Pathway In Prostate Cancer

**5a. CONTRACT NUMBER**
W81XWH-11-1-0334

**5b. GRANT NUMBER**
W81XWH-11-1-0334

**5c. PROGRAM ELEMENT NUMBER**

**6. AUTHOR(S)**
Thomas H. Beckham

E-Mail: beckham@musc.edu

**5d. PROJECT NUMBER**

**5e. TASK NUMBER**

**5f. WORK UNIT NUMBER**

**7. PERFORMING ORGANIZATION NAME(S) AND ADDRESS(ES)**
Medical University of South Carolina
Charleston, SC 29425-0001

**8. PERFORMING ORGANIZATION REPORT NUMBER**

**9. SPONSORING / MONITORING AGENCY NAME(S) AND ADDRESS(ES)**
U.S. Army Medical Research and Materiel Command
Fort Detrick, Maryland 21702-5012

**10. SPONSOR/MONITOR'S ACRONYM(S)**

**11. SPONSOR/MONITOR'S REPORT NUMBER(S)**

**12. DISTRIBUTION / AVAILABILITY STATEMENT**
Approved for Public Release; Distribution Unlimited

**13. SUPPLEMENTARY NOTES**

**14. ABSTRACT**

Prostate cancer is a leading cause of cancer and cancer-related mortality in males in the United States. Acid ceramidase is frequently overexpressed in prostate cancer and catalyzes the deacylation of proapoptotic ceramide into sphingosine. Sphingosine is converted by sphingosine kinases into sphingosine 1-phosphate, which promotes numerous pro-cancer phenotypes. Due to the frequent overexpression of acid ceramidase in prostate cancer and its net cancer promoting signaling effects achieved by reducing ceramide and generating sphingosine 1-phosphate, the impact of acid ceramidase, and the lipid profiles it alters, on prostate cancer cell signaling were studied. Here we report the activation of the oncogenic PI3K/Akt signaling pathway when acid ceramidase is overexpressed both in human prostate tissue and in prostate cancer cell lines. This effect was found to depend on sphingosine kinase 1; potentially reflecting increased accessibility of sphingosine kinase 1 to lysosome-derived sphingosine. Surprisingly, we found that S1P receptor 2 mediates acid ceramidase-induced Akt activation, which challenges the prevailing view in the literature that suggests predominantly tumor suppressive functions for S1P receptor 2. Functionally, acid ceramidase overexpressing cells were found to be resistant to cytotoxic chemotherapies, but profoundly sensitive to inhibition of PI3K or Akt in proliferation assays and soft agar colony formation, suggesting acid ceramidase overexpressing cells become dependent on Akt signaling for their oncogenic phenotypes.

The tumor suppressor PTEN classically antagonizes PI3K-mediated activation of Akt, however emerging evidence suggests that nuclear PTEN is also critically important in suppressing cancer. Thus, mechanisms mediating nucleocytoplasmic shuttling of PTEN are of great interest. Following observations that acid ceramidase promoted net redistribution of PTEN from the nucleus into the cytoplasm, we found that the AC-induced Akt activation pathway described above also promoted nuclear egress of PTEN. Furthermore, we found that acid ceramidase and sphingosine 1-phosphate promote formation of a complex between Crm1 and PTEN, confirming that acid ceramidase promotes Crm1-mediated active export of PTEN. After investigating several potential mechanism including PTEN C-terminus phosphorylation and direct export through an *in silico* predicted PTEN nuclear export sequence, we found that acid ceramidase promotes PTEN nuclear export dependent upon Akt-mediated activation of S6K. Functionally, we found that acid ceramidase was able to promote resistance to Docetaxel chemotherapy, cell proliferation, and tumor formation in cells expressing wild type PTEN, but not in cells expressing nuclear localized PTEN, suggesting that acid ceramidase promotes prostate cancer in part through Akt-mediated nuclear export of PTEN.

**15. SUBJECT TERMS**
Prostate cancer, Akt signaling, PTEN, acid ceramdiase

| 16. SECURITY CLASSIFICATION OF: | 17. LIMITATION OF ABSTRACT | 18. NUMBER OF PAGES | 19a. NAME OF RESPONSIBLE PERSON |
|---|---|---|---|
| | | | USAMRMC |

| a. REPORT | b. ABSTRACT | c. THIS PAGE | | | 19b. TELEPHONE NUMBER *(include area code)* |
|---|---|---|---|---|---|
| U | U | U | UU | 44 | |

**Table of Contents**

**Introduction:**
The goals of this research are to 1) test the hypothesis that acid ceramdiase (AC) overexpression causes activation of Akt in PCa cells through AC's effects on bioactive sphingolipids and that AC overexpressing PCa cells are addicted to Akt activation for their aggressive phenotype, 2) test the hypothesis that the activation of Akt due to AC overexpression depends on deficient PTEN activity and 3) test the hypothesis that AC overexpression contributes to PCa tumor formation and metastasis. The purpose of this research is to more completely evaluate the cancer-relevant signaling alterations that result from AC overexpression so that future thereapeutic modalities can properly identify and target specific cancer susceptibilities.

**Key Research Accomplishments**

Aim 1: Test the hypothesis that acid ceramdiase (AC) overexpression causes activation of Akt in PCa cells through AC's effects on bioactive sphingolipids and that AC overexpressing PCa cells are addicted to Akt activation for their aggressive phenotype

Figure 1: AC and phosphorylation of Akt correlate in prostate adenocarcinoma

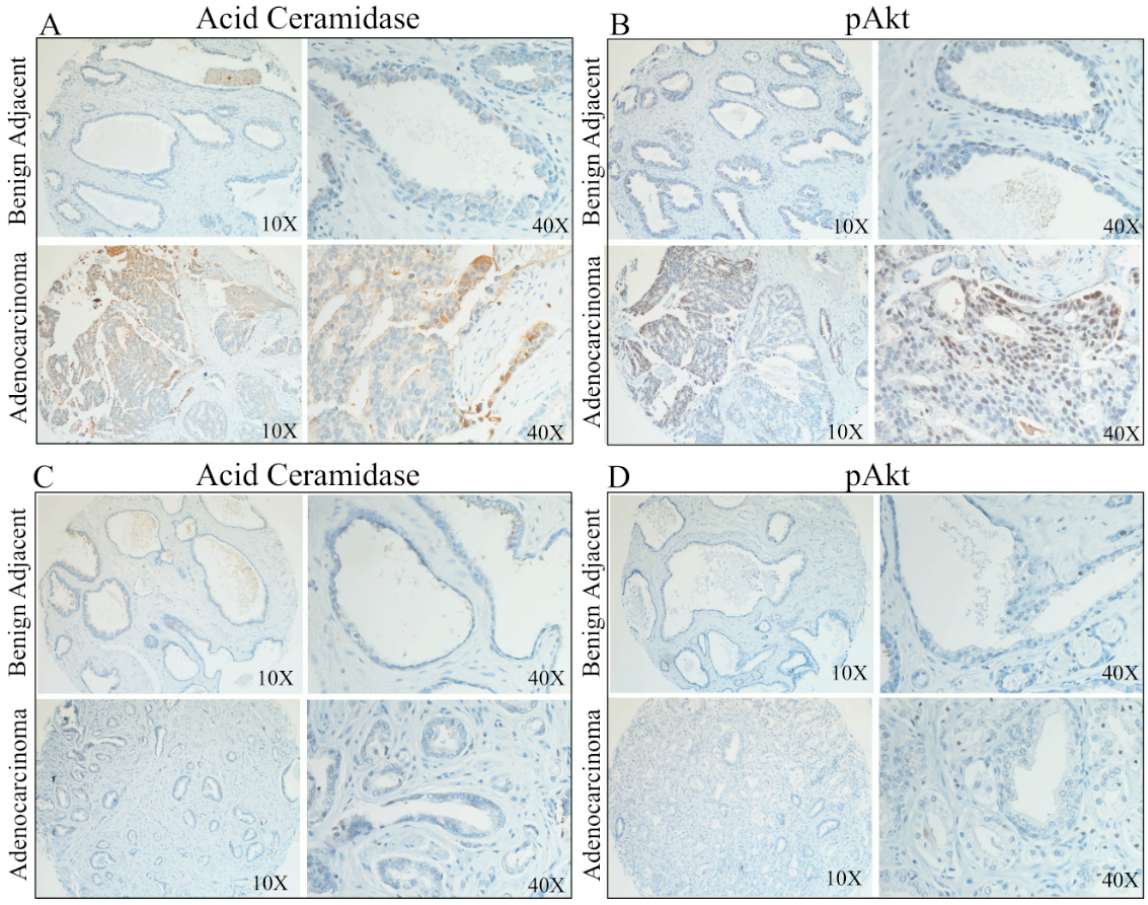

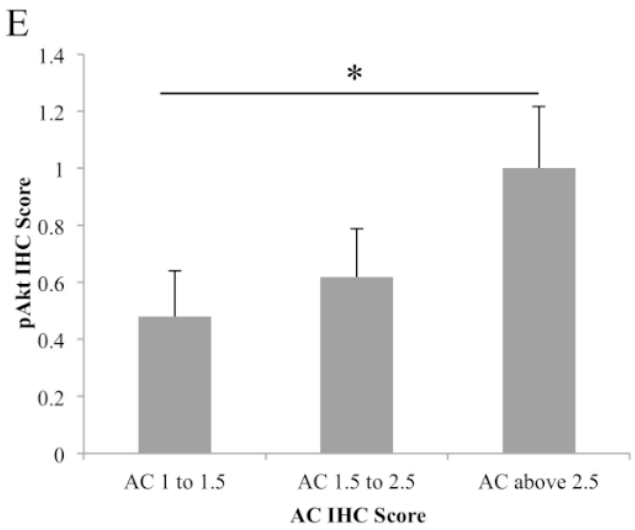


**Figure 1:** *Acid ceramidase correlates with pAkt in prostate cancer. a-d)* A 27 patient tissue microarray with patient-matched prostate adenocarcinoma and adjacent benign tissue was immunostained for AC and pAkt (Ser473). Staining intensity was evaluated by a blinded pathologist. *e)* 56 prostate tumor biopsies were immunostained for AC and pAkt. Tumors were grouped by AC intensity as indicated in the figure, and the mean pAkt score for tumors in the indicated group is plated. *p<.05, Student's t-test.

**Acid ceramidase activates Akt**

The relationship between AC and Akt activation was investigated using several approaches. We stably expressed AC in PPC1 and DU145 prostate cancer cell lines and found that high levels of AC increased phosphorylation of Akt at Serine 473 compared to vector control cells, indicating activation (Fig. 2A). In cells with stable shRNA knockdown of AC, we observed a reduction in basal Akt phosphorylation in both DU145 and PPC1 cells versus vector control (Fig. 2B). Transient adenoviral expression of AC (Ad-AC) compared to Ad-GFP also revealed increased Akt phosphorylation in MIA, Panc01, SCC14A, PPC1 (Fig. 2C) and DU145 (Fig. 2D) cells, suggesting a generalizable phenomenon of AC-induced Akt activation in cancer. Furthermore, shRNA delivered by adenovirus (Ad-shAC) decreased pAkt (Fig. 2D). In order to validate that we are observing functional signaling through Akt when we express AC, we probed for phospho-proteins downstream of Akt (Fig. 2E). We observed activation of the mTOR pathway (p-mTOR and p-p70S6K) as well as inhibition of GSK-3beta, which is involved in regulation of cell proliferation and metabolism(164).

Figure 2: AC expression and activity correlates with Akt activation

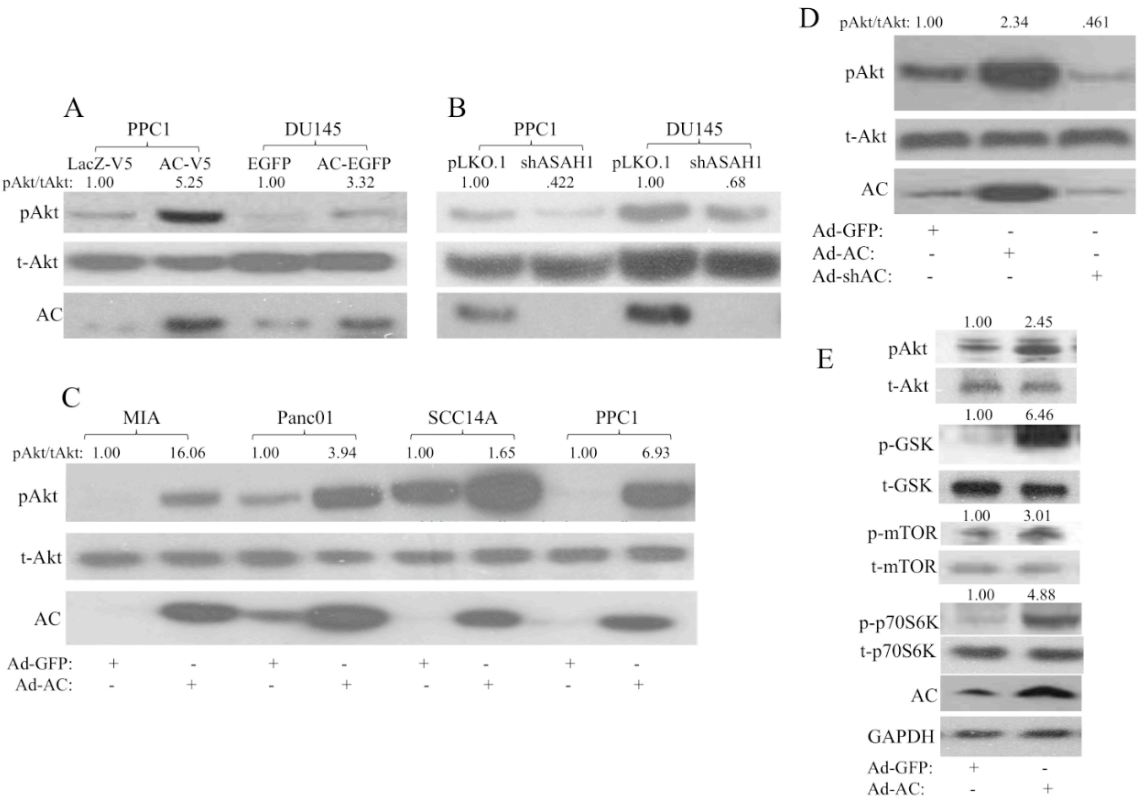


**Figure 2:** *Acid ceramidase activates Akt.* PPC1 and DU145 prostate cancer cells stably expressing *a)* AC or control (PPC1: AC-V5 or LacZ-V5; DU145 AC-EGFP or EGFP) or *b) ASAH1* antisense or empty vector (shAC or pLKO.1) were analyzed by western blotting. *c)* MIA, Panc01, SCC14A, and PPC1 cells were infected with Ad-AC or Ad-GFP. 48 hours after infection, cells were analyzed by western blotting. *d)* DU145 cells were infected with Ad-GFP, Ad-AC, or Ad-shAC. 48 hours after infection, cells were analyzed by western blotting. *e)* PPC1 cells were infected with Ad-AC or Ad-GFP. 48 hours after infection, cells were analyzed by western blotting. pAkt/tAkt is the ratio of phosphorylated Akt to total Akt normalized to the reference (i.e. Ad-GFP is the reference of Ad-AC).

**SphK1 mediates AC-induced Akt activation**

The bioactive lipids ceramide, sphingosine, and S1P have all been linked to regulation of Akt. We observed no change in total cell ceramide in Ad-AC infected PPC1 cells compared to Ad-GFP (Fig. 3A), though species-specific alterations were observed (data not shown). Sphingosine and S1P were significantly elevated in Ad-AC infected cells (Fig. 3A). In order to measure secreted S1P, we treated Ad-AC/GFP infected PPC1 cells with C17-C6-ceramide, finding significant C17-S1P increase in the cells (Fig. 3G) and medium (Fig. 3H). Treatment of cells with exogenous sphingosine did not activate Akt, rather decreasing pAkt moderately after 6 hours of treatment (Fig. 3B). Addition of the dual-isoform SphK inhibitor SKI-II decreased Akt activation at 6 hours, and did not augment Akt activation alone or in combination with sphingosine (Fig. 3B). We then infected PPC1 cells with Ad-AC or Ad-GFP in the presence of SKI-II, and observed a dose-dependent reduction in Akt activation (Fig. 3C), suggesting that SphK activity is necessary for AC-induced Akt activation. Infection of wild type (WT) or SphK2 knockout (SphK2 KO) mouse embryonic fibroblasts (MEFs) with Ad-AC promoted strong activation of Akt, whereas AC had no impact on Akt activation in SphK1 KO MEFs (Fig. 3D). Ad-AC increased S1P cell content (Fig. 3I) and secretion into the medium (Fig. 3J) in WT and SphK2 KO MEFs, but not in SphK1 KO MEFs. To confirm the observation that SphK1 may be necessary for AC-induced Akt activation, we used shRNA (Fig. 3E) and siRNA (Fig. 3F) to knockdown each SphK isoform and confirmed that knockdown of SphK1, but not SphK2, abrogated AC-induced Akt activation.

Figure 3: SphK1 mediates AC-induced Akt activation

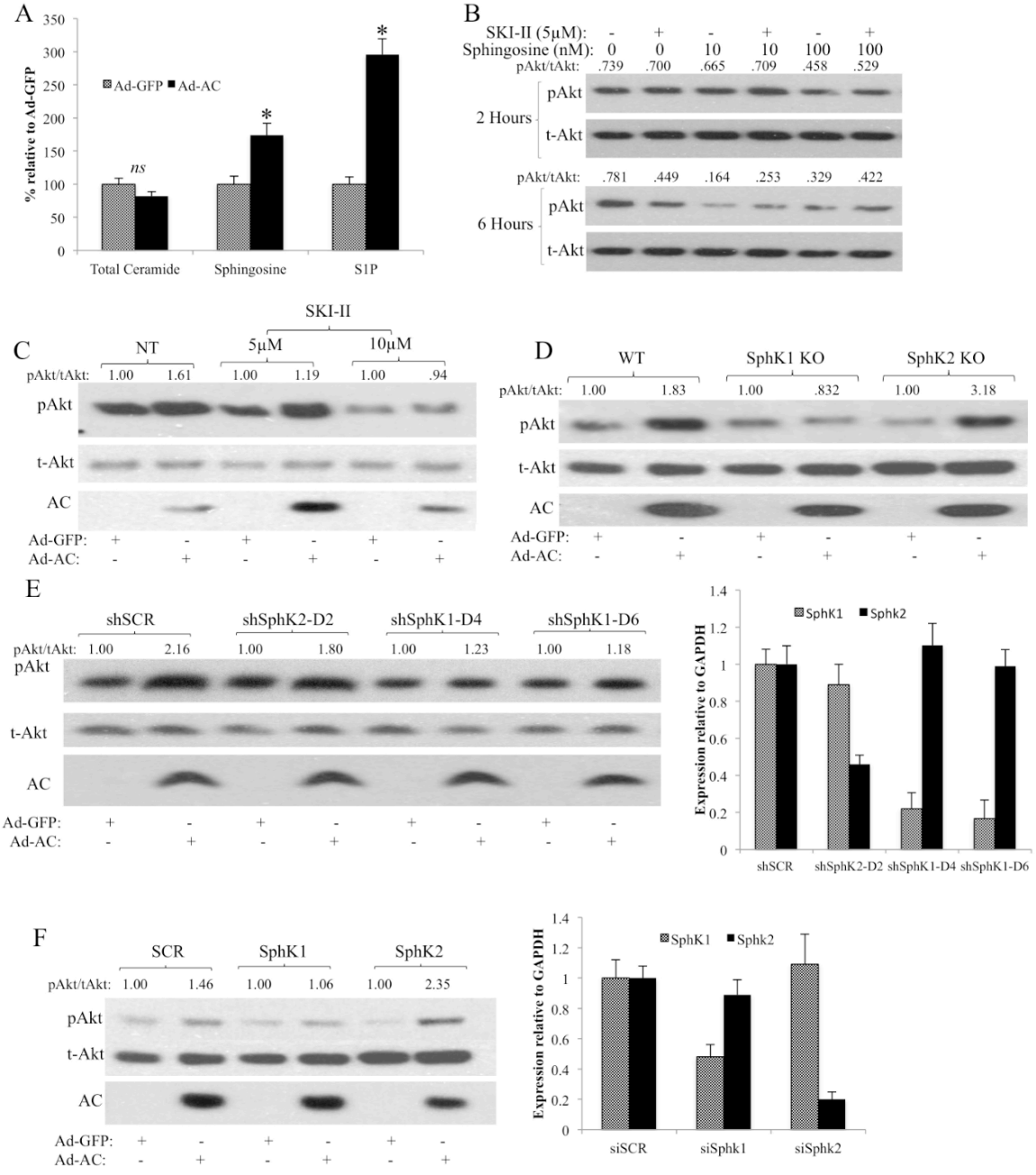

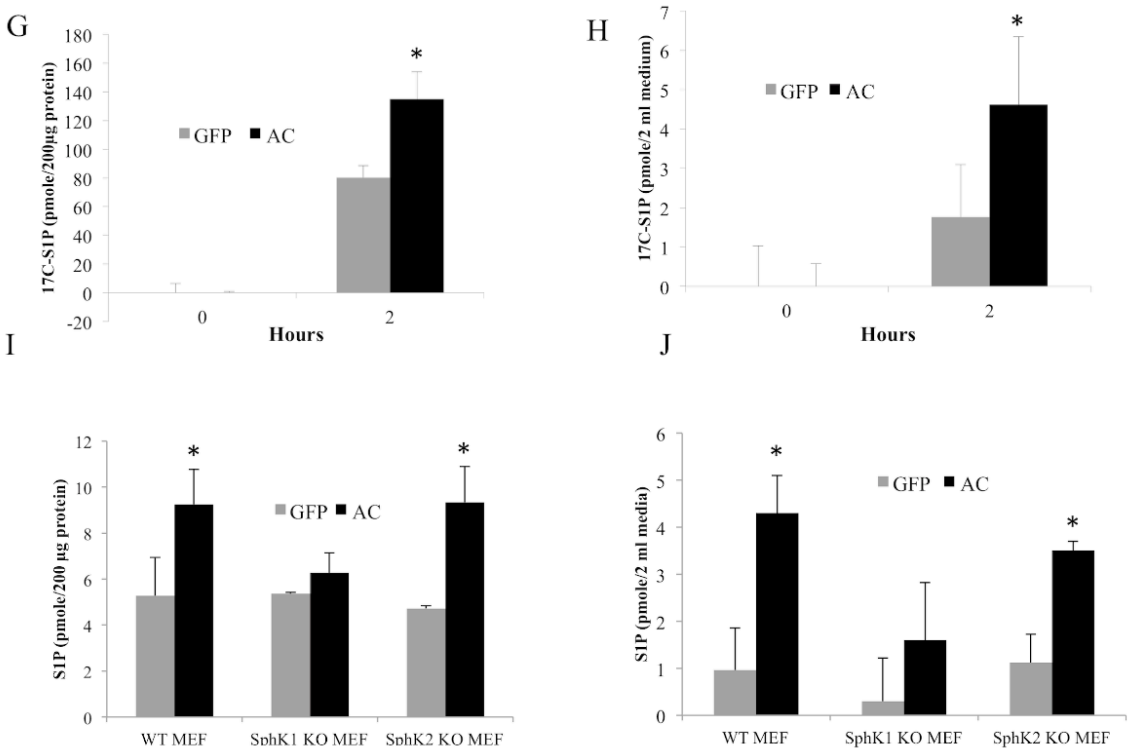


**Figure 3:** *SphK1 mediates AC-induced Akt activation. a)* Ad-GFP or Ad-AC infected PPC1 cell pellets were analyzed by LC/MS for ceramide, sphingosine, and S1P. Bars represent sphingolipid level relative to Ad-GFP. *b)* PPC1 cells were treated for 2 hours with the indicated dose of SphK inhibitor SKI-II or vehicle (DMSO) before treatment with the indicated doses of sphingosine or vehicle (EtOH). Cells were collected 2 or 6 hours after addition of sphingosine, as indicated. pAkt/tAkt ratios were generated using NIH ImageJ band densitometries, and are represented as raw ratios so that multiple comparisons can be made. *c)* PPC1 cells were infected with Ad-AC or Ad-GFP in the presence of the indicated dose of SKI-II. 48 hours after infection, cells were analyzed by western blotting. *d)* WT, SphK1 KO, and SphK2 KO MEFs were infected with Ad-AC or Ad-GFP at MOI 100. 48 hours after infection, cells were analyzed by western blotting. *e)* PPC1 cells were transfected with non-targeting (SCR) or SphK1 or SphK2 targeting shRNA vectors. 6 hours after transfection, cells were infected with Ad-GFP or Ad-AC. 48 hours after infection, cells were analyzed by western blotting and qRT-PCR. *f)* PPC1 cells were transfected with nontargeting (SCR) or SphK1 or Sphk2 targeting siRNA. 6 hours after transfection, cells were infected with Ad-GFP or Ad-AC. 48 hours after infection, cells were analyzed by western blotting and qRT-PCR. PPC1 cells were infected with Ad-GFP or Ad-AC for 48 hours and then treated with 5µM C17-C6-Ceramide for the indicated time and then cells (*g)* and medium *(h)* were collected and analyzed for C17-S1P by LC/MS. *i-j)* WT, SphK1 and SphK2 knockout MEFs were infected with Ad-GFP or Ad-AC. After 48 hours, cells *(i)* and medium *(j)* were collected and S1P was analyzed by LC/MS. *p<.05 analyzed by student's t test.

**S1PR2 stimulates PI3K to activate Akt**

To determine whether AC/S1P-induced Akt activation was mediated by S1PRs, we expressed AC in PPC1 cells in the presence of the S1PR1 antagonist W146 or the S1PR2 antagonist JTE013. While W146 had no impact on reducing AC-induced Akt activation (Fig. 4A), JTE013 strongly inhibited AC-induced Akt activation (Fig. 4B). Similarly, AC-induced Akt activation was also prevented by JTE013 in WT MEFs, confirming that this phenomenon is intact in PTEN positive as well as PTEN negative (PPC1) cells (Fig. 4C). When we transfected PPC1 cells with shRNA sequences against S1PR1, S1PR2, or S1PR3, Ad-AC-induced Akt activation was unaffected in multiple S1PR1 and 3 knockdown cells despite 60-70% reduction in mRNA (Fig. 4D, O-P). Both S1PR2 shRNA sequences greatly reduced Ad-AC-

induced Akt activation, confirming a prominent role for S1PR2 signaling in activation of Akt downstream of AC. Because the observation that S1PR2 activates an oncogenic signaling pathway challenges the dogma on the role of S1PR2 in cancer cell signaling, we performed a proliferation experiment and found that the proliferation advantage of AC overexpressing prostate cancer cells is diminished by treatment with JTE013 (Fig. 4E). Basal S1PR1-3 expression was evaluated in PPC1 and DU145, both of which had predominate S1PR2 mRNA with markedly less S1PR1 and 3 (Fig. 4J). Further analysis revealed that S1PR2 mRNA is induced slightly (1.3-2 fold) but significantly upon AC expression (Fig. 4K). Expression of the other ceramidases was not affected by AC expression, except for a reduction in ACER1 mRNA in PPC1 (Fig. 4L). S1PRs are GPCRs known to stimulate Akt activation by activating $G_i$-mediated stimulation of PI3K. Pertussis toxin (PTX), which inactivates $G_i$, $G_0$, and $G_t$, prevented AC-induced Akt activation (Fig. 4F), and the $G_i$ inhibitor NF023 abrogated AC-induced Akt activation (Fig. 4G), suggesting a role for G proteins, specifically $G_i$, in AC-induced Akt activation. Expressing PTEN in PPC1 cells antagonized AC-induced Akt activation (Fig. 4H), and the PI3K inhibitor LY294002 effected dose-dependent abrogation of pAkt (Fig. 4I), supporting an S1PR2, PI3K-dependent mechanism. To test whether exogenous S1P works in the same way on these cell lines, we treated PPC1 and DU145 with 500nM S1P for 2 hours in the presence or absence of JTE013 (Fig. 4M-N). JTE013 blocked S1P-induced Akt activation in both cell lines, supporting the findings using AC expression to drive increased S1P signaling.

Figure 4: S1PR2 stimulates PI3K to activate Akt

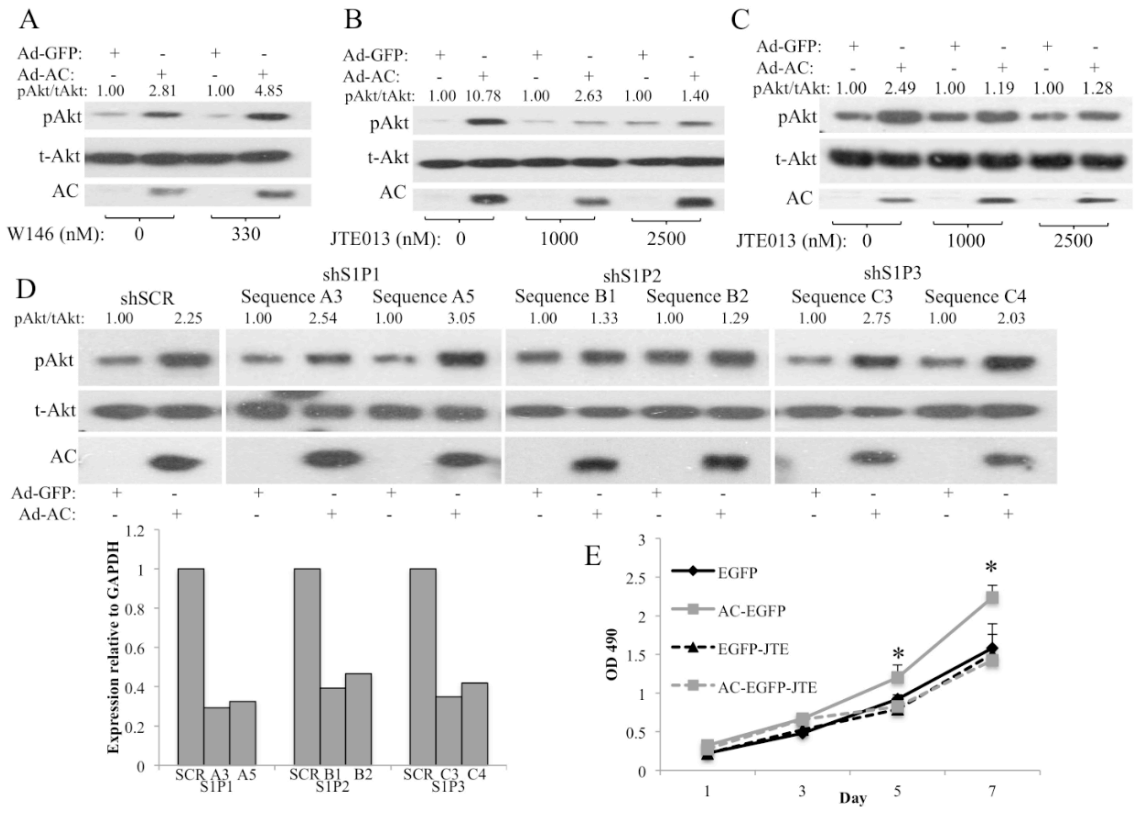

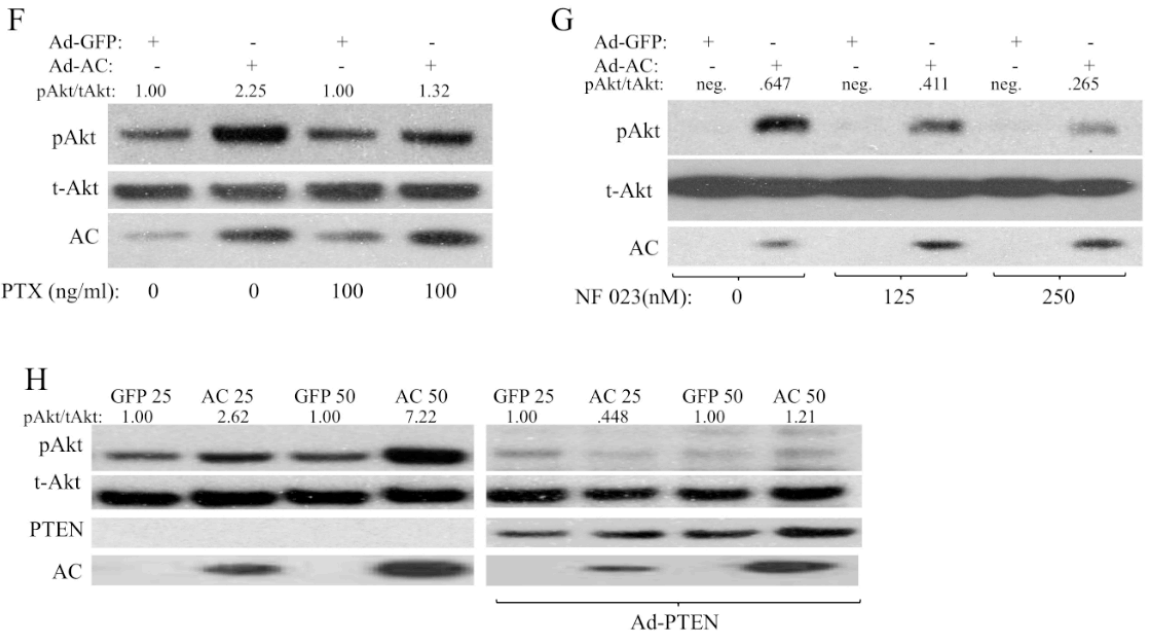
F
Ad-GFP: + - + -
Ad-AC: - + - +
pAkt/tAkt: 1.00 2.25 1.00 1.32
pAkt
t-Akt
AC
PTX (ng/ml): 0 0 100 100
G
Ad-GFP: + - + - + -
Ad-AC: - + - + - +
pAkt/tAkt: neg. .647 neg. .411 neg. .265
pAkt
t-Akt
AC
NF 023(nM): 0 125 250
H
GFP 25 AC 25 GFP 50 AC 50 GFP 25 AC 25 GFP 50 AC 50
pAkt/tAkt: 1.00 2.62 1.00 7.22 1.00 .448 1.00 1.21
pAkt
t-Akt
PTEN
AC
Ad-PTEN
I
Ad-GFP: + - - - -
Ad-AC: - + + + +
pAkt/tAkt: 1.00 1.71 1.07 .987 .435
pAkt
t-Akt
AC
Vehicle
10 25 50
LY294002 (μM)
J
mRNA expression relative to GAPDH
0.0016
0.0014
0.0012
0.001
0.0008
0.0006
0.0004
0.0002
0
***
***
PPC1
DU145
S1P1 S1P2 S1P3
K
Fold Change in mRNA expression (Ad-AC vs. Ad-GFP
7
6
5
4
3
2
1
0
ns
ns
*
*
ns
ns
PPC1
DU145
S1P1 S1P2 S1P3
L
Fold Change in mRNA expression (Ad-AC vs. Ad-GFP
14
12
10
8
6
4
2
0
*
***
***
PPC1
DU145
ACER1 ACER2 ACER3 NCER ASAH1

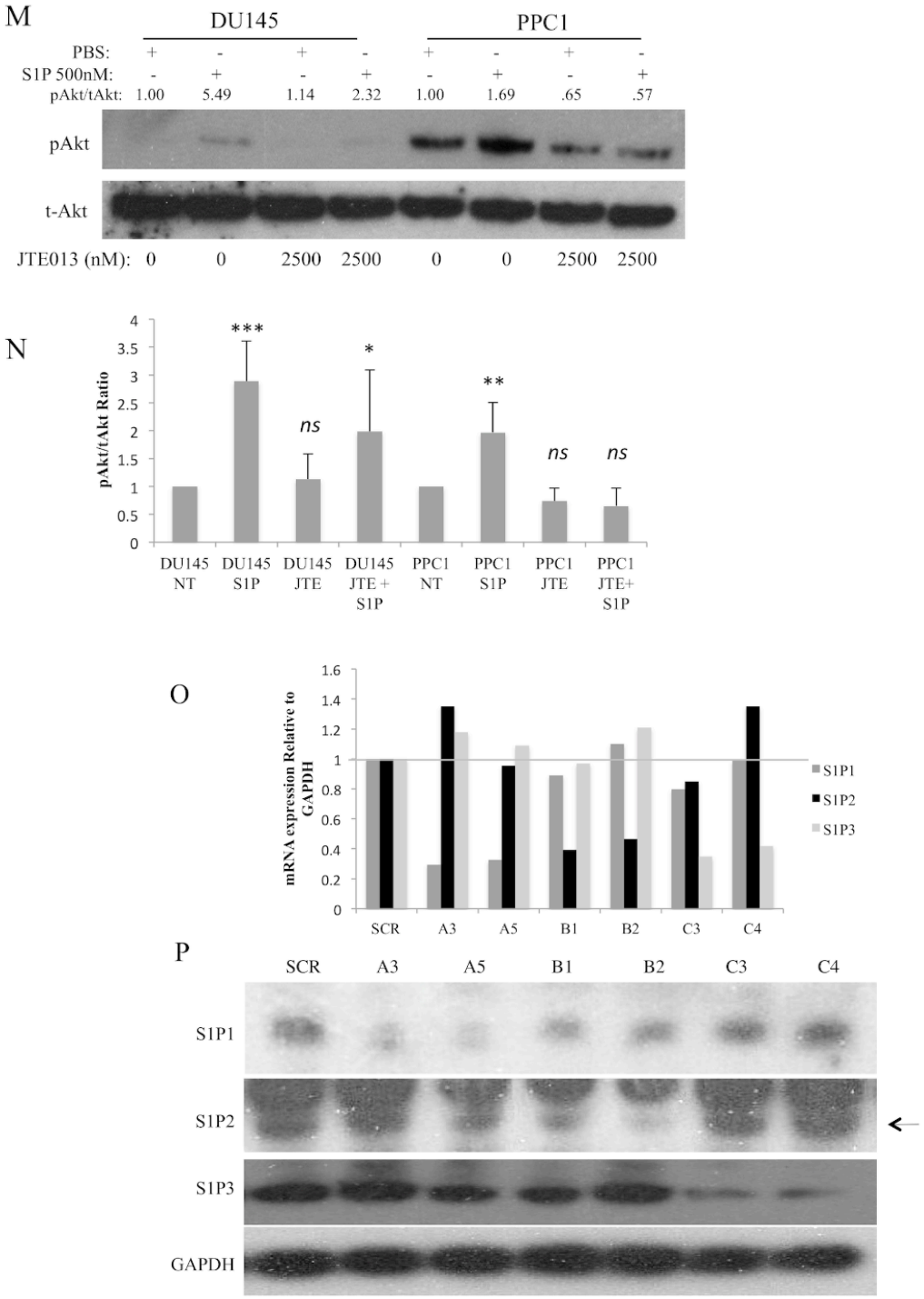


**Figure 4:** *S1PR2 stimulates PI3K to activate Akt. a and b)* PPC1 cells were infected with Ad-AC or Ad-GFP. After 6 hours, cells were treated with the indicated dose of either a) W146 or b) JTE013. After 48 hours of infection, cells were analyzed by western blotting. *c)* WT MEFs were infected with Asd-AC or Ad-GFP (MOI 100). After 6 hours, cells were treated with the indicated dose of JTE013. After 48 hours, cells were collected for western blotting. *d)* PPC1 cells were transfected with non-targeting (SCR) or S1PR1-3 targeting shRNA vectors. 6 hours after transfection, cells were infected with Ad-GFP or Ad-AC. 48 hours after infection, cells were analyzed by western blotting and qRT-PCR. *e)* DU145 EGFP and AC-EGFP cells were plated at low density in 96 well plates in the presence or absence of 1μM JTE013 and analyzed by MTS assay at the indicated days. Statistical analysis was performed using a one-way ANOVA with Bonferroni correction, *p<.05. PPC1 cells were infected with Ad-AC or Ad-GFP.

After 24 hours, cells were treated with the indicated dose of *f)* PTX, *g)* NF023, *i)* LY294002. After another 24 hours, cells were analyzed by western blotting. *h)* PPC1 cells were co-infected with Ad-AC or Ad-GFP and Ad-PTEN (MOI 20), as indicated, after 48 hours cells were analyzed by western blotting. qRT-PCR analysis was carried out on *j)* Unstimulated or *k,l):* Ad-GFP/AC infected PPC1 and DU145 cells. Basal mRNA abundance of S1PR1-3 relative to GAPDH are shown in *j)*, whereas fold change in mRNA expression in Ad-AC versus Ad-GFP infected cells for the indicated gene target is shown in *k)* and *l)*. PPC1 and DU145 cells were plated and stimulated for 2 hours with 500nM S1P with or without 2 hour pretreatment with 2500 nM JTE013. Cells were collected and analyzed by immunoblotting *(m)*. Three independent experiments were done, and the statistical analysis and mean pAkt to Akt ratio, normalized to untreated (NT) or JTE013 alone are shown in *(n)*. *o)* relative mRNA expression of S1PR1-3 in cells transfected with the indicated shRNA construct. *p)* Immunoblot showing protein expression of the indicated S1PR in cells transfected with the indicated shRNA construct.

**AC promotes chemotherapy resistance, but confers sensitivity to Akt inhibition**

Cytotoxic chemotherapy depends in part on ceramide accumulation to cause cell death(165-167). PPC1 cells were subjected to a wide dose range of the cytotoxic chemotherapeutic agents Docetaxel, Gemcitabine (GMZ) and 5'-Fluorouracil (5'-FU). PPC1 cells infected with Ad-AC were found to be less sensitive to all three compounds (Docetaxel: 413%, GMZ: 55% and 5'-FU: 96% less sensitive) reflected by an increased EC50 (Fig. 5, Table 1). Conversely, AC overexpressing cells were more sensitive to inhibition of Akt with Akt inhibitor X (AktX), Perifosine, or MK2206 with AC-expressing cells being approximately 30-40% more sensitive than Ad-GFP infected cells.

Figure 5: AC promotes chemotherapy resistance, but confers sensitivity to Akt inhibition

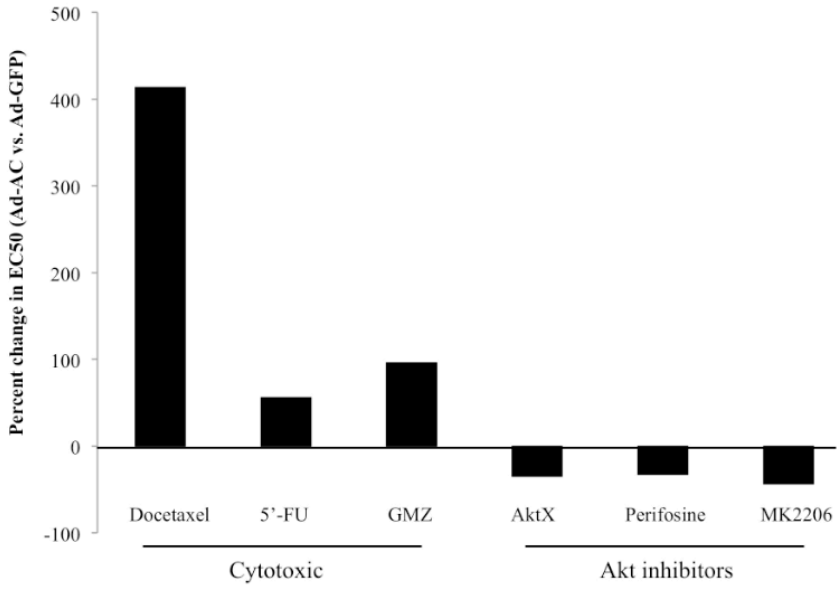

| Table 1: EC50 of various compounds | | |
|---|---|---|
| | **Ad-GFP** | **Ad-AC** |
| **Docetaxel (nM)** | 1.89 | 9.74 |
| **5'-Fu (μM)** | 4.36 | 6.80 |
| **GMZ (μM)** | 31.80 | 62.45 |
| **AktX (μM)** | 13.70 | 8.92 |
| **Perifosine (μM)** | 29.54 | 19.89 |
| **MK 2206 (μM)** | 3.50 | 1.97 |

**Figure 5:** *AC promotes chemotherapy resistance, but confers sensitivity to Akt inhibition. a.* PPC1 cells infected 24 hours prior with Ad-GFP or Ad-AC were treated with various doses of the indicated compounds. After 48 hours, cell viability was measured by MTS assay. Prism software was used to calculate the EC50 of each compound (Table 1) and the EC50 of Ad-AC infected cells was compared to that of Ad-GFP infected cells to determine the percent change in EC50 of Ad-AC infected cells.

**Proliferation in AC overexpressing cells is profoundly sensitive to Akt inhibition.**

Akt signaling promotes cancer in numerous ways, including increased cell proliferation. To determine whether AC-induced proliferation is Akt-dependent, we evaluated prostate cancer cell proliferation in the presence of AktX and Perifosine. In DU145-AC-EGFP cells stably expressing AC, we noted significantly more rapid cell proliferation compared to vector control (Fig 6A). Treatment with AktX (Fig. 6A) and Perifosine (Fig. 6C) both reduced proliferation in AC-EGFP and EGFP cell lines. However, directly comparing cell number at Day 7 revealed that AktX and Perifosine more strongly inhibited proliferation in AC-EGFP cells (Fig. 6B,D). EGFP cell proliferation was reduced 30% (AktX) and 52% (Perifosine), whereas AC-EGFP cell proliferation was reduced 52% (AktX) and 91% (Perifosine). The same effect was observed in PPC1 cells infected with Ad-AC, in which AktX inhibited cell proliferation 52%, in contrast with Ad-GFP infected cells, which were only slightly impacted with 9% reduction in cell number compared to untreated (Fig. 6E,F).

Figure 6: Proliferation in AC overexpressing cells is profoundly sensitive to Akt inhibition

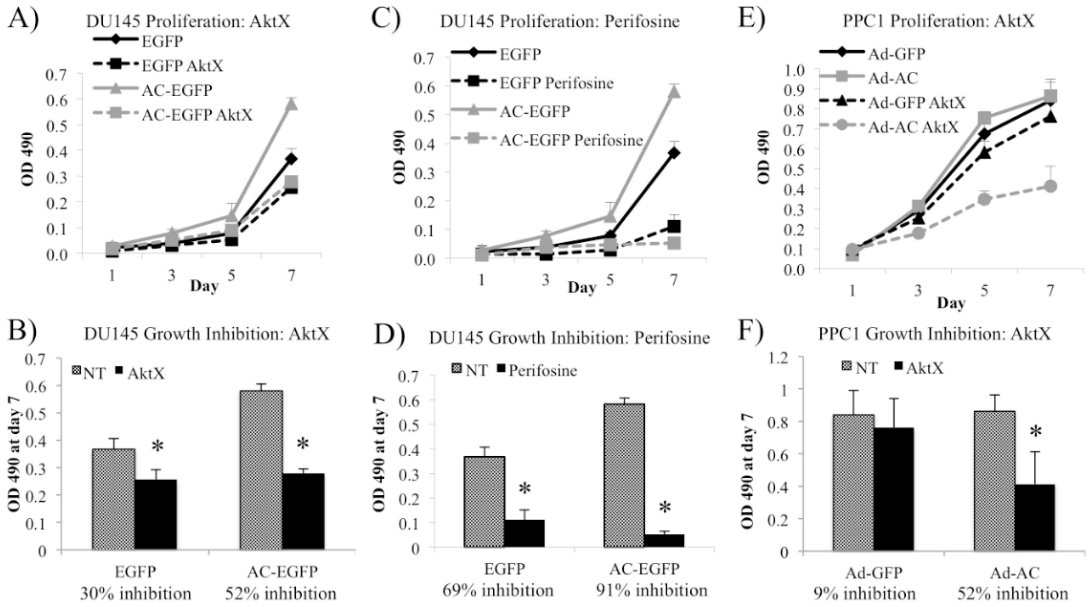

**Figure 6:** *Proliferation in AC overexpressing cells is profoundly sensitive to Akt inhibition. a, c, e)* 500 cells were plated on 96 well plates of DU145 AC-EGFP and EGFP (a and c) or PPC1 cells infected with Ad-GFP or Ad-AC (e). After overnight cell attachment cells were treated with 2.5μM AktX (a, e) or 5μM Perifosine (c). At the indicate day, MTS assay was used to determine relative cell proliferation. *b, d, f)* OD 490 values at day 7 were compared and used to calculate the percent inhibition in cell proliferation in each cell type by the indicated compound. *p<.05 calculated by the student's t test.

**AC-induced Akt signaling promotes soft agar colony formation.**

Anchorage independent growth is a hallmark of oncogenic potential. PPC1 cells infected with Ad-AC formed more colonies on soft agar compared to Ad-GFP infected cells (Fig. 7A,C). Interestingly, while inhibition of Akt signaling with AktX and JTE013, the S1PR2 antagonist did not have an impact on soft agar colony formation in Ad-GFP infected PPC1 cells, Ad-AC infected cells were sensitive to both Akt inhibition and S1PR2 antagonism, consistent with the hypothesis that AC-induced Akt activation is oncogenic. Similarly, when cells were infected with an adenovirus delivering an anti-AC short hairpin, Ad-shASAH1, fewer colonies were formed than when cells were infected with non-targeting shRNA (Fig. 7B,D).

Figure 7: AC-induced Akt signaling promotes soft agar colony formation

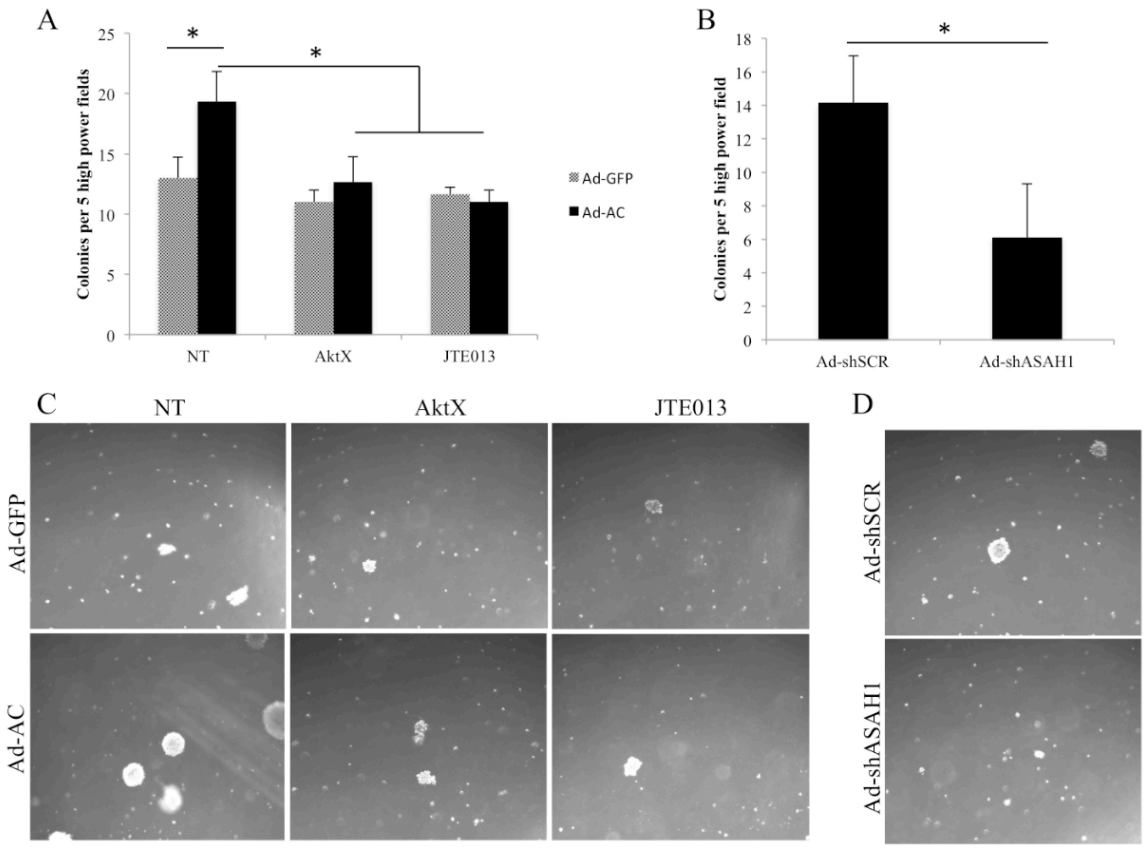


**Figure 7:** *AC-induced Akt signaling promotes soft agar colony formation. a,b)* PPC1 cells were infected with Ad-GFP, Ad-AC (MOI 50), Ad-shSCR, or Ad-shASAH1 (MOI 20) one day prior to plating in 6-well plates in a total volume of 4 ml soft agar. *a)* 4 hours after plating, 5μM JTE013, 10μM AktX, or vehicle (DMSO) was added in 1 ml complete medium. Colonies, represented in *c,d,* were counted two weeks after plating.

Aim 2: Test the hypothesis that the activation of Akt due to AC overexpression depends on deficient PTEN activity

The relationship between AC and Akt activation was investigated using several approaches. We stably expressed AC in PPC1 and DU145 prostate cancer cell lines and found that high levels of AC increased phosphorylation of Akt at Serine 473 compared to vector control cells, indicating activation (Fig. 8A). In cells with stable shRNA knockdown of AC, we observed a reduction in basal Akt phosphorylation in both DU145 and PPC1 cells versus vector control (Fig. 8B). This shows that AC expression correlates with Akt activation in PTEN positive (DU145) and negative (PPC1) cell lines. Figure 8H shows that when we express PTEN in PPC1 cells we significantly reduce AC-induced Akt activation. These observations suggest that while PTEN significantly reduces AC-induced Akt activation, AC can activate Akt in the presence or absence of PTEN.

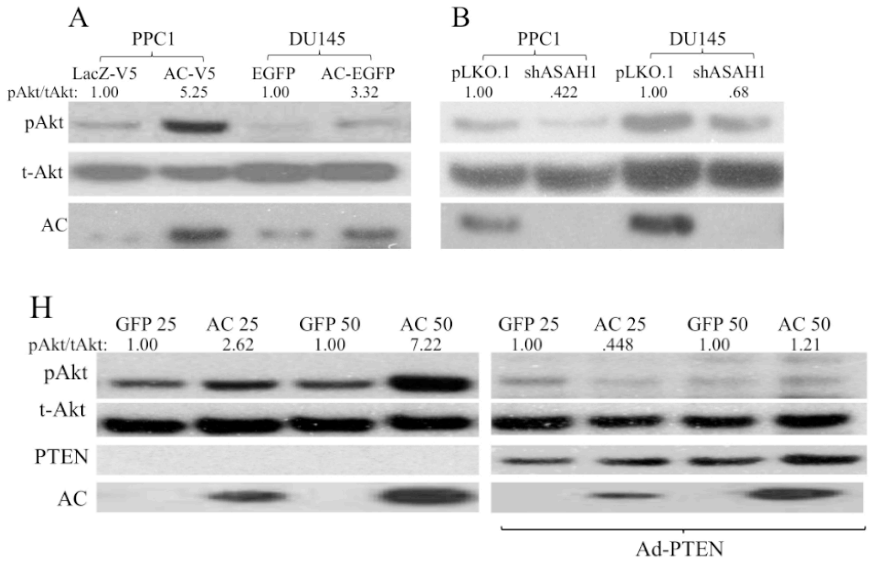


**Figure 8***: Acid ceramidase activates Akt.* PPC1 and DU145 prostate cancer cells stably expressing *a)* AC or control (PPC1: AC-V5 or LacZ-V5; DU145 AC-EGFP or EGFP) or *b) ASAH1* antisense or empty vector (shAC or pLKO.1) were analyzed by western blotting. *h)* PPC1 cells were co-infected with Ad-AC or Ad-GFP and Ad-PTEN (MOI 20), as indicated, after 48 hours cells were analyzed by western blotting.

Aim 3: Test the hypothesis that AC overexpression contributes to PCa tumor formation and metastasis.

**AC promotes oncogenic features of prostate cancer cells in vitro and in vivo.**
We co-infected PPC1 cells with Ad-GFP or Ad-AC and Ad-GFP, Ad-WT-PTEN, or Ad-PTEN-NLS. AC promoted nuclear egress of WT-PTEN, but not NLS-PTEN, which remained confined to the nucleus in all cells (Fig. 8A-B). Treatment of cells with 1.5 nM Docetaxel induced apoptosis in cells expressing both WT-PTEN and PTEN-NLS more strongly than cells not expressing PTEN (Fig. 8C), consistent with the role of PTEN in potentiating apoptotic stimuli. Interestingly, while Ad-AC was able to suppress Docetaxel induced apoptosis in Ad-GFP and Ad-WT-PTEN infected cells, Ad-PTEN-NLS infected cells were not protected from apoptosis by Ad-AC. Moreover, the EC50s of these treatments to Docetaxel were increased by Ad-AC, indicating desensitization or protection from cell death due to Docetaxel, however Ad-PTEN-NLS infected cells had no change in EC50 when AC was expressed (Fig. 8D). These results suggest that AC is able to protect cells from chemotherapy-induced apoptosis and cell death when it is able to promote nuclear egress of PTEN, but not when nuclear expression of PTEN is enforced. In a study of cell proliferation, Ad-GFP and Ad-WT-PTEN infected cells expressing AC proliferated more rapidly than their Ad-GFP infected controls (Fig. 8E). Interestingly, while the overall rate of proliferation in WT-PTEN expressing cells was slower, Ad-AC promoted proliferation more robustly (1.84 fold at day 8) compared to cells expressing no PTEN (1.2 fold at day 8), suggesting that while AC can promote

proliferation in the presence and absence of PTEN, it exerts a more powerful influence in PTEN expressing cells. Cells expressing PTEN-NLS proliferated the least of all treatments, and Ad-AC provided no advantage in proliferation, further suggesting that the ability of AC to promote proliferation depends upon its ability to promote nuclear egress of PTEN. In a study of the ability of AC to promote tumor engraftment in a xenograft study, we found that AC trended towards promotion of formation of tumors more rapidly in cells expressing GFP (control) or a WT-PTEN construct (p=0.1), but not in cells expressing NLS-PTEN (p=0.7) (Fig. 8F).

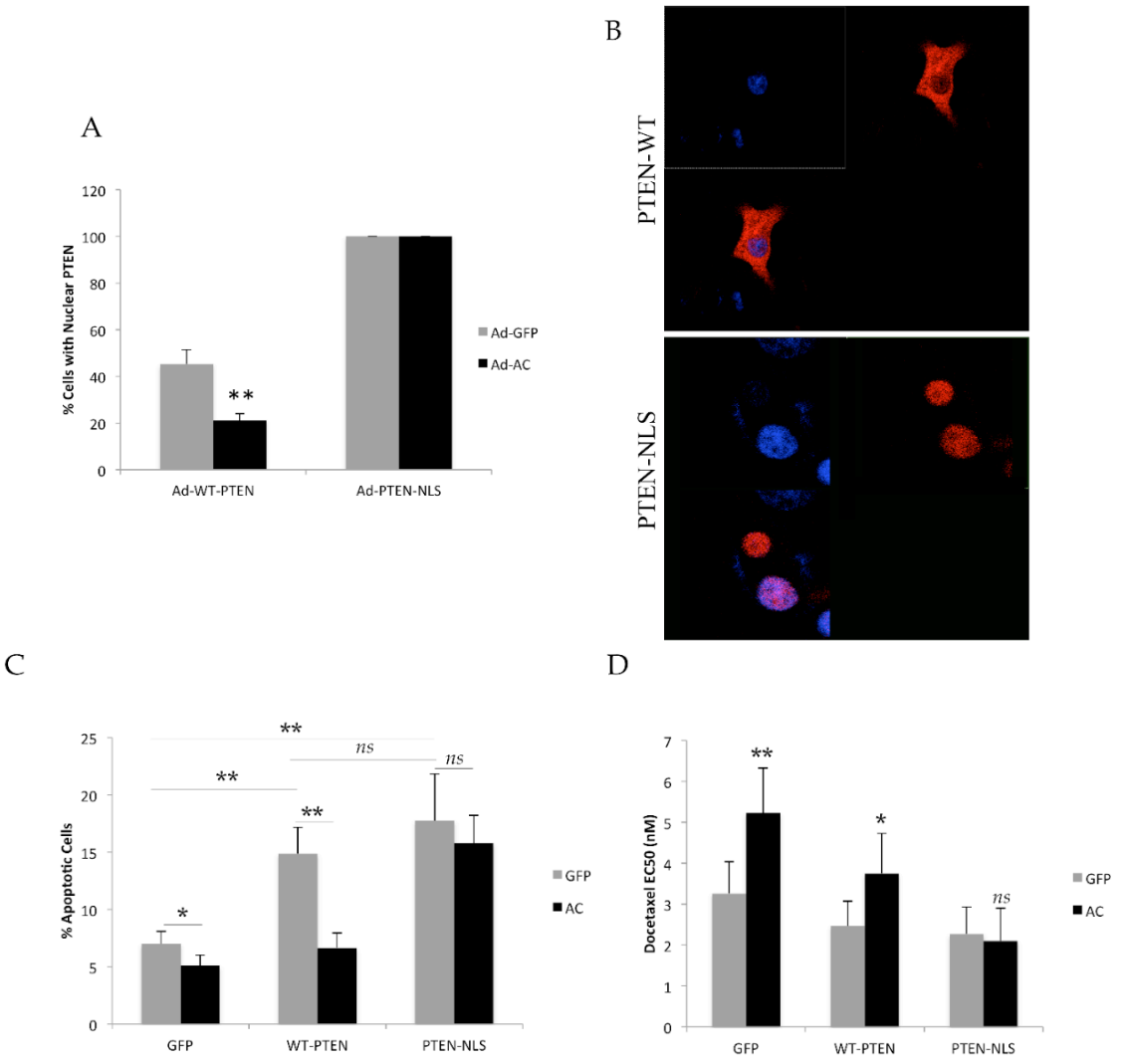

E

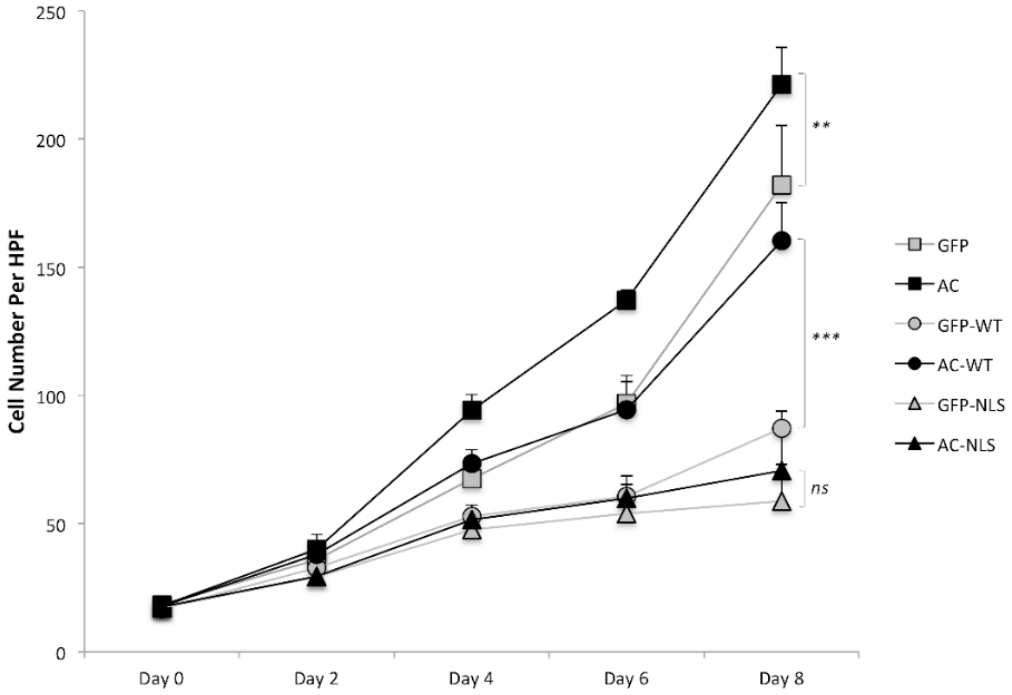


D

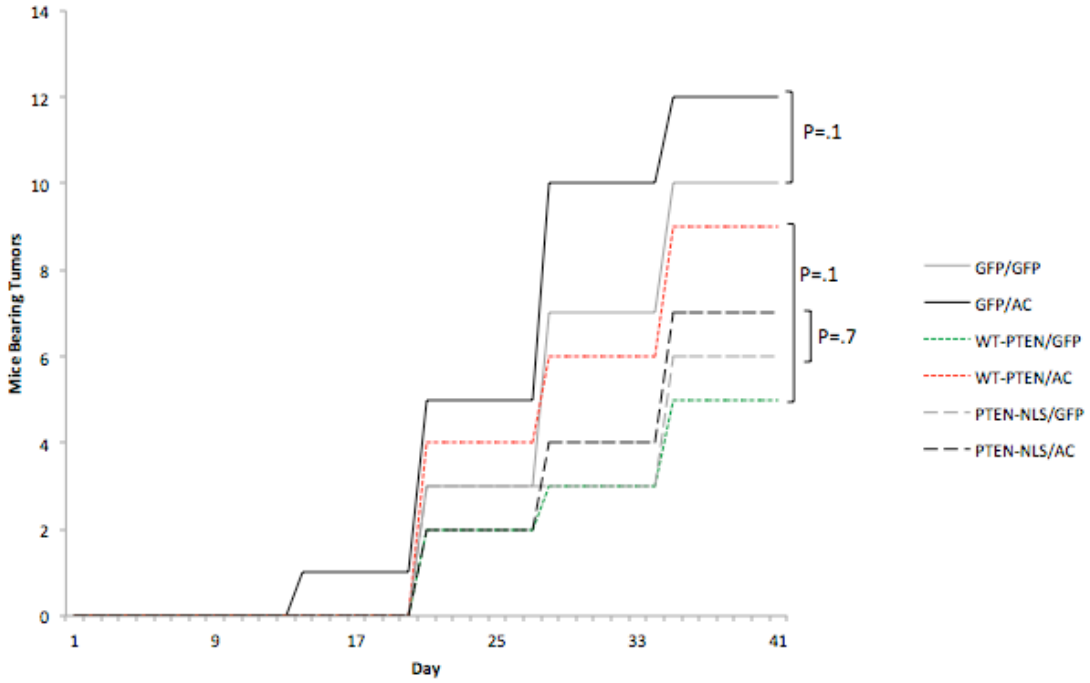


**Figure 8:** *AC promotes tumor formation and Docetaxel resistance in cells with wild type, but not nuclear localized, PTEN. a)* PPC1 cells transfected with WT-PTEN or PTEN-NLS were infected with Ad-GFP or Ad-AC for 48 hours. Cells were immunostained for PTEN, and the percentage of cells which had nuclear PTEN in each treatment is graphed. Representative cells are shown in *b). c-f)* PPC1 cells were infected with 25 MOI Ad-GFP or Ad-AC and either 25 MOI Ad-GFP, Ad-WT-PTEN, or Ad-PTEN-NLS. *c)* After 24 hours plating, cells were treated with 1.5nM Docetaxel and after a further 48 hours, stained with propidium iodide and analyzed for apoptotic cells using FACS. *d)* After 24 hour attachment, cells were

treated with a dose course (.01 to 100nM) Docetaxel and analyzed for relative cell viability using MTS assay after a further 48 hours. The EC50 was estimated using Prism 4 software. *e)* Cells were counted on the indicated day (day 0 being the day of plating). Student's t-test, *p<.05, **p<.01. F) 4x10^6 cells were injected into the flanks of nu/nu mice and observed for 6 weeks for the formation of palpable tumors.

**Reportable outcomes:**

2012 MUSC MSTP Research Day
Charleston, SC
Title: Sphingolipid-mediated regulation of nuclear PTEN
Selected for oral presentation

2012 University of California San Diego Rady School of Management Student Venture Open Competition
San Diego, CA
Title: Small Molecule Platform for Improving Radiation Therapy of Prostate Cancer.
Selected for oral presentation
Awarded First Place

2012 Hollings Cancer Center Research Retreat
Charleston, SC
Title: Sphingolipid-mediated regulation of nuclear PTEN

**Beckham TH**, Cheng JC, Lu P, Shao Y, Troyer D, Lance R, et al. Acid ceramidase induces sphingosine kinase 1/S1P receptor 2-mediated activation of oncogenic Akt signaling. *Oncogenesis*. 2013;2:e49. doi: 10.1038/oncsis.2013.14. PubMed PMID: 23732709.

**Beckham, T.H.,** Cheng, J.C., Lu, P., Marrison, S.T., Norris, J.S., and Liu, X. 2013. Acid Ceramidase Promotes Nuclear Export of PTEN through Sphingosine 1-Phosphate Mediated Akt Signaling. *PLoS One* 8:e76593. PMID: 24098536

The training supported by this award has resulted in successful completion of requirements for the trianee's PhD in June 2013.

**Conclusions:**

We have described a pathway by which AC promotes oncogenic Akt signaling through S1P signaling. Several aspects of this pathway are novel including the tumor promoting function of S1PR2, which is often described as a tumor suppressor. We have also concluded that AC promotes PTEN nuclear export via an Akt-S6K-Crm1 mechanism. This was found to be tumor promoting, as enforced nuclear expression of PTEN prevented AC from promoting resistance to Docetaxel and proliferation of prostate cancer cells.

**Supporting Data**

- See attached manuscripts

OPEN

Citation: Oncogenesis (2013) **2**, e49; doi:10.1038/oncsis.2013.14

www.nature.com/oncsis

ORIGINAL ARTICLE

# Acid ceramidase induces sphingosine kinase 1/S1P receptor 2-mediated activation of oncogenic Akt signaling

TH Beckham[1], JC Cheng[1], P Lu[1], Y Shao[2], D Troyer[3,4], R Lance[5], ST Marrison[1], JS Norris[1] and X Liu[1]

Acid ceramidase (AC) is overexpressed in most prostate tumors and confers oncogenic phenotypes to prostate cancer cells. AC modulates the cellular balance between ceramide, sphingosine and sphingosine 1-phosphate (S1P). These bioactive sphingolipids have diverse, powerful and often oppositional impacts on cell signaling, including the activation status of the oncogenic kinase Akt. Our studies show that AC expression correlates with phosphorylation of Akt in human prostate tumors, and elevation of phosphorylated Akt in tumor versus patient-matched benign tissue is contingent upon AC elevation. Investigation of the mechanism for AC-induced Akt activation revealed that AC activates Akt through sphingosine kinase 1 (SphK1)-derived generation of S1P. This signaling pathway proceeds through S1P receptor 2 (S1PR2)-dependent stimulation of PI3K. Functionally, AC-overexpressing cells are insensitive to cytotoxic chemotherapy, however, these cells are more susceptible to targeted inhibition of Akt. AC-overexpressing cells proliferate more rapidly than control cells and form more colonies in soft agar; however, these effects are profoundly sensitive to Akt inhibition, demonstrating increased dependence on Akt signaling for the oncogenic phenotypes of AC-overexpressing cells. These observations may have clinical implications for targeted therapy as PI3K and Akt inhibitors emerge from clinical trials.

*Oncogenesis* (2013) **2,** e49; doi:10.1038/oncsis.2013.14; published online 3 June 2013

**Subject Categories:** molecular oncology

**Keywords:** acid ceramidase; sphingosine 1-phosphate; Akt; sphingolipids; sphingosine kinase

## INTRODUCTION

AC has been shown to be overexpressed at the mRNA[1] and protein levels[2] in prostate tumors, and has been shown to mediate proliferation, chemo- and radioresistance,[3,4] and cell invasion.[5] Despite the important processes mediated by AC, the signaling mechanisms underlying these oncogenic phenotypes have been understudied. AC deacylates ceramide to form sphingosine, which can be phosphorylated by sphingosine kinase (SphK)1 or SphK2 to form sphingosine 1-phosphate (S1P).[6] These bioactive lipids have been shown to mediate numerous physiologic and pathologic processes. Ceramide has a well-studied role in Protein phosphatase 2A (PP2A)-mediated deactivation of Akt.[7] The role of sphingosine in regulating Akt is equivocal, with reports of sphingosine-induced Akt activation[8] and deactivation.[9] On the other hand, S1P has been convincingly shown to activate Akt downstream of its G protein-coupled receptors (GPCRs). A number of studies ascribe oncogenic roles to S1PR1 and 3, both of which activate Akt through $G_i$-mediated stimulation of PI3K.[10] S1PR3 also transactivates platelet-derived growth factor receptors (PDGFR) to directly stimulate PI3K.[11,12] In contrast, S1PR2 is thought to primarily couple to $G_{12/13}$ to mediate Rac/Rho-dependent inhibition of cell migration, and through Rho-mediated PTEN (phosphatase and tensin homolog) activation, antagonize Akt activation.[13] However, S1PR2 couples to $G_i$, $G_{12/13}$ and $G_q$, and thus may mediate a diverse set of signals.[14]

The present study uncovers an important oncogenic signal elicited by AC. We show that AC promotes activation of Akt through SphK1-generated S1P. Interestingly, this signal depends on S1PR2-mediated stimulation of PI3K, challenging the dogma that S1PR2 is tumor-suppressive. AC overexpression confers resistance to nontargeted chemotherapies; however, the oncogenic phenotypes of AC-overexpressing cells are uniquely sensitive to Akt inhibition. This set of observations has immediate clinical implication, as the success of nascent PI3K/Akt inhibitors is likely to depend on determining which tumors are susceptible to interdiction of this pathway, as we here suggest AC-overexpressing prostate tumors may be.

## RESULTS

### AC and phosphorylation of Akt correlate in prostate adenocarcinoma

Our previous studies have demonstrated that most prostate tumors overexpress AC, compared with benign prostate tissue.[15] As Akt activation is a common feature of many tumors, including prostate, we sought to determine whether there was a relationship between AC expression and Akt activation in the progression to prostate adenocarcinoma. Using a tissue microarray made up of prostate adenocarcinoma and patient-matched benign adjacent biopsy cores from 27 prostate cancer patients, we determined that the 22 patients whose tumor AC immunohistochemistry staining was elevated compared with their benign AC score (Figure 1a); 12 had the same trend in pAkt

[1]Department of Microbiology and Immunology, Hollings Cancer Center, Medical University of South Carolina, Charleston, SC, USA; [2]Department of Pathology and Laboratory Medicine, Medical University of South Carolina, Charleston, SC, USA; [3]Department of Pathology, Leroy T Canoles Cancer Center, Eastern Virginia Medical School, Norfolk, VA, USA; [4]Department of Microbiology and Cell Biology, Leroy T Canoles Cancer Center, Eastern Virginia Medical School, Norfolk, VA, USA and [5]Department of Urology, Leroy T Canoles Cancer Center, Eastern Virginia Medical School, Norfolk, VA, USA. Correspondence: Professor X Liu, Department of Microbiology and Immunology, Hollings Cancer Center, Medical University of South Carolina, 86 Jonathan Lucas Street, Charleston, SC 29425, USA.
E-mail: liux@musc.edu
Received 24 April 2013; accepted 26 April 2013

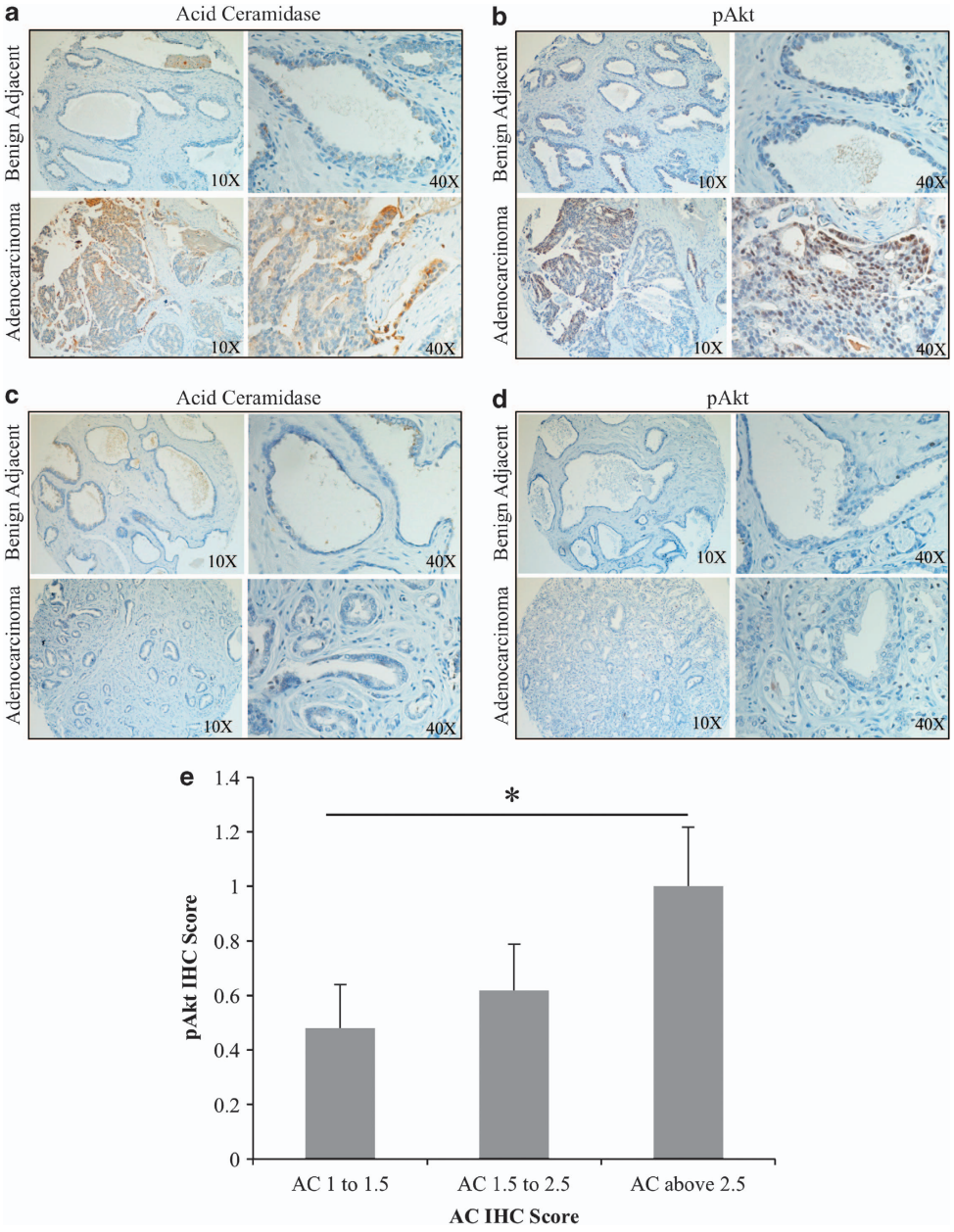


**Figure 1.** AC correlates with pAkt in prostate cancer. (**a**–**d**) A 27-patient tissue microarray with patient-matched prostate adenocarcinoma and adjacent benign tissue was immunostained for AC and pAkt (Ser473). Staining intensity was evaluated by a blinded pathologist. (**e**) A total of 56 prostate tumor biopsies were immunostained for AC and pAkt. Tumors were grouped by AC intensity as indicated in the figure, and the mean pAkt score for tumors in the indicated group is plated. *$P<0.05$, Student's *t test*.

staining (Figure 1b). Conversely, none of the five patients whose tumor AC staining was not elevated compared with their benign tissue (Figure 1c) had increased pAkt staining (Figure 1d). Analysis of these data with Fisher's exact test demonstrates that pAkt elevation from benign to tumor is contingent on AC elevation, with a *P*-value of 0.0307. In a further analysis of 56 prostate tumors immunostained for AC and pAkt, we found that tumors which scored high (above 2.5) for AC also had elevated pAkt scoring compared with AC-low (below 1.5) tumors (Figure 1e).

## AC activates Akt

The relationship between AC and Akt activation was investigated using several approaches. We stably expressed AC in PPC1 and DU145 prostate cancer cell lines and found that high levels of AC increased phosphorylation of Akt at Serine 473 compared with vector control cells, indicating activation (Figure 2a, Supplementary Figure 1A) In cells with stable short-hairpin RNA (shRNA) knockdown of AC, we observed a reduction in basal Akt phosphorylation in both DU145 and PPC1 cells versus vector control (Figure 2b, Supplementary Figure 1B). Transient adenoviral expression of AC (Ad-AC) compared with adenoviral expression of green-fluorescent protein (Ad-GFP) also revealed increased Akt phosphorylation in MIA, Panc01, SCC14A, PPC1 (Figure 2c, Supplementary Figure 1C) and DU145 (Figure 2d, Supplementary Figure 1D) cells, suggesting a generalizable phenomenon of AC-induced Akt activation in cancer. Furthermore, shRNA delivered by adenovirus (Ad-shAC) decreased pAkt (Figure 2d, Supplementary Figure 1D). In order to validate that we are observing functional signaling through Akt when we express AC, we probed for phosphoproteins downstream of Akt (Figure 2e,

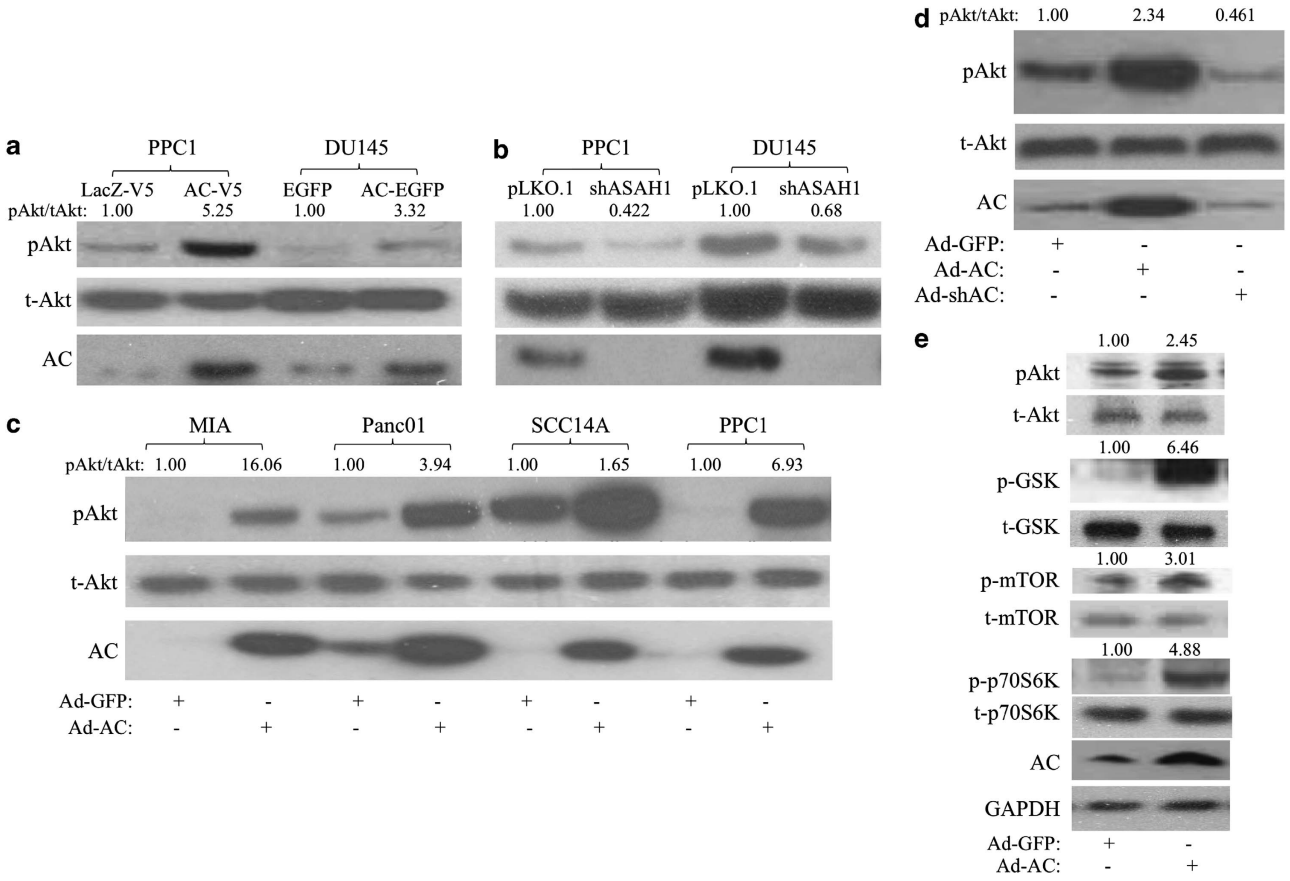


**Figure 2.** AC activates Akt. PPC1 and DU145 prostate cancer cells stably expressing (**a**) AC or control (PPC1: AC-V5 or LacZ-V5; DU145-AC-EGFP or EGFP), or (**b**) *ASAH1* antisense or empty vector (shAC or pLKO.1) were analyzed by western blotting. (**c**) MIA, Panc01, SCC14A and PPC1 cells were infected with Ad-AC or Ad-GFP. After 48 h of infection, cells were analyzed by western blotting. (**d**) DU145 cells were infected with Ad-GFP, Ad-AC or Ad-shAC. After 48 h of infection, cells were analyzed by western blotting. (**e**) PPC1 cells were infected with Ad-AC or Ad-GFP. After 48 h of infection, cells were analyzed by western blotting. pAkt/tAkt is the ratio of phosphorylated Akt to total Akt normalized to the reference (that is, Ad-GFP is the reference of Ad-AC).

Supplementary Figure 1E). We observed activation of the mammalian target of rapamycin (mTOR) pathway (p-mTOR and p-p70S6K), as well as inhibition of GSK-3beta, which is involved in regulation of cell proliferation and metabolism.[16]

### SphK1 mediates AC-induced Akt activation

The bioactive lipids ceramide, sphingosine and S1P have all been linked to the regulation of Akt. We observed no change in total cell ceramide in Ad-AC-infected PPC1 cells compared with Ad-GFP (Figure 3a), though species-specific alterations were observed (data not shown). Sphingosine and S1P were significantly elevated in Ad-AC-infected cells (Figure 3a). In order to measure secreted S1P, we treated Ad-AC/GFP-infected PPC1 cells with C17-C6 ceramide, finding significant C17-S1P increase in the cells (Supplementary Figure 2A) and medium (Supplementary Figure 2B). Treatment of cells with exogenous sphingosine did not activate Akt, rather decreasing pAkt moderately after 6 h of treatment (Figure 3b). Addition of the dual-isoform sphingosine kinase inhibitor SKI–II decreased Akt activation at 6 h, and did not augment Akt activation alone or in combination with sphingosine (Figure 3b). We then infected PPC1 cells with Ad-AC or Ad-GFP in the presence of SKI–II, and observed a dose-dependent reduction in Akt activation (Figure 3c, Supplementary Figure 1F), suggesting that sphingosine kinase activity is necessary for AC-induced Akt activation. Infection of wild-type (WT) or sphingosine kinase 2-knocked out (SphK2 KO) mouse embryonic fibroblasts (MEFs) with Ad-AC promoted strong activation of Akt, whereas AC had no impact on Akt activation in SphK1 KO MEFs (Figure 3d, Supplementary Figure 1G). Ad-AC increased S1P cell content (Supplementary Figure 2C) and secretion into the medium (Supplementary Figure 2D) in WT and SphK2 KO MEFs, but not in SphK1 KO MEFs. To confirm the observation that SphK1 may be necessary for AC-induced Akt activation, we used shRNA (Figure 3e, Supplementary Figure 1H) and small-interfering RNA (siRNA) (Figure 3f, Supplementary Figure 1I) to knock down each SphK isoform and confirmed that knockdown of SphK1, but not SphK2, abrogated AC-induced Akt activation.

### S1PR2 stimulates PI3K to activate Akt

To determine whether AC/S1P-induced Akt activation was mediated by S1PRs, we expressed AC in PPC1 cells in the presence of the S1PR1 antagonist W146, or the S1PR2 antagonist JTE013. Whereas W146 had no impact on reducing AC-induced Akt activation (Figure 4a, Supplementary Figure 1J), JTE013 strongly inhibited AC-induced Akt activation (Figure 4b, Supplementary Figure 1K). W146 was validated in Supplementary Figure 3. Similarly, AC-induced Akt activation was also prevented by JTE013 in WT MEFs, confirming that this phenomenon is intact in PTEN-positive as well as PTEN-negative (PPC1) cells (Figure 4c, Supplementary Figure 1I). When we transfected PPC1 cells with shRNA sequences against S1PR1,

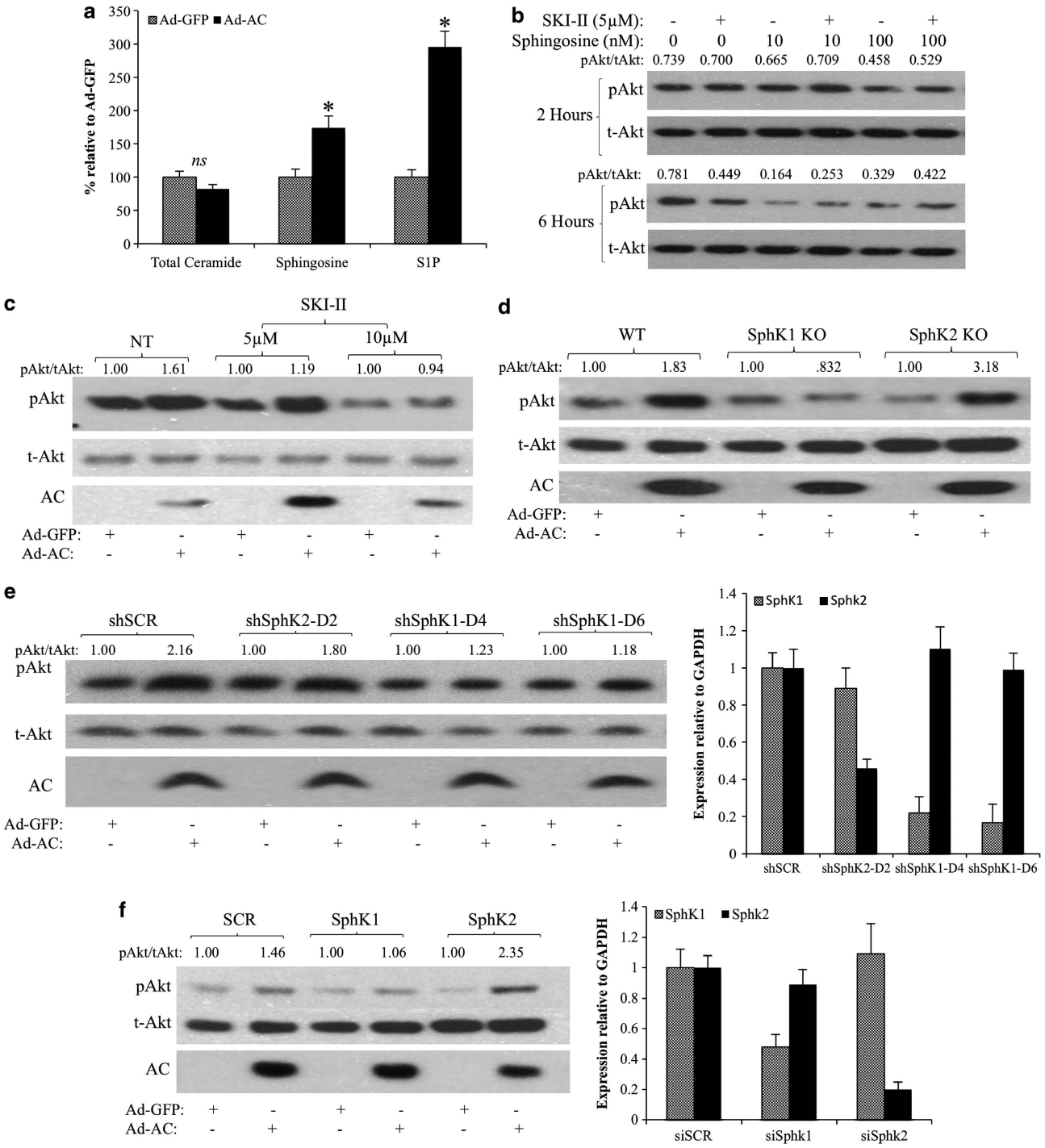


**Figure 3.** SphK1 mediates AC-induced Akt activation. (**a**) Ad-GFP- or Ad-AC-infected PPC1 cell pellets were analyzed by LC/MS for ceramide, sphingosine and S1P. Bars represent sphingolipid level relative to Ad-GFP. *$P < 0.05$ analyzed by Student's *t*-test. (**b**) PPC1 cells were treated for 2 h with the indicated dose of SphK inhibitor SKI–II or vehicle (dimethyl sulphoxide, DMSO) before treatment with the indicated doses of sphingosine or vehicle (EtOH). Cells were collected 2 or 6 h after addition of sphingosine, as indicated. pAkt/tAkt ratios were generated using NIH ImageJ band densitometries, and are represented as raw ratios so that multiple comparisons can be made. (**c**) PPC1 cells were infected with Ad-AC or Ad-GFP in the presence of the indicated dose of SKI–II. After 48 h of infection, cells were analyzed by western blotting. (**d**) WT, SphK1 KO and SphK2 KO MEFs were infected with Ad-AC or Ad-GFP at multiplicity of infection (MOI) 100. After 48 h of infection, cells were analyzed by western blotting. (**e**) PPC1 cells were transfected with nontargeting (SCR) or SphK1, or SphK2-targeting shRNA vectors. After 6 h of transfection, cells were infected with Ad-GFP or Ad-AC. After 48 h of infection, cells were analyzed by western blotting and qRT–PCR. (**f**) PPC1 cells were transfected with nontargeting (SCR) or SphK1, or Sphk2-targeting siRNA. After 6 h of transfection, cells were infected with Ad-GFP or Ad-AC. After 48 h of infection, cells were analyzed by western blotting and qRT–PCR.

S1PR2 or S1PR3, Ad-AC-induced Akt activation was unaffected in multiple S1PR1- and 3-knocked down cells, despite 60–70% reduction in mRNA (Figure 4d, Supplementary Figures 1M and 6). Both S1PR2 shRNA sequences greatly reduced Ad-AC-induced Akt activation, confirming a prominent role for S1PR2 signaling in the activation of Akt downstream of AC. As the observation that S1PR2

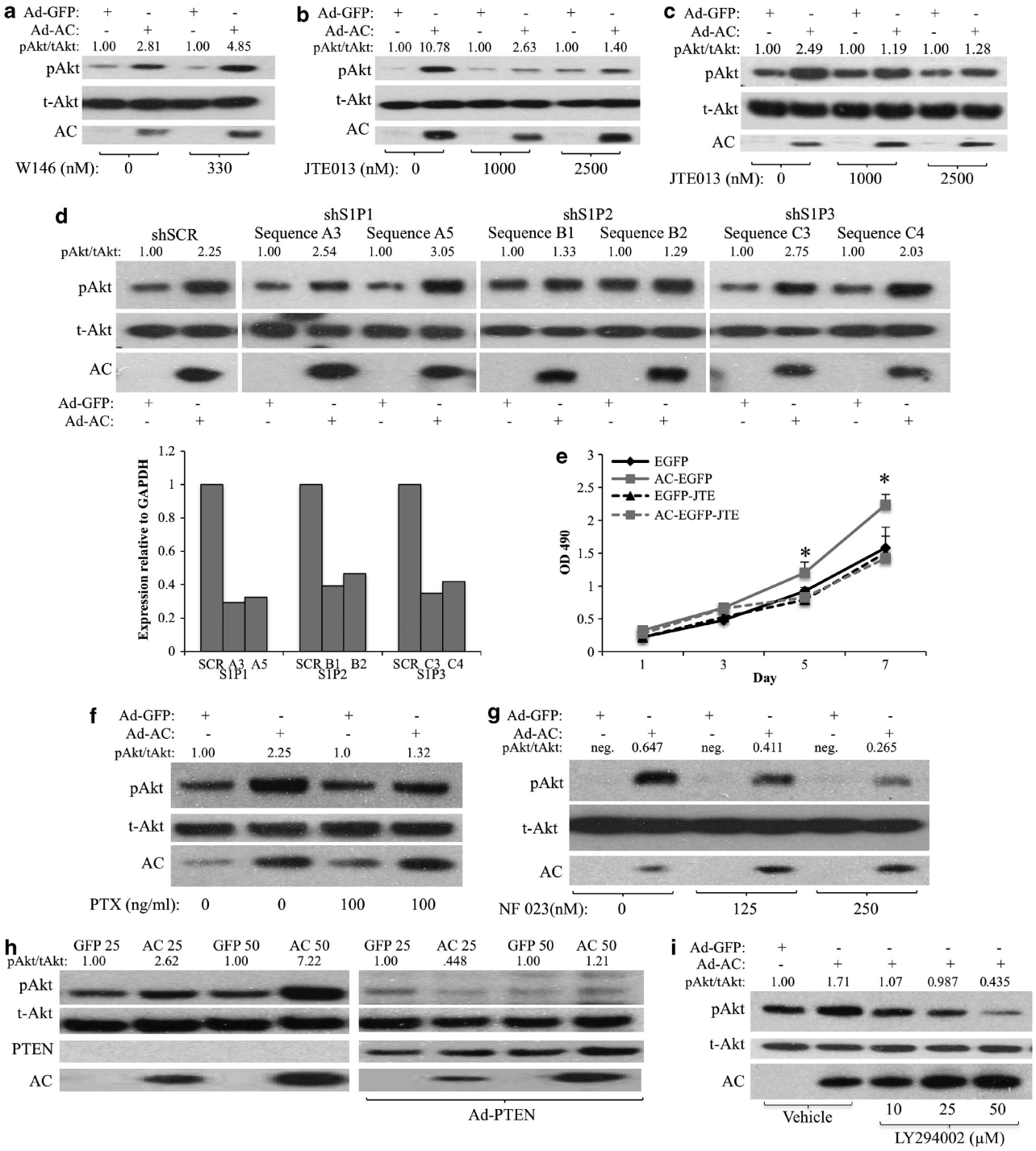


**Figure 4.** S1PR2 stimulates PI3K to activate Akt. (**a** and **b**) PPC1 cells were infected with Ad-AC or Ad-GFP. After 6 h, cells were treated with the indicated dose of either (**a**) W146 or (**b**) JTE013. After 48 h of infection, cells were analyzed by western blotting. (**c**) WT MEFs were infected with Asd-AC or Ad-GFP (MOI 100). After 6 h, cells were treated with the indicated dose of JTE013. After 48 h, cells were collected for western blotting. (**d**) PPC1 cells were transfected with nontargeting (SCR) or S1PR1–3-targeting shRNA vectors. After 6 h of transfection, cells were infected with Ad-GFP or Ad-AC. After 48 h of infection, cells were analyzed by western blotting and qRT–PCR. (**e**) DU145 EGFP and AC-EGFP cells were plated at low density in 96-well plates in the presence or absence of 1 μM JTE013, and analyzed by MTS assay on the indicated days. Statistical analysis was performed using a one-way ANOVA with Bonferroni correction, $^*P<0.05$. PPC1 cells were infected with Ad-AC or Ad-GFP. After 24 h, cells were treated with the indicated dose of (**f**) pertussis toxin, (**g**) NF023 and (**i**) LY294002. After another 24 h, cells were analyzed by western blotting. (**h**) PPC1 cells were coinfected with Ad-AC or Ad-GFP and Ad-PTEN (MOI 20), as indicated; after 48 h cells were analyzed by western blotting.

activates an oncogenic signaling pathway challenges the dogma on the role of S1PR2 in cancer cell signaling, we performed a proliferation experiment and found that the proliferation advantage of AC-overexpressing prostate cancer cells is diminished by treatment with JTE013 (Figure 4e). Basal S1PR1–3 expression was evaluated in PPC1 and DU145, both of which

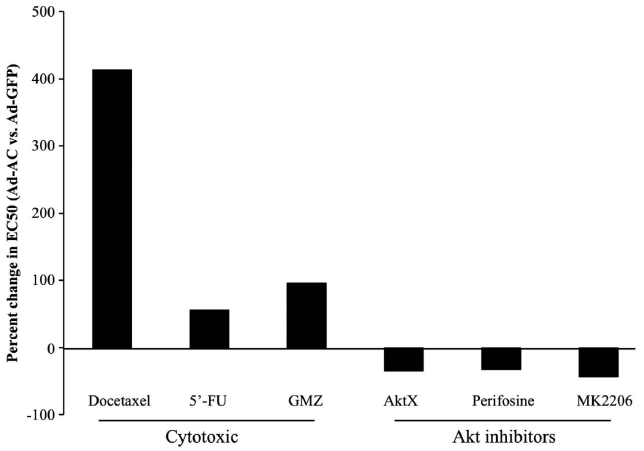


**Figure 5.** AC promotes chemotherapy resistance, but confers sensitivity to Akt inhibition. (**a**) PPC1 cells infected 24 h prior with Ad-GFP, or Ad-AC were treated with various doses of the indicated compounds. After 48 h, cell viability was measured by MTS assay. Prism software was used to calculate the EC50 of each compound (Table 1) and the EC50 of Ad-AC-infected cells was compared with that of Ad-GFP-infected cells to determine the percent change in EC50 of Ad-AC-infected cells.

had predominate S1PR2 mRNA with markedly less S1PR1 and 3 (Supplementary Figure 4A). Further analysis revealed that S1PR2 mRNA is induced slightly (1.3–2 fold), but significantly, upon AC expression (Supplementary Figure 4B), whereas the other ceramidases are not affected by AC expression, except for a reduction in ACER1 mRNA in PPC1 (Supplementary Figure 4C). S1PRs are GPCRs known to stimulate Akt activation by activating $G_i$-mediated stimulation of PI3K. Pertussis toxin, which inactivates $G_i$, $G_0$ and $G_t$, prevented AC-induced Akt activation (Figure 4f Supplementary Figure 1N), and the $G_i$ inhibitor NF023 abrogated AC-induced Akt activation (Figure 4g), suggesting a role for G proteins, specifically $G_i$, in AC-induced Akt activation. Expressing PTEN in PPC1 cells antagonized AC-induced Akt activation (Figure 4h, Supplementary Figure 1O), and the PI3K inhibitor LY294002 effected dose-dependent abrogation of pAkt (Figure 4i, Supplementary Figure 1P), supporting an S1PR2, PI3K-dependent mechanism. To test whether exogenous S1P works in the same way on these cell lines, we treated PPC1 and DU145 with 500 nM S1P for 2 h in the presence or absence of JTE013 (Supplementary Figure 5). JTE013 blocked S1P-induced Akt activation in both cell lines, supporting the findings using AC expression to drive increased S1P signaling.

### AC promotes chemotherapy resistance, but confers sensitivity to Akt inhibition

Cytotoxic chemotherapy depends, in part, on ceramide accumulation to cause cell death.[17–19] PPC1 cells were subjected to a wide dose range of the cytotoxic chemotherapeutic agents Docetaxel, Gemcitabine and 5′-Fluorouracil. PPC1 cells infected with Ad-AC were found to be less sensitive to all the three compounds (Docetaxel: 413%, Gemcitabine: 55% and 5′-Fluorouracil: 96% less sensitive), reflected by an increased EC50 (Figure 5, Table 1). Conversely, AC-overexpressing cells were more sensitive to inhibition of Akt with Akt inhibitor X (AktX), Perifosine or MK2206, with AC-expressing cells being ~30–40% more sensitive than Ad-GFP-infected cells.

### Proliferation in AC-overexpressing cells is profoundly sensitive to Akt inhibition

Akt signaling promotes cancer in numerous ways, including increased cell proliferation. To determine whether AC-induced proliferation is Akt-dependent, we evaluated prostate cancer cell proliferation in the presence of AktX and Perifosine. In DU145-AC-EGFP cells stably expressing AC, we noted significantly more rapid cell proliferation compared with the vector control (Figure 6a). Treatment with AktX (Figure 6a) and Perifosine (Figure 6c) both reduced proliferation in AC-EGFP and EGFP cell lines. However, directly comparing cell number on day 7 revealed that AktX and Perifosine more strongly inhibited proliferation in AC-EGFP cells (Figures 6b and d). EGFP cell proliferation was reduced 30% (AktX) and 52% (Perifosine), whereas AC-EGFP cell proliferation was reduced 52% (AktX) and 91% (Perifosine). The same effect was observed in PPC1 cells infected with Ad-AC, in which AktX inhibited cell proliferation 52%, in contrast to Ad-GFP-infected cells, which had no significant reduction in cell number compared with untreated cells (Figures 6e and f).

**Table 1.** EC50 of various compounds

| | *Ad-GFP* | *Ad-AC* |
|---|---|---|
| Docetaxel (nM) | 1.89 | 9.74 |
| 5′-Fu (μM) | 4.36 | 6.8 |
| GMZ (μM) | 31.8 | 62.45 |
| AktX (μM) | 13.7 | 8.92 |
| Perifosine (μM) | 29.54 | 19.89 |
| MK 2206 (μM) | 3.5 | 1.97 |

Abbreviations: AC, acid ceramidase; Ad-AC, adenoviral expression of AC; 5′-Fu, Fluorouracil, GMZ, Gemcitabine.

### AC-induced Akt signaling promotes soft agar-colony formation

Anchorage-independent growth is a hallmark of oncogenic potential. PPC1 cells infected with Ad-AC formed more colonies on soft agar compared with Ad-GFP-infected cells (Figures 7a and c). Interestingly, while inhibition of Akt signaling with AktX and JTE013, the S1PR2 antagonist did not have an impact on soft agar-colony formation in Ad-GFP-infected PPC1 cells, Ad-AC-infected cells were sensitive to both Akt inhibition and S1PR2 antagonism, consistent with the hypothesis that AC-induced Akt activation is oncogenic. Similarly, when cells were infected with an adenovirus delivering an anti-AC short hairpin, Ad-shASAH1, fewer colonies were formed than when cells were infected with nontargeting shRNA (Figures 7b and d).

## DISCUSSION

AC occupies a powerful position in the balance between ceramide, sphingosine and S1P. As AC is frequently overexpressed in prostate cancer and multiple other malignancies,[15,20,21] understanding the dominant downstream signaling consequences of the impact of AC on the ceramide–sphingosine–S1P balance is of great interest. AC expression did not reduce total ceramide, as one might predict; however, species-specific alterations were prominent, particularly reduced C16 ceramide and increased C24 and C24:1 (data not shown). The lack of impact on total ceramide diminished the likelihood that alterations in ceramide-mediated PP2A signaling were responsible for increased Akt activation. Literature on the direct impact of sphingosine on Akt activation is sparse. One report demonstrated in hepatoma cells that exogenous sphingosine promoted apoptosis by decreasing serum-stimulated Akt activation.[22] This is consistent with our observation of exogenous sphingosine decreasing pAkt; however, we cannot conclude whether this is a direct role for sphingosine, as it is a substrate of both SphKs and ceramide synthases. Of interest, AC was shown to drive sphingosine-mediated activation of Akt in alveolar macrophages.[8] Several observations in this study pointed to a direct functional role for sphingosine. However, AC-mediated

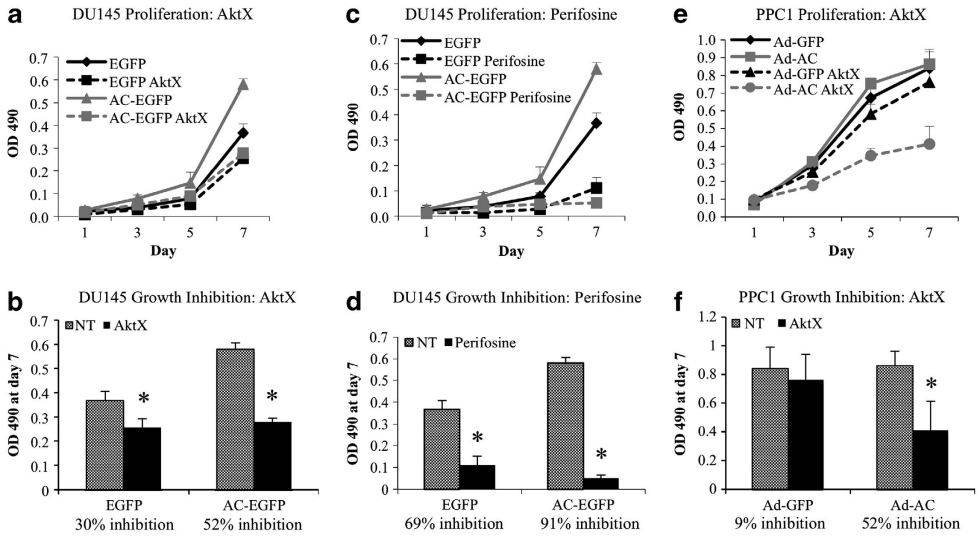


**Figure 6.** Proliferation in AC-overexpressing cells is profoundly sensitive to Akt inhibition. (**a**, **c**, **e**) 500 cells were plated on 96-well plates of DU145-AC-EGFP and EGFP (**a**, **c**), or PPC1 cells infected with Ad-GFP or Ad-AC (**e**). After overnight cell attachment, cells were treated with 2.5 μM AktX (**a**, **e**) or 5 μM Perifosine (**c**). On the indicate day, MTS assay was used to determine relative cell proliferation. (**b**, **d**, **f**) OD 490 values on day 7 were compared and used to calculate the percent inhibition in cell proliferation in each cell type by the indicated compound. *$P < 0.05$ calculated by the Student's *t*-test.

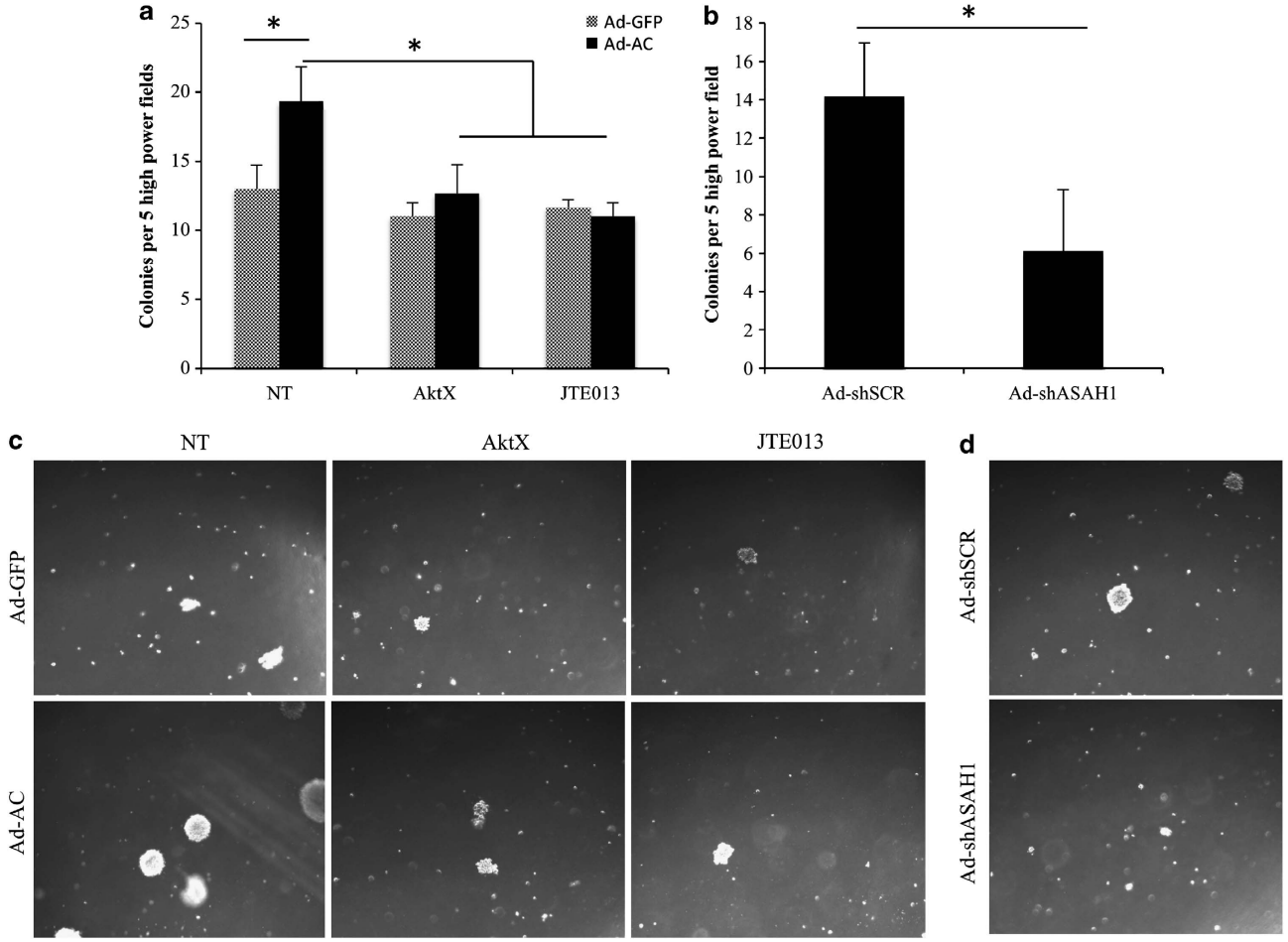


**Figure 7.** AC-induced Akt signaling promotes soft agar-colony formation. (**a**, **b**) PPC1 cells were infected with Ad-GFP, Ad-AC (MOI 50), Ad-shSCR or Ad-shASAH1 (MOI 20) 1 day prior to plating on six-well plates in a total volume of 4 ml soft agar. (**a**) Four hours after plating, 5 μM JTE013, 10 μM AktX or vehicle (DMSO) was added in 1 ml complete medium. Colonies, represented in (**c**, **d**), were counted 2 weeks after plating.

Akt signaling was not studied in the context of genetic manipulation or inhibition of SphK, which would have provided strength to the authors' conclusions. In the present study, no role for sphingosine in activating Akt could be demonstrated. Moreover, it appears that treatment with sphingosine caused deactivation of Akt. One explanation for this is feedback inhibition of AC by exogenous sphingosine, which would lead not only to a reduction of S1P, but also an increase in ceramide, whose role in PP2A-dependent deactivation of Akt is well studied. Salvage generation of ceramide by ceramide synthases could also account for the deactivation of Akt upon addition of exogenous sphingosine.[23]

Our data implicate S1P in mediating activation of Akt in the context of AC expression. The vast majority of S1P-mediated phenomena have been attributed to the signaling of its five GPCRs, S1PR1–5. S1PR 4 and 5 are relatively restricted in their expression to the immune system (S1PR4) and the nervous system (S1PR5).[24] S1PR1–3 are ubiquitously expressed, and have numerous roles in diverse phenomena. S1P is characterized to mediate $G_i$ stimulation of PI3K, and thereby cause activation of Akt as well as MAPK signaling. These effects have been associated with S1PR1 and, to a lesser degree, with S1PR3, and both receptors have been shown to enhance cell proliferation and migration through Rac activation.[25–28] In contrast, S1PR2 is thought to predominantly couple with $G_{12/13}$,[24,29] and thereby antagonize Akt activation by Rho-mediated recruitment of PTEN to the cell membrane.[13] This effect, coupled with its suppression of Rac activity, has resulted in S1P2 being designated as an antimigratory, antiproliferative receptor, which largely opposes the oncogenic signaling of S1PR1 and 3. The present study breaks this dogma by showing that S1PR2 can activate oncogenic Akt signaling in prostate cancer. It is important to note that S1PR2 couples to $G_i$, $G_{12/13}$ and $G_q$, with effects of $G_{12/13}$ predominating in many functional assays. In our study, interdiction of $G_i$ signaling substantially reduced AC-induced Akt activation, suggesting that S1PR2 has adopted a $G_i$ -dominant downstream signal. Interestingly, the prostate cancer cell lines studied here had far more abundant S1PR2 mRNA than S1PR1 or 3, which may explain why inhibition of S1PR2 had an strong impact on cell signaling and phenotype, however it does not explain why a typically tumor-suppressive receptor now signals to activate Akt. One hypothesis is that S1PR2 is initially upregulated in response to AC overexpression in neoplastic tissues as a means to suppress the oncogenic effects of AC. In the hyperselective tumor environment, cancer cells may evolve to favor $G_i$ signaling through S1PR2, compounding the oncogenic insult of AC by further increasing the impact of the downstream metabolite S1P. In support of this, we found that primary prostate epithelial cells had equal expression of S1PR1–3 (data not shown), suggesting that receptor expression is altered at some point during malignant transformation, although we did not observe AC-induced upregulation of S1PR2 in primary cells.

Our study clearly identifies a role for SphK1 in mediating AC-induced Akt activation, with knockout or knockdown of SphK2 having little or no effect. We believe that this may be due to the cellular localizations of the different SphK isoforms. SphK1 has been found to be primarily cytoplasmic or associated with the plasma membrane, whereas SphK2 is largely located in the nucleus or endoplasmic reticulum.[30] As AC resides in the lysosome, thus producing sphingosine primarily in this compartment, it may be that SphK1 has preferential or exclusive access to lysosomal sphingosine. We found that SphK2 KO MEFs had an increase in S1P equivalent to WT MEFs when we overexpressed AC, however SphK1 KO MEFs had no increase in S1P, consistent with this hypothesis.

The observations in this study that AC promotes resistance to cytotoxic chemotherapies but sensitivity to agents that target Akt demonstrate important differences of the diverse functions mediated by AC. An exceedingly common and critical event in cell death in response to nonspecific stressors like radiation and chemotherapy is the accumulation of ceramide, which activates apoptosis through well-characterized mechanisms.[19,31] The efficacy of cytotoxic chemotherapies in this and previous studies have been shown to be lessened by expression of AC, presumably by dampening the accumulation of ceramide and thus downstream apoptotic signals.[3] In contrast, targeted inhibition of Akt proves especially effective in cells overexpressing AC, indicating that AC-overexpressing cancer cells, and thus potentially AC-overexpressing tumors, are reliant on oncogenic Akt activation through the pathway defined in this study for their oncogenic phenotypes. Chemotherapy for hormone-refractory prostate cancer is currently limited to Docetaxel, which provides minimal benefit.[32] Biopsy-based diagnostic methods could be readily adapted for evaluation of AC expression and Akt activation, potentially informing treatment decisions in the near future as PI3K and Akt inhibitors enter clinical use. Thus, while AC contributes to death resistance in the context of diverse cell stressors such as radiation and chemotherapy by attenuating ceramide accumulation, the identification in this study of AC-mediated Akt activation provides critical insight into specific susceptibilities downstream of AC that could inform future clinical decisions.

Akt signaling promotes proliferation indirectly by activating the mTOR pathway that controls translation of peptides necessary for cell growth, and directly by phosphorylating multiple cyclin-dependent kinase inhibitors.[33] Our study of the functional consequences of AC-induced Akt signaling reveals three important observations: (1) AC-expressing cells proliferate more rapidly, (2) AC promotes soft agar-colony formation and (3) these oncogenic phenotypes are profoundly sensitive to Akt inhibition. That AC promotes cell proliferation is not surprising, given the signaling mechanism outlined in this study—Akt phosphorylates Wee1 and Myt1 both of which promote mitotic entry by activating cdc2,[34–36] and Akt directly inactivates the cyclin-dependent kinase inhibitor p27kip1 whose inactivation allows transition from G1/S.[37] More interesting is the finding that AC-overexpressing cells are more sensitive to Akt inhibition with regards to these functional assays than are controls cells. This indicates that AC-overexpressing cells not only rely heavily on Akt signaling for the growth advantages incurred by increased AC signaling, but also for their baseline cell proliferation and tumor formation properties, on the whole suggesting that AC expression causes Akt signaling pathway addiction.

The importance of the pathway outlined in this study is made clear by our tissue microarray studies of human prostate cancer patients. Our ability to study the pattern of expression of AC and pAkt in prostate tumors, and patient-matched benign tissue was critical in understanding whether a statistical relationship existed between AC and pAkt. Simply put, due to the numerous factors that contribute to Akt activation, a prohibitively large sample size would have been required to demonstrate a direct correlation between AC level and phosphorylation of Akt. Instead, we were able to show that when a patient's tumor had more AC than his benign tissue, pAkt tended to increase as well. In patients whose AC did not increase in their tumors, pAkt was not elevated. Analyzing these tissues in a contingency table revealed that a statistically meaningful relationship does exist between AC and pAkt in the benign to adenocarcinoma progression of human prostate tissue. In an analysis of 56 patients' tumors, grouping AC immunohistochemistry score into low-, middle- and high-intensity staining groups revealed that pAkt scores were significantly higher in the AC-high versus AC-low groups, providing more evidence that AC-induced Akt activation is a relevant process in human prostate cancer.

In summary, the present study uncovers a mechanistic basis for oncogenic processes mediated by AC. Cancer cells

expressing high levels of AC have increased activated Akt. This is due to generation of S1P by Sphk1, which stimulates S1PR2 to effect PI3K-dependent Akt activation. Moreover, whereas AC-overexpressing cells are resistant to cytotoxic chemotherapy, proliferate more rapidly and exhibit enhanced anchorage-independent growth compared with control cells, they are significantly more sensitive to Akt inhibition. As most prostate tumors overexpress AC and as we show here a correlation between AC and Akt activation in human prostate biopsy tissue, Akt addiction in AC-overexpressing tumors may inform targeting of specific cancers with nascent Akt inhibitors.

## MATERIALS AND METHODS

### Cell lines and culture

PPC1 (a gift of Dr Yi Lu, University of Tennessee), SCC14A (shared by Dr Besim Ogretmen, Medical University of South Carolina), MIA, Panc01 and DU145 (ATCC, Manassas, VA, USA) were maintained in RPMI 1640 with 10% bovine growth serum (BGS) and incubated in 5% $CO_2$ at 37 °C. WT, SphK1 KO and SphK2 KO MEFs (shared by Dr Besim Ogretmen) were cultured in DMEM with 10% fetal bovine serum and incubated in 5% $CO_2$ at 37 °C. DU145-AC-EGFP/DU145-EGFP and PPC1-AC-V5/PPC1-LacZ-V5 have been described.[3,5] PPC1 pLKO.1/pLKO.1-shAC were generated by transfection of vectors obtained from Open Biosystems (Huntsville, AL, USA), and stable selection was done with puromycin.

### Reagents

Synthesis of sphingosine (2-amino-4-octadecene-1,3-diol) and 17C-C6-ceramide were conducted in the Lipidomics Shared Resource. Reagents used include: SKI–II, Docetaxel (Thermo Fisher, Lafayette, CO, USA), LY294002, Wortmannin, AktX (Cayman Chemical, Ann Arbor, MI, USA), W146, JTE013, NF023 (Tocris, Bristol, UK), Perifosine (BioVision, Milpitas, CA, USA) and pertussis toxin (Sigma Aldrich, St Louis, MO, USA).

### Preparation of tumor tissue microarray

Twenty-seven formalin-fixed paraffin-embedded prostate carcinomas were obtained from the Hollings Cancer Center Tissue Biorepository (Medical University of South Carolina). Tissues were obtained in accordance with an Institutional Review Board approved protocol (no. 426). Three tissue cores were sampled from each tumor, and one core was sampled from adjacent normal tissue. Four-micrometer sections of the tissue microarray were cut and processed for immunohistochemistry. Furthermore, human prostate tissues from the Eastern Virginia Medical School, assembled as described,[38] were immunostained as described below.

### Immunohistochemistry

Formalin-fixed paraffin-embedded sections were deparaffinized in xylene, rehydrated in alcohol and processed for pretreatment as follows: the sections were incubated with target retrieval solution (Dako, Glostrup, Denmark) in a steamer (Rival, Mill Valley, CA, USA) for 45 min, and then 3% hydrogen peroxide solution for 10 min and protein block (Dako) for 20 min at room temperature. Primary antibody incubation overnight in a humid chamber at 4 °C, followed by biotinylated secondary antibody (Vector, Burlingame, CA, USA) for 30 min and ABC reagent (Vector) for 30 min. Immunocomplexes of horseradish peroxidase were visualized by DAB (Dako) reaction, and sections were counterstained with hematoxylin before mounting. Immunoreactivity was scored using a semiquantitative system, combining intensity of staining (0–3) and percentage of cells staining positive (0–3).

### Adenovirus infection

AC complementary DNA was purchased from Origene (Rockville, MD, USA) and Ad-AC (adenovirus expressing AC and GFP), and Ad-GFP were developed by Vector Biolabs (Philadelphia, PA, USA). Ad-PTEN was purchased from Vector Biolabs. The short-hairpin sequence (5′-CCGGGCTGTTATTGACAGCGATATACTGAGTATATCGCTGT CAATAACAGCTTTTT-3′) obtained from Open Biosystems was validated and developed into an adenoviral delivery vector (Ad-shAC) by Vector Biolabs. A total of $2 \times 10^5$ cells were infected in suspension in growth medium and plated on 35-mm dishes. Multiplicity of infection was 50, unless stated otherwise in the figure legend. After overnight attachment, infection was verified by fluorescent microscopy, and the medium was replaced to contain the indicated treatments. For infections following si/shRNA transfection, medium was replaced 24 h after transfection to contain the indicated adenovirus.

### Transfections

Dharmacon siGENOME SMART POOL siRNA against SphK1 and SphK2 were purchased from Thermo Fisher, and nontargeting siRNA was purchased from Qiagen (Valencia, CA, USA). siRNA transfections were performed using Oligofectamine (Qiagen) according to the manufacturer's instructions. The following MISSION shRNA sequences were obtained from Sigma Aldrich encoded in pLKO.1 vectors.

| | |
|---|---|
| SCR | 5′-CCGGGCGCGATAGCGCTAATAATTTCTCGAGAAA TTATTAGCGCTATCGCGCTTTTT-3′ |
| SphK1-D4 | 5′-CCGGGCAGCTTCCTTGAACCATTATCTCGA GATAATGGTTCAAGGAAGCTGCTTTTTG-3′ |
| SphK1-D6 | 5′-CCGGCGCTGTGCCTTAGTGTCTACTCTCGAG AGTAGACACTAAGGCACAGCGTTTTTG-3′ |
| SphK2-D2 | 5′-CCGGCTTCGTGTCAGATGTGGATATCTCGAGA TATCCACATCTGACACGAAGTTTTTG-3′ |
| S1PR1-A3 | 5′-CCGGCCACAAGCACTATATCCTCTTCTCG AGAAGAGGATATAGTGCTTGTGGTTTTT-3′ |
| S1PR1-A5 | 5′-CCGGGACAAGGAGAACAGCATTAA ACTCGAGTTTAATGCTGTTCTCCTTGTCTTTTT-3′ |
| S1PR2-B1 | 5′-CCGGAGGTCCAGGAACACTATAATTCTCGA GAATTATAGTGTTCCTGGACCTTTTTT-3′ |
| S1PR2-B2 | 5′-CCGGCCTCTCTACGCCAAGCATTATCTCG AGATAATGCTTGGCGTAGAGAGGTTTTT-3′ |
| S1PR3-C3 | 5′-CCGGGCGGCACTTGACAATGATCAACTC GAGTTGATCATTGTCAAGTGCCGCTTTTT-3′ |
| S1PR3-C4 | 5′-CCGGCATCGCTTACAAGGTCAACATCTCGAG ATGTTGACCTTGTAAGCGATGTTTTT-3′ |

These were transfected using Lipofectamine 2000 (Life Technologies, Carlsbad, CA, USA), according to the manufacturer's instructions.

### qRT–PCR

si/shRNA knockdown validation was carried out by isolation of RNA using TRI Reagent (Molecular Research Center, Cincinnati, OH, USA) and complementary DNA synthesis using the Bio-Rad (Hercules, CA, USA) iScript complementary DNA synthesis kit, according to the manufacturer's instructions. qRT–PCR was performed by using iCycler iQ real-time PCR detection system (Bio-Rad) using annealing temperature 58 °C and the following primers:

Sphk1: forward-5′-TGAGCAGGTCACCAATGAAG-3′; reverse-5′-TGTGCAGA GACAGCAGGTTC-3′

SphK2: forward-5′-GGAGGAAGCTGTGAAGATGC-3′; reverse-5′-GCAACA GTGAGCAGTTGAGC-3′

S1PR1: forward-5′-GAAGGGGGAGAATACGAACA-3′; reverse-5′-GCCAAAT GAACCCTTTAGGA-3′

S1PR2: forward-5′-CACCTGGAAAGGCCAGATAA-3′; reverse-5′-CAGTGCAA GATTCCGTCTCA-3′

S1PR3: forward-5′-GCCGACGGAGGAGCCCTTTTTC-3′; reverse-5′-ATGCTC CCGCAGGGTCTCGTT-3′

ACER1: forward-5′-GCCTAGCATCTTCGCCTATCAG-3′; reverse-5′-GGAAGT TGCTCTCACACCAGTC-3′

ACER2: forward-5′-AGTGTCCTGTCTGCGGTTACG-3′; reverse-5′-TGTTGTTG ATGGCAGGCTTGAC-3′

ACER3: forward-5′-TGGACTGGTGCGAGGAGAAC-3′; reverse-5′-TCCAGAA CTCGGCGATGTACC-3′

ASAH2: forward-5′-TTACCCTTGGGTCCTTGGCCATAA-3′; reverse-5′-TCTGC CACGATGTTGAAGTAGCCT-3′

GAPDH: forward-5′-CAATGACCCCTTCATTGACC-3′; reverse-5′-GATCTCGC TCCTGGAAGATG-3′

### Western blotting

Cell lysates were prepared and analyzed as previously described,[4] using the following antibodies: pAkt (D9E, no. 4060), total Akt (C67E7, no. 4691), p-mTOR S2448, no. 2971), p-4E-BP1 (236B4, no. 2855), p-P70S6K (108D2, no. 9234), p-GSK-3beta (S9, no. 9336), Erk1/2 (137F5, no. 4695), p-Erk1/2 (197G2, no. 4377) and PTEN (138G6, no. 9559) (Cell Signaling

Technologies, Danvers, MA, USA), AC (BD Transduction no. 612302), S1P1 (H-60, Santa Cruz Biotechnology, Santa Cruz, CA, USA), S1P2 (6E8.1, Millipore, Billerica, MA, USA) and S1P3 (no. PA5-28762, Pierce, Rockford, IL, USA). Band densitometries were quantified using NIH ImageJ software (Bethesda, MD, USA). Unless otherwise stated, pAkt/tAkt ratios are represented normalized to the reference (set at 1.00) to allow rapid evaluation of increases or decreases from control. Western blots are representative of a minimum of three independent experiments.

### Cell viability assays

A total of 5000 cells per well were infected with Ad-AC or Ad-GFP and plated in 96-well plates. After overnight attachment, medium containing the indicated compound was added. For each compound tested, a broad dose range was selected encompassing doses effecting little to complete cell death. After 48 h, the Promega CellTiter 96 AQueous One Solution Cell Proliferation Assay (MTS) (Promega, Madison, WI, USA) was used to approximate the number of viable cells. Prism v4 (GraphPad, La Jolla, CA, USA) was used to determine the EC50 of the various compounds.

### Proliferation

A total of 500 cells were plated per well in 96-well plates. After overnight attachment, medium containing the indicated compound was added to the indicated final concentration. On the indicated day (day 1 being the day after plating), the Promega CellTiter 96 AQueous One Solution Cell Proliferation Assay (MTS) was used to approximate the number of viable cells. All readings were performed 1 h after addition of assay reagent.

### Soft agar-colony-formation assay

A base layer composed of 2 ml 0.5% agar, 10% serum and 1 × RPMI was prepared in six-well plates. A top layer was prepared to a final composition of 0.35% agar, 10% serum and 1 × RPMI, with 2500 cells per 2 ml. This layer was prepared at 40 °C and plated on top of the base layer. After 4 h at 37 °C, 1 ml complete medium containing the indicated compound was carefully added to the top of each well. In 2 weeks, colony formation was analyzed by counting the number of colonies per × 100 microscope field. Five fields were counted for each well, and the average of three wells was used to generate data.

### Sphingolipid analysis

Ceramide species, sphingosine and S1P from cell pellets were collected and analyzed with LC-MS/MS by the Lipidomics Shared Resource, MUSC, as previously described.[4]

### Statistical analysis

Independent experiments were performed a minimum of three times. Statistical analyses on experiments performed in triplicate were performed by unpaired one-tailed Student's *t*-test, one-way analysis of variance with Bonferroni correction using Prism (version 4.0) from GraphPad, or Fisher's exact test. $^*P < 0.05$ was considered significant.

## CONFLICT OF INTEREST

The authors declare no conflict of interest.

## ACKNOWLEDGEMENTS

PPC1 cells were a kind gift from Dr Yi Lu, University of Tennessee. WT, SphK1 and SphK2 KO MEFs were a kind gift of Dr Besim Ogretmen, Medical University of South Carolina. Grant support provided by the Department of Defense PCTA PC101962 and NCI 5P01CA097132, and Award Number UL1RR029882 from the National Center For Research Resources. Research supported in part by the Lipidomics Shared Resource, Hollings Cancer Center, Medical University of South Carolina (P30 CA138313) and the Lipidomics Core in the SC Lipidomics and Pathobiology COBRE (P20 RR017677).

## REFERENCES

1 Seelan RS, Qian C, Yokomizo A, Bostwick DG, Smith DI, Liu W. Human acid ceramidase is overexpressed but not mutated in prostate cancer. *Genes Chromosomes Cancer* 2000; **29**: 137–146.
2 Norris JS, Bielawska A, Day T, El-Zawahri A, Elojeimy S, Hannun Y *et al.* Combined therapeutic use of AdGFPFasL and small molecule inhibitors of ceramide metabolism in prostate and head and neck cancers: a status report. *Cancer Gene Ther* 2006; **13**: 1045–1051.
3 Saad AF, Meacham WD, Bai A, Anelli V, Elojeimy S, Mahdy AE *et al.* The functional effects of acid ceramidase overexpression in prostate cancer progression and resistance to chemotherapy. *Cancer Biol Ther* 2007; **6**: 1455–1460.
4 Mahdy AE, Cheng JC, Li J, Elojeimy S, Meacham WD, Turner LS *et al.* Acid ceramidase upregulation in prostate cancer cells confers resistance to radiation: AC inhibition, a potential radiosensitizer. *Mol Ther* 2009; **17**: 430–438.
5 Beckham TH, Lu P, Cheng JC, Zhao D, Turner LS, Zhang X *et al.* Acid ceramidase-mediated production of sphingosine 1-phosphate promotes prostate cancer invasion through upregulation of cathepsin B. *Int J Cancer* 2012; **131**: 2034–2043.
6 Ogretmen B, Hannun YA. Biologically active sphingolipids in cancer pathogenesis and treatment. *Nat Rev Cancer* 2004; **4**: 604–616.
7 Schubert KM, Scheid MP, Duronio V. Ceramide inhibits protein kinase B/Akt by promoting dephosphorylation of serine 473. *J Biol Chem* 2000; **275**: 13330–13335.
8 Monick MM, Mallampalli RK, Bradford M, McCoy D, Gross TJ, Flaherty DM *et al.* Cooperative prosurvival activity by ERK and Akt in human alveolar macrophages is dependent on high levels of acid ceramidase activity. *J Immunol* 2004; **173**: 123–135.
9 Thayyullathil F, Chathoth S, Shahin A, Kizhakkayil J, Hago A, Patel M *et al.* Protein phosphatase 1-dependent dephosphorylation of Akt is the prime signaling event in sphingosine-induced apoptosis in Jurkat cells. *J Cell Biochem* 2011; **112**: 1138–1153.
10 Radeff-Huang J, Seasholtz TM, Matteo RG, Brown JH. G protein mediated signaling pathways in lysophospholipid induced cell proliferation and survival. *J Cell Biochem* 2004; **92**: 949–966.
11 Baudhuin LM, Jiang Y, Zaslavsky A, Ishii I, Chun J, Xu Y. S1P3-mediated Akt activation and cross-talk with platelet-derived growth factor receptor (PDGFR). *FASEB J* 2004; **18**: 341–343.
12 Baudhuin LM, Cristina KL, Lu J, Xu Y. Akt activation induced by lysophosphatidic acid and sphingosine-1-phosphate requires both mitogen-activated protein kinase kinase and p38 mitogen-activated protein kinase and is cell-line specific. *Mol Pharmacol* 2002; **62**: 660–671.
13 Sanchez T, Skoura A, Wu MT, Casserly B, Harrington EO, Hla T. Induction of vascular permeability by the sphingosine-1-phosphate receptor-2 (S1P2R) and its downstream effectors ROCK and PTEN. *Arterioscler Thromb Vasc Biol* 2007; **27**: 1312–1318.
14 Means CK, Brown JH. Sphingosine-1-phosphate receptor signalling in the heart. *Cardiovasc Res* 2009; **82**: 193–200.
15 Elojeimy S, Liu X, McKillop JC, El-Zawahry AM, Holman DH, Cheng JY *et al.* Role of acid ceramidase in resistance to FasL: therapeutic approaches based on acid ceramidase inhibitors and FasL gene therapy. *Mol Ther* 2007; **15**: 1259–1263.
16 Lin CF, Chen CL, Chiang CW, Jan MS, Huang WC, Lin YS. GSK-3beta acts downstream of PP2A and the PI 3-kinase-Akt pathway, and upstream of caspase-2 in ceramide-induced mitochondrial apoptosis. *J Cell Sci* 2007; **120**: 2935–2943.
17 Ogretmen B, Hannun Y. Updates on functions of ceramide in chemotherapy-induced cell death and in multidrug resistance. *Drug Resist Updat* 2002; **4**: 368–377.
18 Charles AG, Han T-Y, Liu YY, Hansen N, Giuliano AE, Cabot MC. Taxol-induced ceramide generation and apoptosis in human breast cancer cells. *Cancer Chemother Pharmacol* 2001; **47**: 444–450.
19 Wang XZ, Beebe JR, Pwiti L, Bielawska A, Smyth MJ. Aberrant sphingolipid signaling is involved in the resistance of prostate cancer cell lines to chemotherapy. *Cancer Res* 1999; **59**: 5842–5848.
20 Musumarra G, Barresi V, Condorelli DF, Scire S. A bioinformatic approach to the identification of candidate genes for the development of new cancer diagnostics. *Biol Chem* 2003; **384**: 321–327.
21 Shah MV, Zhang R, Irby R, Kothapalli R, Liu X, Arrington T *et al.* Molecular profiling of LGL leukemia reveals role of sphingolipid signaling in survival of cytotoxic lymphocytes. *Blood* 2008; **112**: 770–781.
22 Chang HC, Tsai LH, Chuang LY, Hung WC. Role of AKT kinase in sphingosine-induced apoptosis in human hepatoma cells. *J Cell Physiol* 2001; **188**: 188–193.
23 Kitatani K, Idkowiak-Baldys J, Hannun YA. The sphingolipid salvage pathway in ceramide metabolism and signaling. *Cell Signal* 2008; **20**: 1010–1018.
24 Takuwa N, Du W, Kaneko E, Okamoto Y, Yoshioka K, Takuwa Y. Tumor-suppressive sphingosine-1-phosphate receptor-2 counteracting tumor-promoting sphingosine-1-phosphate receptor-1 and sphingosine kinase 1—Jekyll Hidden behind Hyde. *Am J Cancer Res* 2011; **1**: 460–481.

25 Okamoto H, Takuwa N, Gonda K, Okazaki H, Chang K, Yatomi Y *et al.* EDG1 is a functional sphingosine-1-phosphate receptor that is linked via a Gi/o to multiple signaling pathways, including phospholipase C activation, Ca2+ mobilization, Ras-mitogen-activated protein kinase activation, and adenylate cyclase inhibition. *J Biol Chem* 1998; **273**: 27104–27110.
26 Liu F, Verin AD, Wang P, Day R, Wersto RP, Chrest FJ *et al.* Differential regulation of sphingosine-1-phosphate- and VEGF-induced endothelial cell chemotaxis. Involvement of G(ialpha2)-linked Rho kinase activity. *Am J Respir Cell Mol Biol* 2001; **24**: 711–719.
27 Windh RT, Lee MJ, Hla T, An S, Barr AJ, Manning DR. Differential coupling of the sphingosine 1-phosphate receptors Edg-1, Edg-3, and H218/Edg-5 to the G(i), G(q), and G(12) families of heterotrimeric G proteins. *J Biol Chem* 1999; **274**: 27351–27358.
28 Sugimoto N, Takuwa N, Okamoto H, Sakurada S, Takuwa Y. Inhibitory and stimulatory regulation of Rac and cell motility by the G12/13-Rho and Gi pathways integrated downstream of a single G protein-coupled sphingosine-1-phosphate receptor isoform. *Mol Cell Biol* 2003; **23**: 1534–1545.
29 Arikawa K, Takuwa N, Yamaguchi H, Sugimoto N, Kitayama J, Nagawa H *et al.* Ligand-dependent inhibition of B16 melanoma cell migration and invasion via endogenous S1P2 G protein-coupled receptor. Requirement of inhibition of cellular RAC activity. *J Biol Chem* 2003; **278**: 32841–32851.
30 Pitson SM. Regulation of sphingosine kinase and sphingolipid signaling. *Trends Biochem Sci* 2011; **36**: 97–107.
31 Haimovitz-Friedman A, Kan CC, Ehleiter D, Persaud RS, McLoughlin M, Fuks Z *et al.* Ionizing radiation acts on cellular membranes to generate ceramide and initiate apoptosis. *J Exp Med* 1994; **180**: 525–535.
32 Domingo-Domenech J, Vidal SJ, Rodriguez-Bravo V, Castillo-Martin M Quinn SA, Rodriguez-Barrueco R *et al.* Suppression of acquired docetaxel resistance in prostate cancer through depletion of notch- and hedgehog-dependent tumor-initiating cells. *Cancer Cell* 2012; **22 373–388.**
33 Engelman JA. Targeting PI3K signalling in cancer: opportunities, challenges and limitations. *Nat Rev Cancer* 2009; **9**: 550–562.
34 Watanabe N, Broome M, Hunter T. Regulation of the human WEE1Hu CDK tyrosine 15-kinase during the cell cycle. *EMBO J* 1995; **14**: 1878–1891.
35 McGowan CH, Russell P. Human Wee1 kinase inhibits cell division by phosphorylating p34cdc2 exclusively on Tyr15. *EMBO J* 1993; **12**: 75–85.
36 Mueller PR, Coleman TR, Kumagai A, Dunphy WG. Myt1: a membrane-associated inhibitory kinase that phosphorylates Cdc2 on both threonine-14 and tyrosine-15. *Science* 1995; **270**: 86–90.
37 Koff A, Polyak K. p27KIP1, an inhibitor of cyclin-dependent kinases. *Prog Cell Cycle Res* 1995; **1**: 141–147.
38 Hawley S, Fazli L, McKenney JK, Simko J, Troyer D, Nicolas M *et al.* A model for the design and construction of a resource for the validation of prognostic prostate cancer biomarkers: the canary prostate cancer tissue microarray. *Adv Anat Pathol* 2013; **20**: 39–44.



Supplementary Information accompanies this paper on the Oncogenesis website (http://www.nature.com/oncsis).

# Acid Ceramidase Promotes Nuclear Export of PTEN through Sphingosine 1-Phosphate Mediated Akt Signaling

**Thomas H. Beckham*, Joseph C. Cheng, Ping Lu, S. Tucker Marrison, James S. Norris, Xiang Liu**

Department of Microbiology and Immunology, Medical University of South Carolina, Charleston, South Carolina, United States of America

## Abstract

The tumor suppressor PTEN is now understood to regulate cellular processes at the cytoplasmic membrane, where it classically regulates PI3K signaling, as well as in the nucleus where multiple roles in controlling cell cycle and genome stability have been elucidated. Mechanisms that dictate nuclear import and, less extensively, nuclear export of PTEN have been described, however the relevance of these processes in disease states, particularly cancer, remain largely unknown. We investigated the impact of acid ceramidase on the nuclear-cytoplasmic trafficking of PTEN. Immunohistochemical analysis of a human prostate tissue microarray revealed that nuclear PTEN was lost in patients whose tumors had elevated acid ceramidase. We found that acid ceramidase promotes a reduction in nuclear PTEN that is dependent upon sphingosine 1-phosphate-mediated activation of Akt. We were further able to show that sphingosine 1-phosphate promotes formation of a complex between Crm1 and PTEN, and that leptomycin B prevents acid ceramidase and sphingosine 1-phosphate mediated loss of nuclear PTEN, suggesting an active exportin-mediated event. To investigate whether the tumor promoting aspects of acid ceramidase in prostate cancer depend upon its ability to export PTEN from the nucleus, we used enforced nuclear expression of PTEN to study docetaxel-induced apoptosis and cell killing, proliferation, and xenoengraftment. Interestingly, while acid ceramidase was able to protect cells expressing wild type PTEN from docetaxel, promote proliferation and xenoengraftment, acid ceramidase had no impact in cells expressing PTEN-NLS. These findings suggest that acid ceramidase, through sphingosine 1-phosphate, promotes nuclear export of PTEN as a means of promoting tumor formation, cell proliferation, and resistance to therapy.

**Citation:** Beckham TH, Cheng JC, Lu P, Marrison ST, Norris JS, et al. (2013) Acid Ceramidase Promotes Nuclear Export of PTEN through Sphingosine 1-Phosphate Mediated Akt Signaling. PLoS ONE 8(10): e76593. doi:10.1371/journal.pone.0076593

**Editor:** Xiaolin Zi, University of California Irvine, United States of America

**Received** May 6, 2013; **Accepted** September 2, 2013; **Published** October 1, 2013



**Funding:** Department of Defense PCTA W81XWH-11-1-0334, NCI 5P01CA097132, and National Center For Research Resources UL1RR029882. All core facilities were supported, in part, by Cancer Center Support Grant P30 CA138313 to the Hollings Cancer Center, Medical University of South Carolina. This work was also supported by Lipidomics Core in the SC Lipidomics and Pathobiology COBRE (P20 RR017677). The funders had no role in study design, data collection and analysis, decision to publish, or preparation of the manuscript.

**Competing interests:** The authors have declared that no competing interests exist.

* E-mail: beckham@musc.edu

## Introduction

PTEN is a critically important tumor suppressor classically known to antagonize oncogenic PI3K/Akt signaling by dephosphorylating the lipid product of PI3K, $PIP_{3,4,5}$, thereby antagonizing pleckstrin homology domain dependent recruitment of Akt and its activating kinase PDK1 to the cell membrane [1,2]. This function, while undoubtedly a key factor in PTEN-mediated tumor suppression, is by no means the only described role for PTEN with interest in recent years focusing on the role of PTEN within the nucleus. Nuclear PTEN is now known to serve lipid-phosphatase-independent functions in regulating the cell cycle by promoting acetylation of p53 and upregulating RAD51 in response to DNA damage [3], and by mediating APC/C tumor suppression by promoting association with the adaptor CDH1 [4]. Besides these molecular functions, nuclear PTEN has been observationally linked to tumor suppression. Histological analysis of PTEN has shown that nuclear PTEN in tumor tissue was a favorable prognostic indicator and correlated with a lower tumor proliferation index in melanoma and colon cancer tissues [5,6]. Interestingly, the most frequent mutation in the hamartomarous condition Cowden Syndrome, in which patients inherit a mutant PTEN allele and are susceptible to cancer, is Lysine289. This mutant form retains its phosphatase activity, but is not imported into the nucleus, providing strong suggestive evidence that nuclear PTEN is important in suppression of neoplasia [7,8].

Several studies describe mechanisms that mediate import of PTEN into the nucleus including active import based on multiple cryptic nuclear localization- signal-like sequences,

mutation of which abrogated RAN-mediated [9] or Major Vault Protein-mediated [10,11] nuclear accumulation of PTEN; PTEN C-terminus phosphorylation [12]; and monoubiquitination [7]. In contrast, little is known about active mechanisms of export of PTEN from the nucleus. One report by Liu, et al, showed that PTEN is exported from the nucleus at the G1/S transition through Akt-mediated activation of S6K [13]. They showed a direct interaction of PTEN with S6K and suggested this is mediated by the master nuclear export protein Crm1.

Here we report Crm1-dependent export of nuclear PTEN in response to sphingosine 1-phosphate (S1P) signaling. We found that expression of acid ceramidase (AC) in prostate cancer cells promoted a loss of nuclear PTEN. Following our recent study outlining AC-mediated Akt activation [14], we determined that AC-induced Akt activation promoted nuclear export of PTEN. Furthermore, we show that S1P strongly promotes formation of a complex between PTEN and Crm1, and that inhibition of Crm1 with Leptomycin B prevents AC/S1P-mediated export of nuclear PTEN. Interestingly, while AC was capable of promoting cell proliferation and resistance to Docetaxel in cells expressing wild type PTEN, it was not able to do so in cells expressing PTEN-NLS (wild type PTEN with an N-terminal nuclear localization signal attached), suggesting that the oncogenic properties of AC in prostate cancer involve its ability to regulate the level of PTEN in nucleus. Because most prostate cancers overexpress AC, we report a disease-relevant active mechanism of AC-mediated nuclear PTEN insufficiency promoting prostate cancer.

## Materials and Methods

### Cell lines and culture

PPC-1 [15] (a kind gift of Dr. Yi Lu, University of Tennessee), 22rv1, and DU145 (ATCC, Manassas, VA) were maintained in RPMI 1640 media supplemented with 10% bovine growth serum and incubated in 5% CO2 at 37°C. DU145-AC-EGFP/DU145-EGFP have been described [16,17].

### Reagents

Synthesis of S1P was conducted in the Lipidomics Shared Resource. S1P dry aliquots were prepared by suspension in methanol and lyophilization under a dry nitrogen stream. Aliquots were stored at -80°C until use at which time they were resuspended in PBS to 100μM. Reagents used include: SKI-II, Docetaxel (Thermo, Fisher, Lafayette, CO), LY294002, AktX (Cayman Chemical, Ann Arbor, MI), W146, JTE013 (Tocris, Bristol, UK), Leptomycin B (Sigma, St. Louis, MO), and S6K1 inhibitor DG2 (Millipore, Billerica, MA).

### Transfections and plasmid constructs

All plasmid transfections were carried out using Lipofectamine 2000 (Life Technologies) according to manufacturer instructions. The following plasmids were used in this study: Origene PTEN cDNA (SC119965), FLAG-Crm1 [18] (Addgene plasmid #17647), FLAG-PTEN [19] (Addgene plasmid #22231), PTEN-E4 [12] (Addgene plasmid #11171), PTEN-A4 [12] (Addgene plasmid #10753), HA-PTEN-NLS [20] (Addgene plasmid #10933) and HA-PTEN-wt [20] (Addgene plasmid #10750). Wild type PTEN cDNA from Origene was used by Genewiz (La Jolla, CA) as a template for site-directed mutagenesis to mutate the codons encoding Leucine residues at amino acids 334, 336 and 338 to Alanine residues. The resulting construct is referred to as PTEN-AAA.

### Preparation of tumor tissue microarray

27 formalin-fixed paraffin-embedded (FFPE) prostate carcinomas were obtained from the Hollings Cancer Center Tissue Biorepository (Medical University of South, Carolina). These tissues were obtained in accordance with an Institutional Review Board approved protocol (426). One-millimeter tissue cylinders were punched from representative tumor areas of a “donor” tissue block and brought into different recipient paraffin blocks each containing 27 individual samples. Three tissue cores were sampled from each tumor, and one core was sampled from patient matched adjacent normal tissue. Four-micrometer thick sections of the TMA were cut and processed for immunohistochemistry.

### Immunohistochemistry

FFPE sections were deparaffinized in xylene, rehydrated in alcohol, and processed for pretreatment as follows: The sections were incubated with target retrieval solution (Dako, Glostrup, Denmark) in a steamer (Rival, CA, USA) for 45 minutes and then 3% hydrogen peroxide solution for 10 minutes and protein block (Dako, Glostrup, Denmark) for 20 minutes at room temperature. Primary antibody incubation overnight in a humid chamber at 4°C followed by biotinylated secondary antibody (Vector, CA, USA) for 30 minutes and ABC reagent (Vector, CA, USA) for 30 minutes. Immunocomplexes of horseradish peroxidase were visualized by DAB (Dako, Glostrup, Denmark) reaction, and sections were counterstained with hematoxylin before mounting. Immunoreactivity was scored using a semiquantitative system combining intensity of staining(0-3) and percentage of cells staining positive(0-3). Separate scores were generated for PTEN staining within the nucleus and the cytoplasm.

### Confocal Microscopy

Cells grown on 8-well chamber slides (Becton-Dickinson, Franklin Lakes, NY) were fixed in 3.7% paraformaldehyde, permeabilized in methanol, blocked with 1.5% bovine serum albumin in PBS, and incubated with PTEN primary antibody in 1% BSA/PBS. Bound primary antibodies were detected with Alexa Fluor 555-conjugated goat anti-rabbit secondary antibodies (Invitrogen). Nuclei were stained by incubation with 1:5000 diluted ToPro3-Iodide for 15 minutes. Confocal microscopy was performed using a Leica Laser Scanning Confocal Microscope maintained by the Medical University of South Carolina Hollings Cancer Center Cell and Molecular Imaging Core (1P30 CA138313-01). For each treatment, a minimum of 100 cells were evaluated visually for presence of nuclear PTEN by an evaluator blinded to the treatment group. NIH ImageJ software was used to measure the cytoplasmic and nuclear PTEN stain intensities and the N/C ratios for each treatment were determined.

### Immunoprecipitation

Cells transfected with either FLAG-Crm1 [18] (Addgene plasmid #17647) or FLAG-PTEN [19] (Addgene plasmid #22231) were used for Immunoprecipitation with the Sigma FLAG IP kit in accordance with manufacturer instructions. Briefly, cells were washed twice with ice cold PBS then lysed by gentle shaking with lysis buffer at 4°C for 20 minutes. Cells were scraped and collected into centrifuge tubes, and cellular debris was pelleted by centrifugation at 12,000 g for 12 minutes. Cell lysates were used to suspend anti-FLAG M2 affinity beads. Following overnight rotation at 4°C, beads were pelleted and washed several times before the bound protein was liberated with boiling for 5 minutes in 2X sample buffer. After pelleting the beads, 15µL of the supernatant was analyzed by immunoblotting as described above.

### Cellular Fractionation

Nuclear and cytoplasmic fractions were obtained using the REAP method [21], with slight modification. Briefly, cells were washed twice with ice cold PBS before mechanical disruption of cytoplasmic membranes by tituration (5X with P-1000 pipetor) with .1% NP-40 in PBS. After a 10 second spin in a table top microcentrifuge, the supernantant was reserved as the cytoplasmic fraction. Following an additional brief tituration (2X with P-1000 pipetor) and a 10 second centrifugation, the supernatant was removed and the pellet was resuspended in 30µL RIPA buffer. After 30 minutes of incubation on ice with aggressive vortexing every 10 minutes, nuclear debris was removed by centrifuging at 20,000 x g for 20 minutes. The supernatant is the nuclear fraction.

### Adenovirus infection

AC cDNA was purchased from Origene (Rockville, MD) and Ad-AC (adenovirus expressing AC and GFP) and Ad-GFP were developed by Vector Biolabs (Philadelphia, PA). Ad-PTEN was purchased from Vector Biolabs. The short hairpin sequence (5'-ccgggctgttattgacagcgatatactgagtatatcgctgtcaataacagcttttt -3') obtained from Open Biosystems (Huntsville, AL) was validated and developed into an adenoviral delivery vector (Ad-shAC) by Vector Biolabs. The HA-PTEN-NLS construct obtained from Addgene was developed into an adenoviral delivery vector by Vector Biolabs by cloning the PTEN-NLS sequence without the HA tag into an adenovirus construct. Cells were infected in suspension with the indicated MOI of the indicated adenovirus in complete medium.

### Western blotting

Cell lysates were prepared and analyzed as previously described [22], using the following antibodies: pAkt (#4060), total-Akt (#4691) p-P70S6K (#9234), P70S6K (#9202), PTEN (#9559), p-PTEN S380(#9551), p-PTEN S380/Thr382/383 (#9554) Histone-H3 (#4499), β-Tubulin (#2128) DYKDDDDK (FLAG) Tag (#2044) (Cell Signaling Technologies, Danvers, MA), AC (BD Transduction #612302), GAPDH (G-9), and Lamin B (C-20) (Santa Cruz, Santa Cruz, CA).

### Cell viability assays

5000 cells per well were infected with Ad-AC or Ad-GFP and plated in 96-well plates. After overnight attachment, medium containing the indicated compound was added. Cells were treated with a broad dose range of Docetaxel from 100 nM to .1 nM, doses encompassing effecting little to complete cell death. After 48 hours, the Promega CellTiter 96® AQueous One Solution Cell Proliferation Assay (MTS) was used to approximate the number of viable cells. Prism v4 was used to determine the EC50 (concentration at which half of the cells are viable).

### Propidium Iodide staining

Cells were trypsinized and washed twice with cold PBS prior to suspension in 100µL PBS followed by 3 ml of -20°C 70% EtOH. After a minimum of one hour incubation at 4°C, cells were washed twice with 2 ml PBS and again resuspended in 100µL PBS. Cells were incubated or one hour with RNase A at a final concentration of 500µg/ml. 20µL of stock solution of propidium iodide (1 mg/ml) was added to a final concentration of 50µg/ml and incubated in the dark at 4°C for 30 minutes prior to analysis for DNA content by flow cytometry with software rendering by ModFit LT 4.0 (Verity Software House).

### Proliferation

2000 cells were plated per well in 24-well plates. On the indicated day (day 0 being the day after plating), one plate was fixed in 3.7% formalin and stained with crystal violet. Cell number was determined by counting a minimum of 5 randomly selected microscopic fields (10X objective).

### Animal studies

For establishment of xenografts, cells were infected at MOI 25 with each of the indicated adenoviruses in suspension at a density of $1x10^6$ cells per mL in serum free medium containing 1% BSA for 4 hours prior to preparation for engraftment by suspension in 1:1 RPMI 1640: Matrigel HC admixture (0.08 mL per injection). Pathogen-free four-week-old female Athymic NCr-nu/nu mice were purchased from the NCI, Frederick Cancer Research Center (Frederick, MD, USA). Animals were monitored for formation of palpable tumors weekly. The mice were maintained under standard conditions according to the institutional guidelines for animal care. All animal experiments were approved by the Committee for the Care and Use of Laboratory Animals of Medical University of SC.

### Statistical Analysis

Independent experiments were performed a minimum of three times. Statistical analyses on experiments performed in triplicate were performed by unpaired one-tailed student's *t* test, one way ANOVA with Bonferroni correction using Prism (version 4.0) from GraphPad, or Fisher's Exact Test. $*p<0.05$ was considered significant. Time to tumor formation was analyzed via Kaplan-Meier methods. Mice that did not develop tumors were censored at 42 days. The log-rank test was used to compare distributions of time to tumor formation across groups for all pairs of groups.

## Results

### Acid ceramidase correlates with loss of nuclear PTEN in prostate adenocarcinoma

Using a tissue microarray (TMA) made up of prostate adenocarcinoma and patient-matched benign adjacent biopsy cores from 27 prostate cancer patients, we determined that in the patients whose tumor AC immunohistochemistry (IHC) staining was elevated compared their benign AC score (benign AC score: .325, adenocarcinoma AC score: 2.55, $p<.001$) (Figure 1A), the percentage of PTEN in the nuclei of the specimens (100*nuclear PTEN score/(cytoplasmic + nuclear PTEN score) was decreased in adenocarcinoma tissue (benign nuclear PTEN: 40.9%, adenocarcinoma nuclear PTEN: 6.25%, $p<.05$) (Figure 1B). Conversely, in patients whose tumor AC staining was not elevated compared to their benign tissue (Figure 1C) no decrease in the percentage of nuclear PTEN was observed (Figure 1D). The AC scores and nuclear PTEN % are displayed in table form (Figure 1E).

### Acid ceramidase causes S1P-dependent loss of nuclear PTEN

PPC1 cells transfected with wild type PTEN were infected with either Ad-GFP or Ad-AC. Figure S1 is provided as a demonstration of the degree of AC expression that is enforced using our adenoviral transfection approach which can be compared to the degree of AC overexpression found in human prostate tumors in our previous study [23]. Immunofluorescence to visualize PTEN localization revealed that expression of AC significantly reduced the number of cells that had PTEN in the nucleus, but not in the presence of the sphingosine kinase inhibitor SKI-II. Representative cells are shown in Figure 2A, and quantified in Figure 2B. Nuclei from cells infected with Ad-GFP or Ad-AC were isolated and evaluated for nuclear PTEN by western blotting (Figure 2C). Nuclear PTEN was reduced in Ad-AC infected cells, but not in the presence of the sphingosine kinase (SphK) inhibitor SKI-II, suggesting that AC promotes a reduction in nuclear PTEN by a SphK-dependent mechanism. Whole cell lysates from this experiment are shown in Figure S2A. In order to maintain consistency throughout the study, we utilized PPC1 cells, which are PTEN null, transfected with PTEN constructs. This allows evaluation of PTEN and PTEN mutant localization without the effects of endogenous PTEN. In order to verify that this phenomenon occurs with endogenous PTEN, key results were confirmed in DU145 cells. Stable (Figure S3A-B) and transient (Figure S3C-D) expression of AC promoted reduction in nuclear PTEN that was blocked by SKI-II, similar to the results obtained in transfected PPC1 cells. To determine whether exogenous S1P could mimic the effects of AC expression, we treated cells with 500 or 1000 nM S1P. Treatment of cells with S1P recapitulated this phenomenon in PTEN-transfected PPC1 (Figure 2D-F, Figure S2B) as well as in DU145 cells (Figure S3E-H), indicating that S1P promotes a reduction in nuclear PTEN in prostate cancer cells.

### S1P promotes Akt-dependent loss of nuclear PTEN

Recent studies from our lab have shown that AC causes activation of Akt through S1P receptor 2 (S1PR2) in prostate cancer cells. To determine whether AC-induced Akt activation mediates loss of nuclear PTEN, we expressed AC in PPC1 cells and analyzed changes in PTEN localization using nuclear fractionation (Figure 3A) and confocal microscopy (Figure 3B-C). Antagonism of S1PR2 with JTE013 abolished AC-mediated nuclear PTEN loss, as did inhibition of Akt with the inhibitor AktX, indicating that AC-induced Akt activation promotes loss of nuclear PTEN. Treatment of cells with exogenous S1P in the presence of JTE013 and AktX demonstrated that S1P, through S1PR2 and activation of Akt, promotes loss of nuclear PTEN (Figure 3D-F). Inhibition of S1PR2 or Akt prevented S1P-mediated nuclear PTEN loss in DU145 as well (Figure S4).

### S1P mediates Crm1-dependent export of nuclear PTEN

To investigate the mechanism of S1P-mediated nuclear loss of PTEN, we used the Crm1 inhibitor Leptomycin B (LMB) to determine whether we were observing a Crm1-dependent PTEN nuclear export. Indeed, LMB abrogated AC- (Figure 4A-C) and S1P- (Figure 4D-F, Figure S5) induced nuclear PTEN loss, suggesting that we are observing activation of Crm1-mediated active export of PTEN upon AC expression or S1P stimulation. To determine whether S1P promotes association of PTEN and Crm1, we transfected cells with either FLAG-Crm1 (Figure 5A) or FLAG-PTEN (Figure 5B) and analyzed FLAG immunoprecipitates. Interestingly, stimulation of cells with S1P significantly promoted PTEN presence in FLAG-Crm1 immunoprecipitates and, reciprocally, Crm1 in FLAG-PTEN immunoprecipitates, suggesting that S1P stimulates formation of a complex between Crm1 and PTEN. Whole cell lysates from this experiment are shown in Figure S6. PTEN does not have a described nuclear export sequence (NES), however *in silico* analysis with NetNES1.1 [24] predicts a weak NES (Figure S7A). Site directed mutagenesis of three Leucine residues in the predicted NES to Alanine residues (L334A, L336A and L338A) did not impact S1P-mediated nuclear export (Figure S7B) or reduce the presence of PTEN in S1P-stimualted Crm1 immunoprecipitates (Figure S7C), suggesting that this predicted NES is not functional. We also evaluated whether phosphorylation of the C-terminus of PTEN was involved in S1P-mediated nuclear export of PTEN, as the phosphorylation status of the C-terminus has been reported to be involved with its nuclear localization [9,25]. Expression of AC did not promote C-terminus phosphorylation of PTEN (Figure S8A), and two mutant versions with Alanine or Glutamate substitutions in phosphorylation residues that were identified as regulating localization of PTEN, A4 (S380A, T382A, T383A, S385A) and E4 (S380E, T382E, T383E, S385E) were both found in S1P-stimulated Crm1 immunoprecipitates (Figure S8B). PTEN-E4 and PTEN-A4 were PTEN were equivalently exported upon S1P stimulation (Figure S8C), thus we concluded that PTEN C-terminus phosphorylation is not involved in AC/S1P induced nuclear export of PTEN.

Figure 1: Human prostate tumors lose nuclear PTEN when AC is elevated

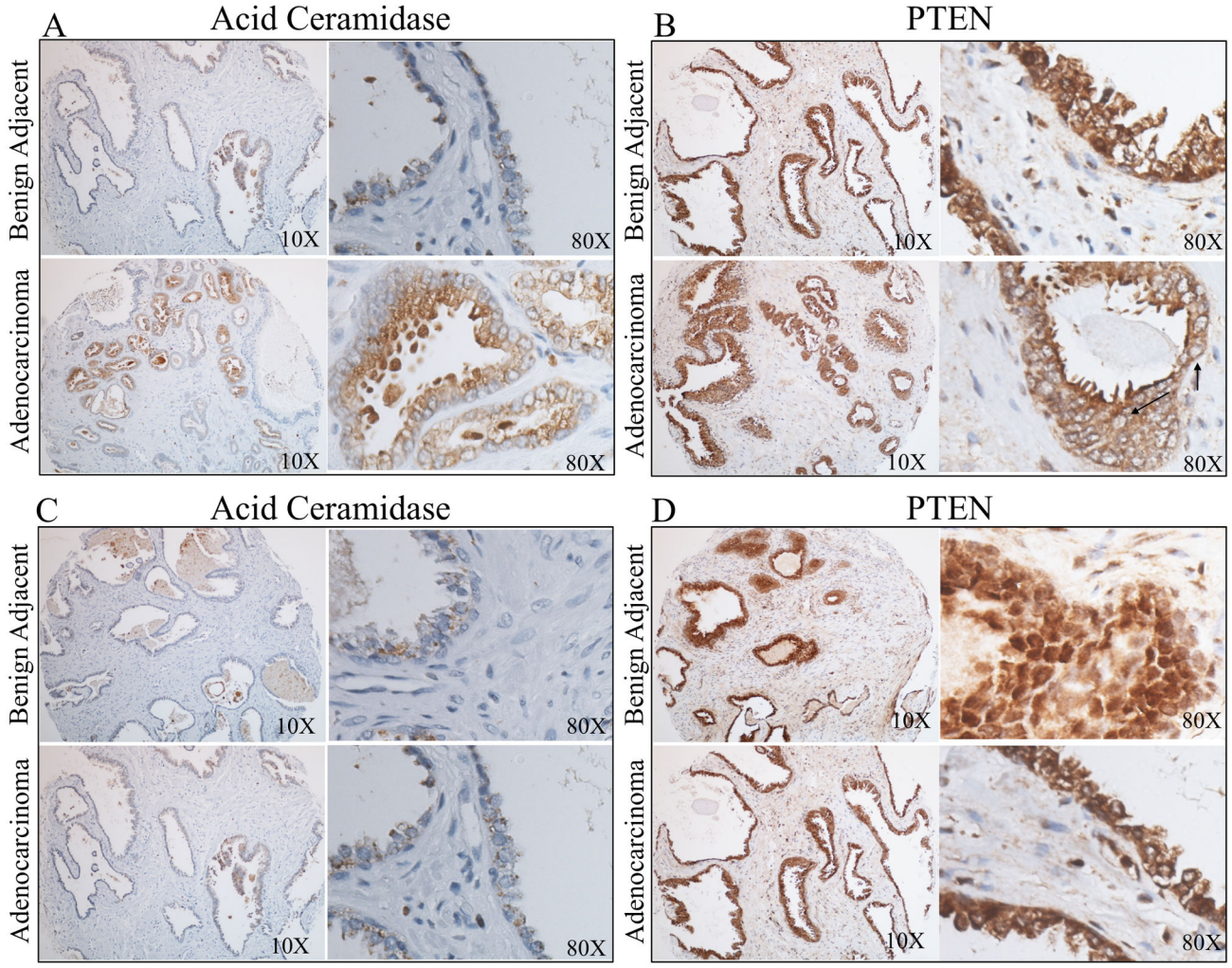


E

| | AC-high | Nuclear PTEN | AC-low | Nuclear PTEN |
|---|---|---|---|---|
| Benign | 0.325 | 40.90% | 0.6 | 12.60% |
| Tumor | 2.55 | 6.25% | 1.12 | 30.20% |
| p-value | <.001 | <.005 | *ns* | *ns* |

**Figure 1. Human prostate tissues lose nuclear PTEN when AC is elevated.** (*a-d*) A 27 patient tissue microarray with patient-matched prostate adenocarcinoma and adjacent benign tissue was immunostained for AC and PTEN. Staining intensities for AC, nuclear PTEN, and cytoplasmic PTEN were evaluated by a blinded pathologist. The arrows in (*b*) are examples of nuclei devoid of PTEN. In patients whose cancer tissue had elevated AC than their benign tissue (*a*), there was also a decrease in the amount of nuclear PTEN, p<.05 (b). Patients whose AC did not increase in their tumor tissue (*c*) did not have a decrease in nuclear PTEN (*d*). AC pathology scores and nuclear PTEN percentage for the AC-high and AC-low patient groups are organized in (*e*).

doi: 10.1371/journal.pone.0076593.g001

Figure 2: Acid ceramidase promotes S1P-mediated loss of nuclear PTEN

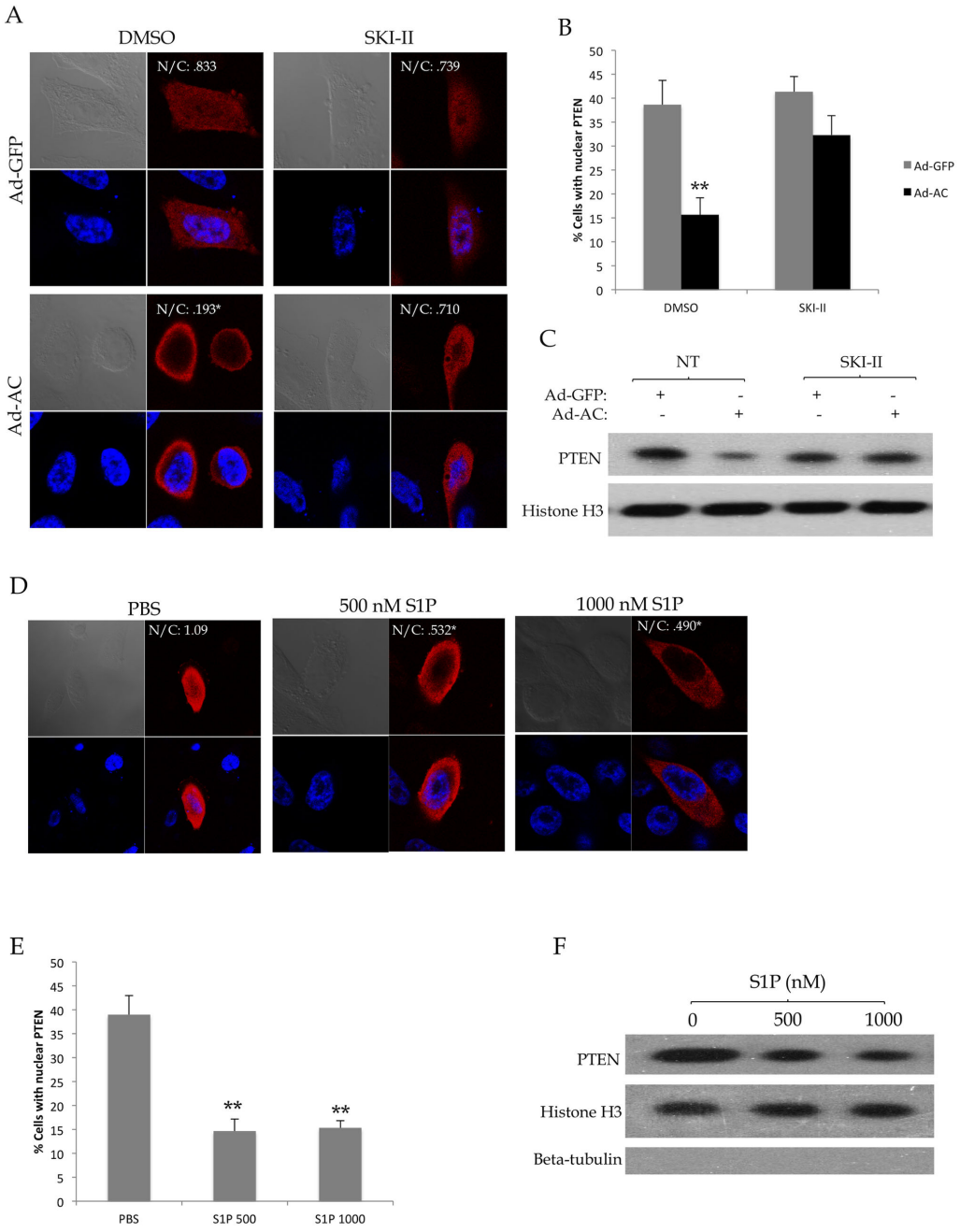


**Figure 2. Acid ceramidase promotes S1P-mediated loss of nuclear PTEN.** PPC1 cells transfected with WT-PTEN were infected with Ad-GFP or Ad-AC for 48 hours in the presence of DMSO (no treatment; NT) or the sphingosine kinase inhibitor SKI-II for 24 hours. A) Cells were immunostained for PTEN (red) and nuclei (blue). Nuclear (N) and cytoplasmic (C) PTEN staining intensity were measured for all cells in a given treatment using ImageJ. N/C indicates the nuclear PTEN to cytoplasmic PTEN ratio. B) The percentage of cells from (A) which had nuclear PTEN in each treatment. C) Nuclear fractions from the indicated treatments were isolated and evaluated for presence of PTEN with Histone H3 as a nuclear loading control and absence of β-tubulin to indicate purity of the nuclear sample. D) PPC1 cells transfected with WT-PTEN were treated with the indicated dose of S1P or PBS for 2 hours prior to fixation and immunostaining for PTEN (red) and nuclei (blue). E) The percentage of cells from (D) which had nuclear PTEN. F) Nuclear fractions from the indicated treatments were isolated and evaluated for presence of PTEN with Histone H3 as a nuclear loading control and absence of β-tubulin to indicate purity of the nuclear sample. One way ANOVA with Bonferroni correction, *p<.05, **p<.01.

doi: 10.1371/journal.pone.0076593.g002

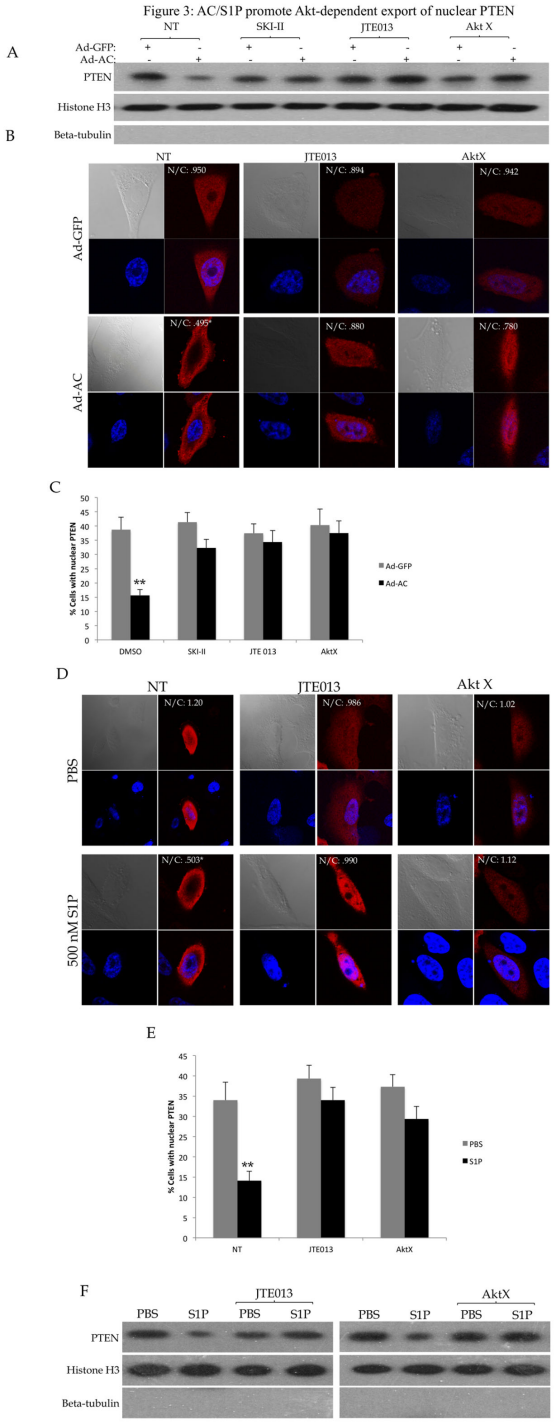


**Figure 3. AC/S1P promote Akt-dependent export of nuclear PTEN.** PPC1 cells were transfected with WT-PTEN were infected with Ad-GFP or Ad-AC for 48 hours in the presence of DMSO (NT) or the indicated compounds for 24 hours. A) Nuclear fractions from the indicated treatments were isolated and evaluated for presence of PTEN with Histone H3 as a nuclear loading control and absence of β-tubulin to indicate purity of the nuclear sample. B) Cells were immunostained for PTEN (red) and nuclei (blue). C) The percentage of cells from (B) which had nuclear PTEN in each treatment. D) PPC1 cells transfected with WT-PTEN were treated with 1μM JTE013 or 5μM AktX for 24 hours prior to treatment with the indicated dose of S1P or PBS for 2 hours followed by fixation and immunostaining for PTEN (red) and nuclei (blue). E) The percentage of cells from (D) which had nuclear PTEN. F) Nuclear fractions from the indicated treatments were isolated and evaluated for presence of PTEN with Histone H3 as a nuclear loading control and absence of β-tubulin to indicate purity of the nuclear sample. One way ANOVA with Bonferroni correction, *p<.05**p<.01.

doi: 10.1371/journal.pone.0076593.g003

Figure 4: AC/S1P promotes Leptomycin B sensitive export of nuclear PTEN.

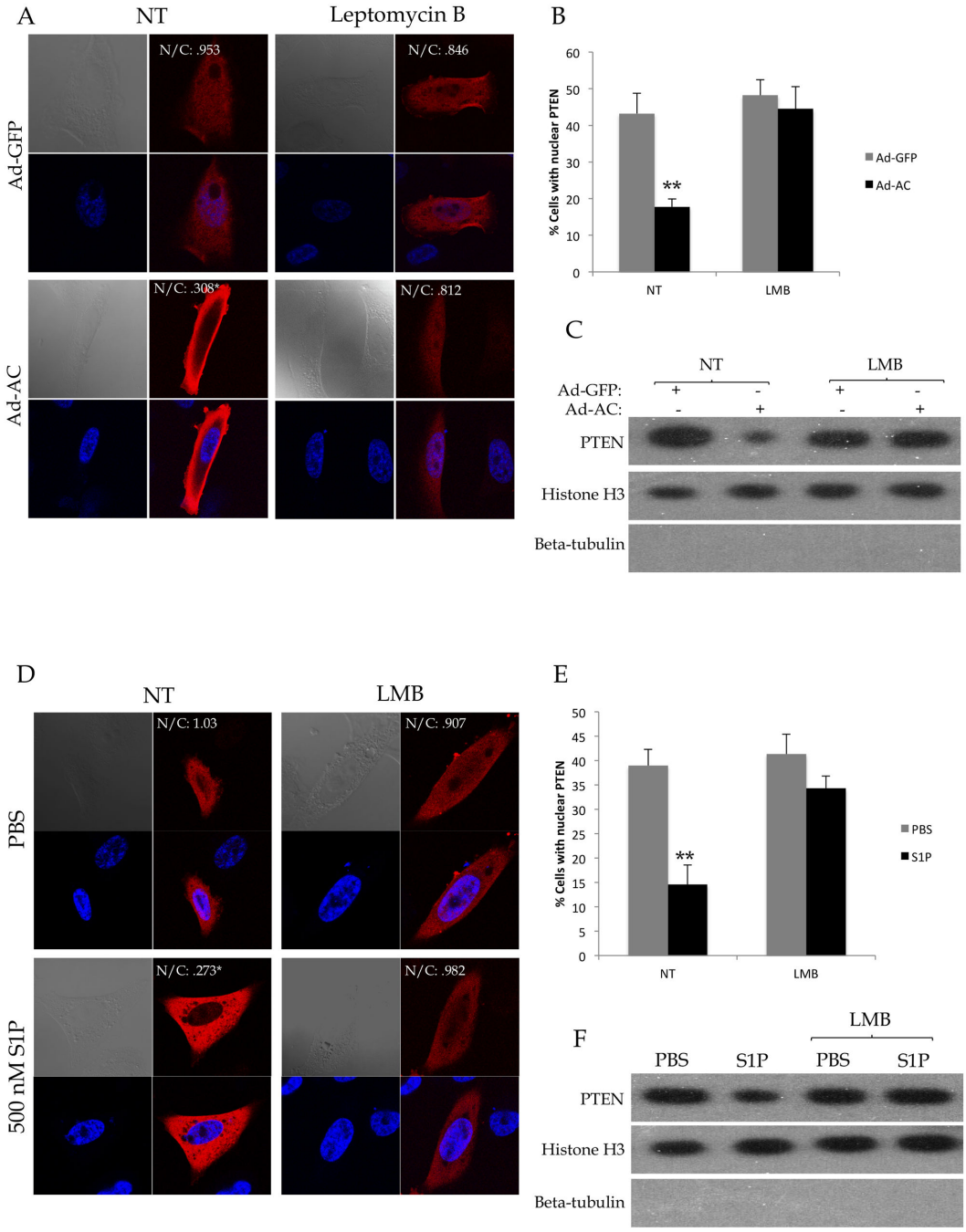


**Figure 4. AC/S1P promotes Leptomycin B sensitive export of nuclear PTEN.** PPC1 cells transfected with WT-PTEN were infected with Ad-GFP or Ad-AC for 48 hours in the presence of EtOH (NT) or 100 nM Leptomycin B (LMB) for 24 hours. A) Cells were immunostained for PTEN (red) and nuclei (blue). B) The percentage of cells from (A) which had nuclear PTEN in each treatment. C) Nuclear fractions from the indicated treatments were isolated and evaluated for presence of PTEN with Histone H3 as a nuclear loading control and absence of β-tubulin to indicate purity of the nuclear sample. D) PPC1 cells transfected with WT-PTEN were treated with 100nM LMB for 24 hours and 500nM S1P or PBS for 2 hours prior to fixation and immunostaining for PTEN (red) and nuclei (blue). E) The percentage of cells from (D) which had nuclear PTEN. F) Nuclear fractions from the indicated treatments were isolated and evaluated for presence of PTEN with Histone H3 as a nuclear loading control and absence of β-tubulin to indicate purity of the nuclear sample. One way ANOVA with Bonferroni correction, *p<.05**p<.01.

doi: 10.1371/journal.pone.0076593.g004

Figure 5: PTEN and Crm1 form an S6K mediated complex upon S1P stimulation

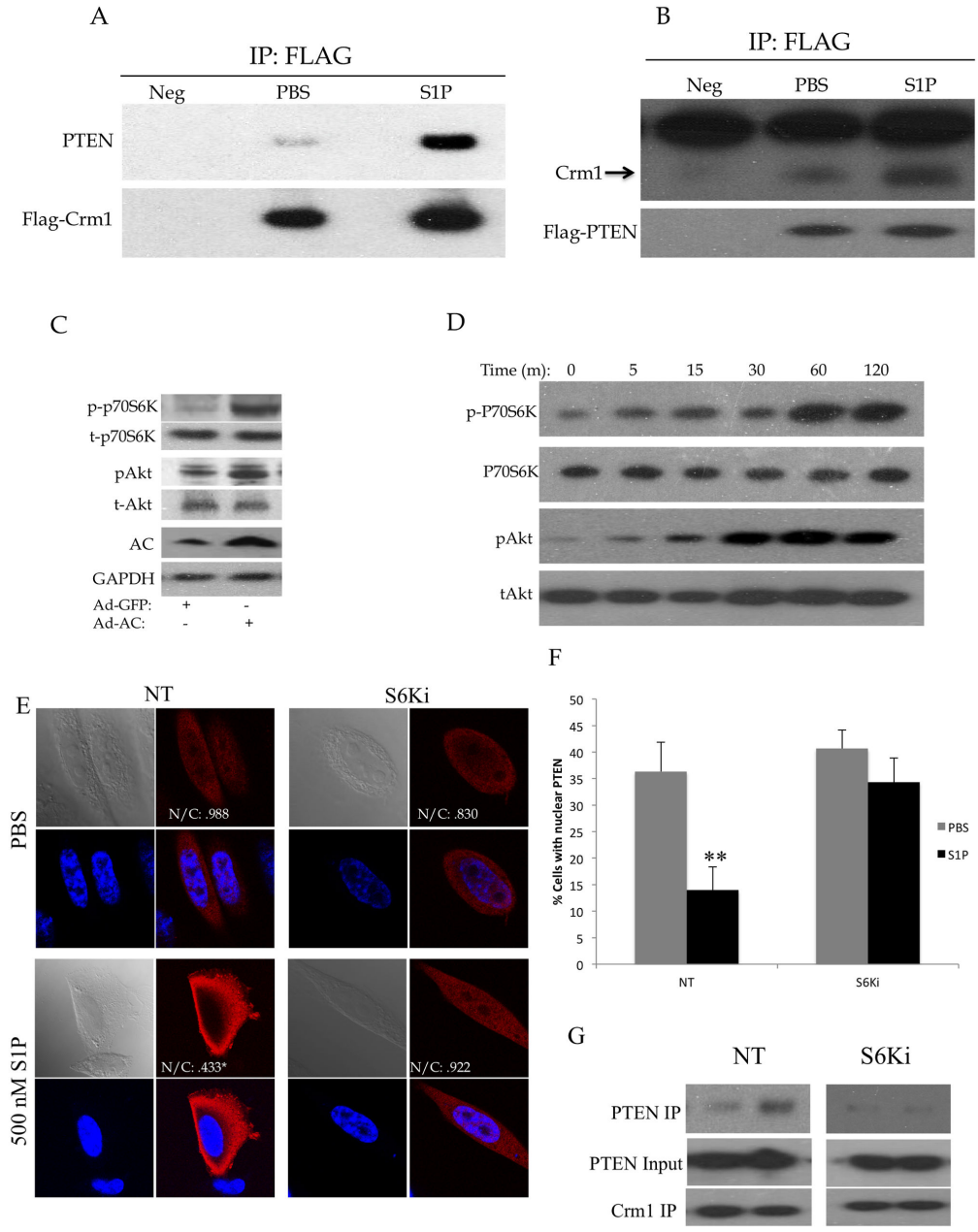


**Figure 5. PTEN and Crm1 form an S6K mediated complex upon S1P stimulation.** A) PPC1 cells were transfected with WT-PTEN and FLAG-Crm1. Cells were collected after 2 hours stimulation with 500nM S1P or PBS and submitted to immunoprecipitation of the FLAG-Crm1 protein. The negative control (Neg) indicates lysate from cells not transfected with FLAG-Crm1. B) PPC1 cells were transfected with FLAG-PTEN and collected after 2 hour stimulation with 500nM S1P or PBS and submitted to immunoprecipitation of the FLAG-PTEN protein. The negative control (Neg) indicates lysate from cells not transfected with FLAG-PTEN. C) PPC1 cells were infected with Ad-AC or Ad-GFP and analyzed for S6K phosphorylation. D) PPC1 cells were treated with 500nM S1P for 2 hours and analyzed for S6K phosphorylation. E) PPC1 cells transfected with WT-PTEN were treated with water (NT) or 2.5 μM S6K1 inhibitor DG2 (S6Ki) for 24 hours then stimulated with 500 nM S1P for 2 hours prior to immunostaining for PTEN (red) and nuclei (blue). F) The percentage of cells from (E) which had nuclear PTEN in each treatment. G) PPC1 cells were transfected with WT-PTEN and FLAG-Crm1 and treated for 24 hours with 2.5 μM S6Ki. Cells were collected after 2 hour stimulation with 500nM S1P or PBS and submitted to immunoprecipitation of the FLAG-Crm1 protein. One way ANOVA with Bonferroni correction, *p<.05**p<.01.

doi: 10.1371/journal.pone.0076593.g005

### AC and S1P mediate Crm1-dependent export of nuclear PTEN through S6K activation

Previous reports have shown that Akt promotes PTEN nuclear export through Crm1, mediated by a physical interaction with S6K [13]. In keeping with our previous findings that AC, through S1P, promotes activation of Akt and its downstream targets, overexpression of AC (Figure 5C) and treatment with exogenous S1P (Figure 5D) promoted phosphorylation of S6K. To evaluate whether S6K-dependent nuclear export of PTEN was involved in our observations, we used the S6K1 inhibitor S6K1 Inhibitor II (here called S6Ki). The S6K inhibitor prevented S1P-mediated PTEN nuclear egress (Figure 5E-F). Moreover, utilization of S6Ki prevented the association of PTEN with Crm1 upon S1P stimulation, as noted by the absence of S1P-stimulated increase in PTEN in FLAG-Crm1 immunoprecipitates in the presence of S6Ki (Figure 5G). These findings strongly suggest that AC/S1P promote nuclear egress of PTEN through the formation of an S6K-mediated complex with Crm1, as previously described.

### Oncogenic features of AC expressing cells are absent in the presence of nuclear localized PTEN

Nuclear PTEN has been found to promote apoptosis and suppress cell proliferation. Therefore, we set out to determine whether the ability of AC to promote nuclear egress of PTEN was functionally important for these phenotypes. We co-infected PPC1 cells with Ad-GFP or Ad-AC and Ad-GFP, Ad-WT-PTEN, or Ad-PTEN-NLS. AC promoted nuclear egress of WT-PTEN, but not NLS-PTEN, which remained confined to the nucleus in all cells (Figure S9A). Moreover, PTEN-NLS and WT-PTEN are expressed at similar levels (Figure S9B) Treatment of cells with 1.5 nM Docetaxel induced apoptosis in cells expressing both WT-PTEN and PTEN-NLS more strongly than cells not expressing PTEN (Figure 6A), consistent with the role of PTEN in potentiating apoptotic stimuli. Interestingly, while Ad-AC was able to suppress Docetaxel induced apoptosis in Ad-GFP and Ad-WT-PTEN infected cells, Ad-PTEN-NLS infected cells were not protected from apoptosis by Ad-AC. Moreover, the EC50s of these treatments to Docetaxel were increased by Ad-AC, indicating desensitization or protection from cell death due to Docetaxel, however Ad-PTEN-NLS infected cells had no change in EC50 when AC was expressed (Figure 6B). These results suggest that AC is able to protect cells from chemotherapy-induced apoptosis and cell death when it is able to promote nuclear egress of PTEN, but not when nuclear expression of PTEN is enforced. In a study of cell proliferation, Ad-GFP and Ad-WT-PTEN infected cells expressing AC proliferated more rapidly than their Ad-GFP infected controls (Figure 6C). Interestingly, while the overall rate of proliferation in WT-PTEN expressing cells was slower, Ad-AC promoted proliferation more robustly (1.84 fold at day 8) compared to cells expressing no PTEN (1.2 fold at day 8), suggesting that while AC can promote proliferation in the presence and absence of PTEN, it exerts a more powerful influence in PTEN expressing cells. Cells expressing PTEN-NLS proliferated the least of all treatments, and Ad-AC provided no advantage in proliferation, further suggesting that the ability of AC to promote proliferation depends upon its ability to promote nuclear egress of PTEN. In a study of the ability of AC to promote tumor engraftment in a xenograft study, we found that AC trended towards promotion of formation of tumors more rapidly in cells expressing GFP (control) or a WT-PTEN construct (p=0.1), but not in cells expressing NLS-PTEN (p=0.7) (Figure 6D).

## Discussion

Once thought to be an exclusively cytoplasmic protein, PTEN has been found in the nuclei of numerous cell types. Interestingly, studies in breast tissue [26], thyroid tissue [27], and pancreatic tissue [28] have all found that nuclear PTEN is generally found in benign or resting cells but tends to be lost in more aggressive cancer cells. Because PTEN is now well known to be a tumor suppressor in the nucleus in addition to its well-appreciated role in cytoplasmic tumor suppression, determining how PTEN gets in and out of the nucleus is of great interest. A number of studies describe mechanisms of PTEN nuclear import [7,9,11,12], however very little information is known about export of PTEN from the nuclear compartment. We initially observed that cells overexpressing AC seemed to have a reduced amount of nuclear PTEN compared to controls, which led us to investigate the mechanism behind this observation. Having recently discovered that AC promotes activation of Akt through S1P receptor 2-mediated stimulation of PI3K [14], we sought to determine whether AC-induced reduction of nuclear PTEN is mediated by S1P-induced activation of Akt. By inhibiting sphingosine kinase, S1PR2, and Akt in AC-overexpressing cells, we found that the previously described pathway of AC-induced Akt activation was indeed necessary for AC to promote nuclear egress of PTEN. The essential role of this pathway was confirmed using S1PR2 and Akt inhibition in cells stimulated with exogenous S1P.

Having found that AC-mediated Akt activation promoted loss of nuclear PTEN, we were interested in determining what mechanisms of PTEN nuclear export might be responsible for the phenomenon we observed. Our mutation of an *in silico* predicted nuclear export sequence (NES) and multiple C-terminus phosphorylation sites did not support classical direct nuclear export or alteration in PTEN C-terminus phosphorylation as contributory to AC/S1P-mediated nuclear export of PTEN [12]. Alfred Yung's group has found evidence that PTEN moves from the nucleus to the cytoplasm in response to Akt activation through mTOR-mediated activation of S6K [13]. In that study, inhibition of PI3K, mTOR, and S6K1 all prevented export of PTEN. They concluded that this export was dependent on Crm1, as the inhibitor Leptomycin B prevented export of PTEN from the nucleus. Overall, they presented compelling evidence of a negative feedback loop through which activation of Akt is suppressed by recruiting a nuclear reservoir of PTEN into the cytoplasm. Because we observed AC-induced, Akt-dependent PTEN nuclear egress, we sought to determine whether the previously discovered Crm1-mediated S6K dependent export was occurring in our system. Indeed, we found that not only does Leptomycin B suppress AC and S1P mediated export of nuclear PTEN, as found in the Yung study, but also the novel observation that

Figure 6: AC promotes tumor formation and Docetaxel resistance in cells with wild type, but not nuclear localized, PTEN

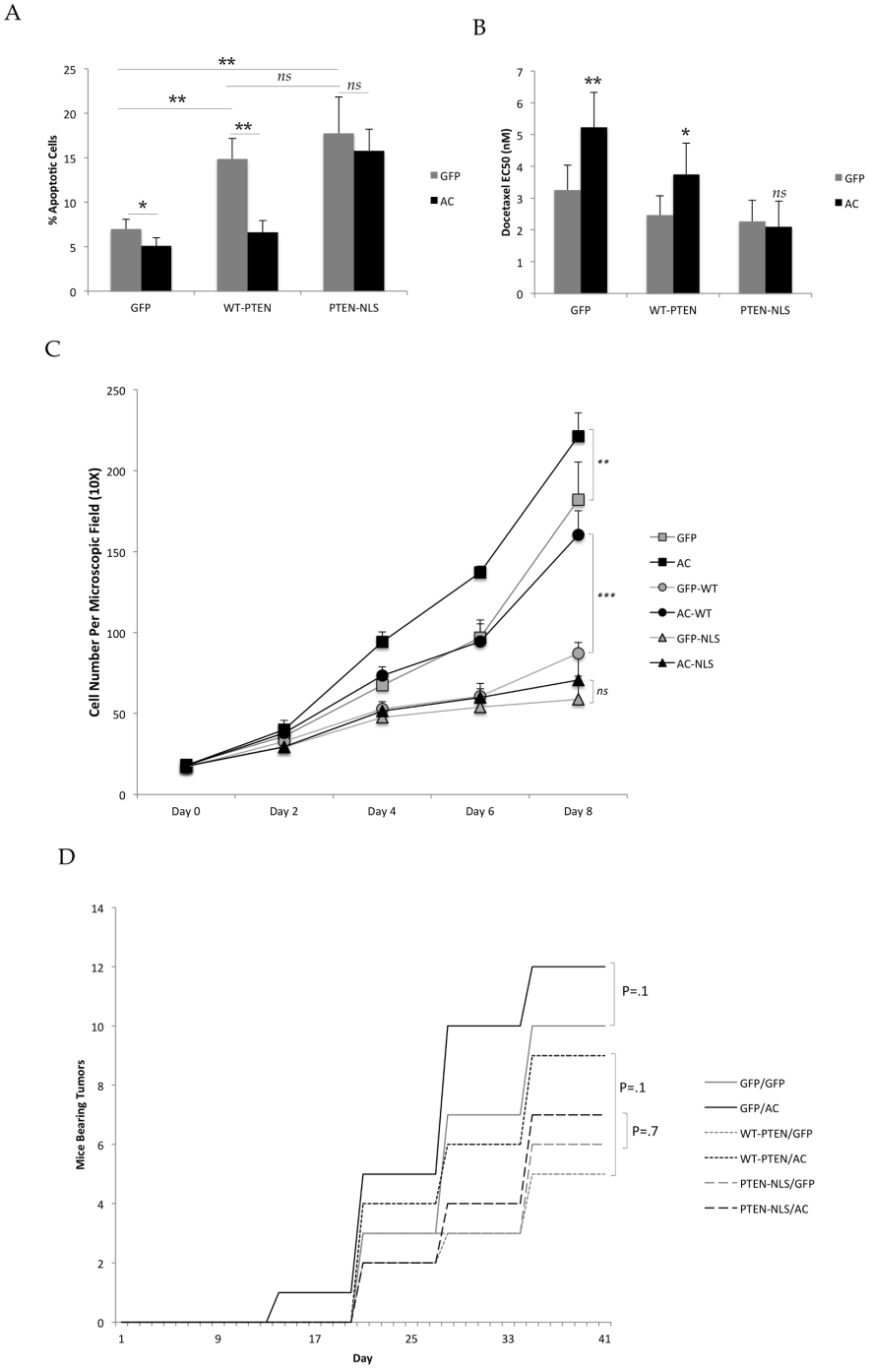


**Figure 6. AC promotes tumor formation and Docetaxel resistance in cells with wild type, but not nuclear localized, PTEN.** A-D) PPC1 cells were infected with 25 MOI Ad-GFP or Ad-AC and either 25 MOI Ad-GFP, Ad-WT-PTEN, or Ad-PTEN-NLS. A) After 24 hours plating, cells were treated with 1.5nM Docetaxel and after a further 48 hours, stained with propidium iodide and analyzed for apoptotic cells using FACS. B) After 24 hour attachment, cells were treated with a dose course (.01 to 100nM) Docetaxel and analyzed for relative cell viability using MTS assay after a further 48 hours. The EC50 was estimated using Prism 4 software. C) Cells were counted on the indicated day (day 0 being the day of plating). Student's t-test, *p<.05, **p<.01. D) 4x106 cells were injected into the flanks of nu/nu mice and observed for 6 weeks. We monitored the mice each week for the formation of palpable tumors and graph the number of mice in the indicated treatment that had established palpable tumor at the indicated day.

doi: 10.1371/journal.pone.0076593.g006

S1P stimulation promotes formation of a physical complex between PTEN and Crm1. Similar to the Yung study, inhibition of S6K prevented export of nuclear PTEN and abolished S1P-mediated formation of the Crm1-PTEN complex, suggesting that the previously described mechanism is active in our observed phenomenon. The Yung study specifically outlined Akt-mediated export of PTEN at the G1/S transition. Our results do not implicate a cell-cycle dependent event as we observed a reduction in nuclear PTEN intensity in 100% of cells following S1P treatment, and synchronization in G1 by serum starvation did not affect the localization of PTEN or the impact of AC/S1P on the percentage of intensity of nuclear PTEN (data not shown). The discrepancy is likely due to the different cell types used between our study and Yung's, in which the majority of the data regarding the G1/S transition was gathered in fibroblasts compared to our study, which uses epithelial prostate carcinoma cells in which derangements in cell cycle processes are severe.

While identifying the mechanism by which AC promoted nuclear loss of PTEN was a chief goal of this study, we were also interested in whether PTEN translocation affects a relevant disease state. AC is overexpressed in the majority of prostate tumors at the mRNA [29] and protein [23] levels, and years of study by our group have shown that AC promotes oncogenic phenotypes in prostate cancer by promoting resistance to chemotherapy [16] and radiotherapy [22] and promoting cell proliferation and xenograft growth [16]. Thus, AC overexpression is a relevant model in which to investigate whether nuclear export of PTEN is an impactful event on the behavior of prostate cancer. To establish this, we evaluated expression of AC and nuclear and cytoplasmic expression of PTEN in a human prostate TMA which contains 27 patient matched adenocarcinoma and benign adjacent tissues, allowing us to evaluate molecular alterations that occur in an individual patient's diseased tissue. In this analysis, we found that in patients whose cancer tissue had elevated AC expression compared to their benign tissue also experienced a loss of nuclear PTEN in the benign to cancer transition. Patients whose tumors did not upregulate AC did not lose nuclear PTEN. This mirrors observations in melanoma, colon cancer, and others in which nuclear PTEN was more prevalent in benign tissue than in cancer [5], with the added implication that AC promotes nuclear egress of PTEN during the development of human prostate cancer. These observations that nuclear PTEN loss may be a consequence of AC overexpression are interesting as nuclear PTEN loss has been found to be a negative prognostic indicator in multiple cancer types.

Functionally, we investigated two of the processes that nuclear PTEN has been found to mediate: apoptosis and proliferation. While some studies have shown that nuclear PTEN does not mediate apoptosis [30], nuclear PTEN is known to regulate p53 acetylation [31,32] and promote apoptosis in response to TNF alpha and doxorubin [9]. To induce apoptosis, we used the standard of care therapy for hormone refractory prostate cancer, Docetaxel, finding that AC expression rescued PPC1 cells expressing wild type PTEN from apoptosis with a concomitant increase in the EC50 of Docetaxel in these cells. This observation is largely consistent with our previous report that AC expression in DU145 cells, which bear wild type PTEN, promotes resistance to taxanes [16]. In contrast, cells expressing nuclear localized PTEN were not protected from Docetaxel by expression of AC, which promoted no change in percentage of apoptotic cells or EC50. This observation identifies a potential mechanism by which active reduction in nuclear PTEN may promote escape from apoptosis in response to chemotherapy and potentially other therapeutics. The Pandolfi group has recently shown impressive evidence that nuclear PTEN suppresses the APC/C (anaphase-promoting complex/cyclosome), which opposes several cell-cycle promoting proteins by promoting their ubiquitin-mediated degradation [4]. This study provides strong mechanistic and functional evidence that nuclear PTEN opposes cell proliferation. Interestingly, expression of AC in cells bearing wild type PTEN promoted cell proliferation 53% more than cells bearing no PTEN, suggesting that while AC promotes cell proliferation in the absence of PTEN, the presence of PTEN allows a more prominent effect, suggesting that the interaction of AC with PTEN is a factor in its ability to promote cell proliferation. It is worth noting that the PTEN-independent promotion of proliferation by AC is not surprising, as Akt has several well-known roles in promoting cell proliferation. In contrast, expressing AC in cells with enforced nuclear expression of PTEN had no impact on cell proliferation, again illustrating that the ability of AC to promote nuclear export of PTEN is an important part of its suppression of oncogenic properties in prostate cancer cells. To test whether the impact of AC on PTEN was important in vivo, we found that while both PTEN-NLS and wild type PTEN suppressed xenoengraftment, AC trended towards promotion of tumor formation only in cells bearing no PTEN or WT-PTEN, although these results were not statistically significant ($p=0.1$). Consistent with sensitivity to Docetaxel and proliferation, AC was unable to promote tumor formation in cells bearing PTEN-NLS ($p=0.7$). The functional studies performed in this work present evidence that AC promotes cell proliferation, resistance to therapy, and potentially tumor formation in part through its ability to cause translocation of PTEN out of the nucleus, effectively promoting nuclear insufficiency of PTEN tumor suppression.

## Conclusion

In this study, we conclude that the Akt activation caused by AC overexpression promotes nuclear export of PTEN in prostate cancer. This phenomenon is dependent upon S1P-mediated activation of Akt which further activates S6K to promote a complex formation between PTEN and the master nuclear exporter Crm1. In human tissues, we found that upregulation of AC during the benign to tumor progression is accompanied by a loss of PTEN in the nucleus. Functional analysis revealed that the ability of AC to promote nuclear egress of PTEN was important for its promotion of proliferation, resistance to standard chemotherapy, and potentially xenoengraftment. This study provides evidence that AC, which is overexpressed in most prostate cancers, exerts its

oncogenic functions in part through promoting insufficiency of PTEN tumor suppression in the nucleus.

## Supporting Information

**Figure S1. PPC1 cells were infected with Ad-AC at MOI ranging from 0 to 50, or Ad-GFP at MOI 50 and probed for expression of AC.** NIH ImageJ was used to measure band densitometries and generate AC/Actin ratios, which were normalized to Ad-GFP MOI 50.
(TIF)

**Figure S2.** PPC1 cells transfected with WT-PTEN were infected with Ad-GFP or Ad-AC for 48 hours in the presence of DMSO (no treatment; NT) or the sphingosine kinase inhibitor SKI-II for 24 hours (A). Whole cell lysates were analyzed by immunoblotting. (B) PPC1 cells transfected with WT-PTEN were treated with the indicated dose of S1P or PBS for 2 hours. Whole cell lysates were analyzed by immunoblotting.
(TIF)

**Figure S3. Nuclear fractions (A) and whole cell lysate (B) of DU145 cells stably expressing AC (AC-EGFP and empty vector (EGFP) were collected and analyzed by western blotting.** Nuclear fractions (C) and whole cell lysates (D) of DU145 cells infected with Ad-GFP or Ad-AC were collected and analyzed by western blotting. E-F) DU145 cells were infected with Ad-GFP or Ad-AC for 48 hours and treated with SKI-II for 24 hours prior to isolation of nuclear fractions (E) and whole cell lysates (F) and western blot analysis.G-H) DU145 cells were stimulated with 500 nM S1P for 2 hours prior to isolation of nuclear fractions (G) and whole cell lysates (H).
(TIF)

**Figure S4. DU145 cells were treated with A) 1μM JTE013 or DMSO (NT) or B) 5μM AktX or water (NT) for 24 hours prior to stimulation with 500 nM S1P or PBS (NT) for 2 hours.** Nuclear fractions were analyzed by western blotting.
(TIF)

**Figure S5. DU145 cells were treated with the indicated concentration of Leptomycin B for 24 hours prior to stimulation with 500 nM S1P for 2 hours.** Nuclear fractions were analyzed by western blotting.
(TIF)

**Figure S6.** PPC1 cells were transfected with WT-PTEN and FLAG-Crm1 (A). Cells were collected after 2 hours stimulation with 500nM S1P or PBS. The negative control (Neg) indicates lysate from cells not transfected with FLAG-Crm1. (B) PPC1 cells were transfected with FLAG-PTEN and collected after 2 hour stimulation with 500nM S1P or PBS. The negative control (Neg) indicates lysate from cells not transfected with FLAG-PTEN.
(TIF)

**Figure S7.** The amino acid sequence of PTEN was analyzed by NetNES1.1 for potential nuclear export signals (A). The identified sequence was mutated (LLL to AAA). (B) WT-PTEN and PTEN-AAA were transfected into PPC1 cells prior to stimulation with 500 nM S1P. Bars indicate the percentage of cells with PTEN in the nucleus. C) PPC1 cells were transfected with FLAG-Crm1 and either WT-PTEN or PTEN-AAA. After 2 hours stimulation with 500 nM S1P, cell lysates were immunoprecipitated with anti- FLAG beads. Student's t-test, **p<.01.
(TIF)

**Figure S8.** DU145 cells were infected with the indicated MOI of Ad-GFP and Ad-AC and analyzed for PTEN phosphorylations by western blotting (A). (B) The PTEN C-terminus phosphorylation site mutants A4 (S380A, T382A,T383A,S385A) and E4 (S380E,T382E,T383E,S385E) were transfected into PPC1 along with FLAG-Crm1 and stimulated for 2 hours with 500 nM S1P or PBS. Cell lysates were immunoprecipitated with anti-FLAG beads. (C) The PTEN A4 and E4 were transfected into PPC1, stimulated for 2 hours with 500 nM S1P or PBS, and immunostained for PTEN. Bars represent the percentage of cells with PTEN in the nucleus. Student's t-test, **p<.01.
(TIF)

**Figure S9. PPC1 cells transfected with WT-PTEN or PTEN-NLS were infected with Ad-GFP or Ad-AC for 48 hours.** A) Cells were immunostained for PTEN, and the percentage of cells which had nuclear PTEN in each treatment is graphed. B) Whole cell lysates were analyzed by immunoblotting. Student's t-test, **p<.01.
(TIF)

## Author Contributions

Conceived and designed the experiments: THB XL JSN. Performed the experiments: THB PL XL. Analyzed the data: THB XL JSN JCC STM. Contributed reagents/materials/ analysis tools: XL JSN. Wrote the manuscript: THB.

## References


1. Maehama T, Dixon JE (1998) The tumor suppressor, PTEN/MMAC1, dephosphorylates the lipid second messenger, phosphatidylinositol 3,4,5-trisphosphate. J Biol Chem 273: 13375-13378. doi:10.1074/jbc.273.22.13375. PubMed: 9593664.
2. Vazquez F, Sellers WR (2000) The PTEN tumor suppressor protein: an antagonist of phosphoinositide 3-kinase signaling. Biochim Biophys Acta 1470: M21-M35. PubMed: 10656987.
3. Li AG, Piluso LG, Cai X, Wei G, Sellers WR et al. (2006) Mechanistic insights into maintenance of high p53 acetylation by PTEN. Mol Cell 23: 575-587. doi:10.1016/j.molcel.2006.06.028. PubMed: 16916644.
4. Song MS, Carracedo A, Salmena L, Song SJ, Egia A et al. (2011) Nuclear PTEN Regulates the APC-CDH1 Tumor-Suppressive Complex in a Phosphatase-Independent Manner. Cell 144: 187-199. doi:10.1016/j.cell.2010.12.020. PubMed: 21241890.
5. Whiteman DC, Zhou XP, Cummings MC, Pavey S, Hayward NK et al. (2002) Nuclear PTEN expression and clinicopathologic features in a

population-based series of primary cutaneous melanoma. Int J Cancer 99: 63-67. doi:10.1002/ijc.10294. PubMed: 11948493.
6. Jang KS, Song YS, Jang SH, Min KW, Na W et al. (2010) Clinicopathological significance of nuclear PTEN expression in colorectal adenocarcinoma. Histopathology 56: 229-239. doi:10.1111/j.1365-2559.2009.03468.x. PubMed: 20102402.
7. Trotman LC, Wang X, Alimonti A, Chen Z, Teruya-Feldstein J et al. (2007) Ubiquitination regulates PTEN nuclear import and tumor suppression. Cell 128: 141-156. doi:10.1016/j.cell.2006.11.040. PubMed: 17218261.
8. Dahia PL, Marsh DJ, Zheng Z, Zedenius J, Komminoth P et al. (1997) Somatic deletions and mutations in the Cowden disease gene, PTEN, in sporadic thyroid tumors. Cancer Res 57: 4710-4713. PubMed: 9354427.
9. Gil A, Andrés-Pons A, Fernández E, Valiente M, Torres J et al. (2006) Nuclear localization of PTEN by a Ran-dependent mechanism enhances apoptosis: Involvement of an N-terminal nuclear localization domain and multiple nuclear exclusion motifs. Mol Biol Cell 17: 4002-4013. doi:10.1091/mbc.E06-05-0380. PubMed: 16807353.
10. Yu Z, Fotouhi-Ardakani N, Wu L, Maoui M, Wang S et al. (2002) PTEN associates with the vault particles in HeLa cells. J Biol Chem 277: 40247-40252. doi:10.1074/jbc.M207608200. PubMed: 12177006.
11. Ginn-Pease ME, Eng C (2003) Increased nuclear phosphatase and tensin homologue deleted on chromosome 10 is associated with G0-G1 in MCF-7 cells. Cancer Res 63: 282-286. PubMed: 12543774.
12. Vazquez F, Ramaswamy S, Nakamura N, Sellers WR (2000) Phosphorylation of the PTEN tail regulates protein stability and function. Mol Cell Biol 20: 5010-5018. doi:10.1128/MCB.20.14.5010-5018.2000. PubMed: 10866658.
13. Liu JL, Mao Z, LaFortune TA, Alonso MM, Gallick GE et al. (2007) Cell cycle-dependent nuclear export of phosphatase and tensin homologue tumor suppressor is regulated by the phosphoinositide-3-kinase signaling cascade. Cancer Res 67: 11054-11063. doi:10.1158/0008-5472.CAN-07-1263. PubMed: 18006852.
14. Beckham TH, Cheng JC, Lu P, Shao Y, Troyer D et al. (2013) Acid ceramidase induces sphingosine kinase 1/S1P receptor 2-mediated activation of oncogenic Akt signaling. Oncogenesis 2: e49. doi:10.1038/oncsis.2013.14. PubMed: 23732709.
15. Brothman AR, Wilkins PC, Sales EW, Somers KD (1991) Metastatic properties of the human prostatic cell line, PPC-1, in athymic nude mice. J Urol 145: 1088-1091. PubMed: 2016798.
16. Saad AF, Meacham WD, Bai A, Anelli V, Elojeimy S et al. (2007) The functional effects of acid ceramidase overexpression in prostate cancer progression and resistance to chemotherapy. Cancer Biol Ther 6: 1455-1460. doi:10.4161/cbt.6.9.4623. PubMed: 17881906.
17. Beckham TH, Lu P, Cheng JC, Zhao D, Turner LS et al. (2012) Acid ceramidase-mediated production of sphingosine 1-phosphate promotes prostate cancer invasion through upregulation of cathepsin B. Int J Cancer 131: 2034-2043. doi:10.1002/ijc.27480.
18. Wang W, Budhu A, Forgues M, Wang XW (2005) Temporal and spatial control of nucleophosmin by the Ran-Crm1 complex in centrosome duplication. Nat Cell Biol 7: 823-830. doi:10.1038/ncb1282. PubMed: 16041368.
19. Mosessian S, Avliyakulov NK, Mulholland DJ, Boontheung P, Loo JA et al. (2009) Analysis of PTEN complex assembly and identification of heterogeneous nuclear ribonucleoprotein C as a component of the PTEN-associated complex. J Biol Chem 284: 30159-30166. doi:10.1074/jbc.M109.027995. PubMed: 19740742.
20. Ramaswamy S, Nakamura N, Vazquez F, Batt DB, Perera S et al. (1999) Regulation of G1 progression by the PTEN tumor suppressor protein is linked to inhibition of the phosphatidylinositol 3-kinase/Akt pathway. Proc Natl Acad Sci U S A 96: 2110-2115. doi:10.1073/pnas.96.5.2110. PubMed: 10051603.
21. Suzuki K, Bose P, Leong-Quong RY, Fujita DJ, Riabowol K (2010) REAP: A two minute cell fractionation method. BMC Res Notes 3: 294. doi:10.1186/1756-0500-3-294. PubMed: 21067583.
22. Mahdy AE, Cheng JC, Li J, Elojeimy S, Meacham WD et al. (2009) Acid ceramidase upregulation in prostate cancer cells confers resistance to radiation: AC inhibition, a potential radiosensitizer. Mol Ther 17: 430-438.
23. Norris JS, Bielawska A, Day T, El-Zawahri A, Elojeimy S et al. (2006) Combined therapeutic use of AdGFPFasL and small molecule inhibitors of ceramide metabolism in prostate and head and neck cancers: a status report. Cancer Gene Ther 13: 1045-1051. doi:10.1038/sj.cgt.7700965. PubMed: 16763610.
24. la Cour T, Kiemer L, Molgaard A, Gupta R, Skriver K et al. (2004) Analysis and prediction of leucine-rich nuclear export signals. Protein Eng Des Sel 17: 527-536. doi:10.1093/protein/gzh062. PubMed: 15314210.
25. Gil A, Andrés-Pons A, Pulido R (2007) Nuclear PTEN: a tale of many tails. Cell Death Differ 14: 395-399. doi:10.1038/sj.cdd.4402073. PubMed: 17186024.
26. Perren A, Weng LP, Boag AH, Ziebold U, Thakore K et al. (1999) Immunohistochemical evidence of loss of PTEN expression in primary ductal adenocarcinomas of the breast. Am J Pathol 155: 1253-1260. doi:10.1016/S0002-9440(10)65227-3. PubMed: 10514407.
27. Gimm O, Perren A, Weng LP, Marsh DJ, Yeh JJ et al. (2000) Differential nuclear and cytoplasmic expression of PTEN in normal thyroid tissue, and benign and malignant epithelial thyroid tumors. Am J Pathol 156: 1693-1700. doi:10.1016/S0002-9440(10)65040-7. PubMed: 10793080.
28. Perren A, Komminoth P, Saremaslani P, Matter C, Feurer S et al. (2000) Mutation and expression analyses reveal differential subcellular compartmentalization of PTEN in endocrine pancreatic tumors compared to normal islet cells. Am J Pathol 157: 1097-1103. doi:10.1016/S0002-9440(10)64624-X. PubMed: 11021813.
29. Seelan RS, Qian C, Yokomizo A, Bostwick DG, Smith DI et al. (2000) Human acid ceramidase is overexpressed but not mutated in prostate cancer. Genes Chromosomes Cancer 29: 137-146. doi:10.1002/1098-2264(2000)9999:9999. PubMed: 10959093.
30. Chung JH, Eng C (2005) Nuclear-cytoplasmic partitioning of phosphatase and tensin homologue deleted on chromosome 10 (PTEN) differentially regulates the cell cycle and apoptosis. Cancer Res 65: 8096-8100. doi:10.1158/0008-5472.CAN-05-1888. PubMed: 16166282.
31. Shen WH, Balajee AS, Wang J, Wu H, Eng C et al. (2007) Essential Role for Nuclear PTEN in Maintaining Chromosomal Integrity. Cell 128: 157-170. doi:10.1016/j.cell.2006.11.042. PubMed: 17218262.
32. Shen Y, White E (2001) p53-dependent apoptosis pathways. Adv Cancer Res 82: 55–84. PubMed: 11447765.